Structure and Functions of *Streptomyces* Subtilisin Inhibitor (SSI): Studies with Site-specifically Modified and Mutated Proteins

Keiko Masuda-Momma

1994

Structure and Functions of *Streptomyces* Subtilisin Inhibitor (SSI): Studies with Site-specifically Modified and Mutated Proteins

Keiko Masuda-Momma

1994

CONTENTS

Abbreviations

API-2c'	Alkaline proteinase inhibitor 2c'
BPSTI	bovine pancreatic secretory trypsin inhibitor
BPTI	bovine pancreatic trypsin inhibitor
CD	circular dichroism
DSC	differencial scanning calorimetry
LB medium	Luria-Bertani medium
OMJPQ3	third domain of ovomucoid inhibitor from Japanese quail
OMSVP3	third domain of ovomucoid inhibitor from silver pheasant
OMTKY3	third domain of ovomucoid inhibitor from turky
PAGE	polyacrylamide gel electrophoresis
Pi	notation for the amino acid residue in protease substrates as used in Schechter & Berger (25)
S-BPN'(wt)	subtilisin BPN' wild type
S-BPN'Y104F	the mutant subtilisin BPN' in which tyrosine 104 is replaced by phenylalanine
SSI	Streptomyces subtilisin inhibitor
SSI(wt)	SSI wild type

SSI*	modified SSI in which the reactive site Met73–Val74 is cleaved
$SSIX_1 p_1 X_2$	a mutant SSI in which the amino acid residue X_1 at p_1th position is replaced by X_2
$SSIX_3 p_2 X_4/X_5 p_3 X_6$	a double mutated SSI in which the amino acid residue X_3 at p_2th position is replaced by X_4 and X_5 at p_3th position is replaced by X_6.
STI	soybean trypsin inhibitor

Introduction

Proteinaceous proteinase inhibitors occur widely in nature and must be closely involved in the control of many important biological functions (1-2). Elucidating the detailed features of the inhibition of the target proteinase is not only necessary for understanding the biological significance of the inhibitor, it is also important for understanding the mechanisms of specific protein-protein interaction and of proteolysis (3-4). Since Kunitz and Northrop isolated a trypsin inhibitor from bovine pancreas in 1936 (5), many proteinase inhibitors have been reported (6) and Laskowski, Jr. and his coworkers presented the general concept on the mechanism of interaction between serine proteinases and their inhibitors (3). Most of serine proteinase inhibitors are bound stoichiometrically and reversibly through noncovalent bonding to inhibit enzymes competitively. The modified inhibitor in which only the reactive site peptide bond is hydrolyzed by the catalytic action of enzyme is observed under the particular condition and it can also inhibit the enzymes. So that the simplest standard mechanism of interaction between serine proteinase and inhibitor has been proposed as follows:

$$E + I \rightleftharpoons C \rightleftharpoons E + I^*$$

where E, I, I*, and C represent an enzyme, an inhibitor, a modified inhibitor, and a stable enzyme-inhibitor complex, respectively. The most fundamental question about proteinaceous proteinase inhibitors concerns the nature of the structural requirements for a protein to be a proteinase inhibitor.

In the present thesis, the equilibrium was studied kinetically and statically to reveal the structure-function relationship of proteinaceous proteinase inhibitor using the system of the interaction between Streptomyces subtilisin inhibitor and subtilisin BPN'.

Streptomyces subtilisin inhibitor (SSI) is a proteinaceous proteinase inhibitor of microorganism origin isolated from the culture broth of Streptomyces albogriseolus S-3253 by Murao and Sato in 1972 (7), and it has been the subject of intensive studies (8). SSI strongly inhibits bacterial alkaline serine proteinases such as subtilisin BPN'. The general properties of SSI are listed in Table I. The primary structure of SSI was determined by Ikenaka et al. in 1974 as shown in Fig. 1 (9). The three-dimensional structures of SSI (10-11) and SSI-subtilisin BPN' complex (12-13) have been resolved by X-ray crystallography (Fig. 2) and NMR study (14). The SSI gene has been isolated (15), and an expression system has been established in a heterologous host, Streptomyces lividans 66 (16).

In this study, the interaction between SSI and subtilisin BPN' was studied with site specifically modified and mutated proteins. In Chapter 1, static and kinetic analysis is performed on the interaction between subtilisin BPN' and mutated SSI of which the P_1 site amino acid residue, Met73, was replaced by site-directed mutagenesis. The rate constant of binding, k_{on}, and the rate constant of dissociation, k_{off}, are determined by using newly derived equations. In Chapter 2, amino acid residues responsible for the changes of absorption and fluorescence spectra on the binding of subtilisin BPN' and SSI are identified by using mutated proteins. Equilibrium constants K_{hyd} for the hydrolysis of

the reactive-site peptide bond of SSI is studied in Chapter 3. The standard mechanism of inhibition on the interaction between SSI and subtilisin BPN' is investigated by measuring the resynthesis of the reactive site in Chapter 4. In Chapter 5, kinetic and thermodynamic studies on the dissociation of a dimeric protein, SSI is carried out. In Chapter 6, role of Pro residues at around the reactive site of SSI is studied on the interaction with subtilisin BPN' and conformational stability.

Table I The general properties of SSI.

		ref.
Source	Streptomyces albogriseolus	
Molecular Weight	11500 /subunit	(9,17-20)
Two identical subunits		
Amino acid residues	113	(9)
reactive site	Met73-Val74	(21)
p*I*	4.3	(20)
A_{278}(1 mg/ml), pH7.0	0.829	(17)

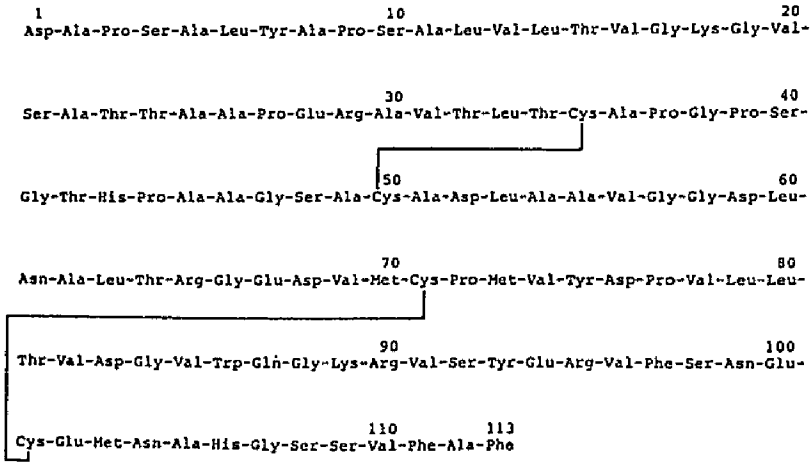

Fig. 1. Primary structure of Streptemyces subtilisin inhibitor. (9)

Fig. 2-a. α-Carbon cahins of a complex of SSI dimer (bold bonds) with 2 subtilisin BPN' molecules (thin bonds). Scale bar represents 10 Å. (13)

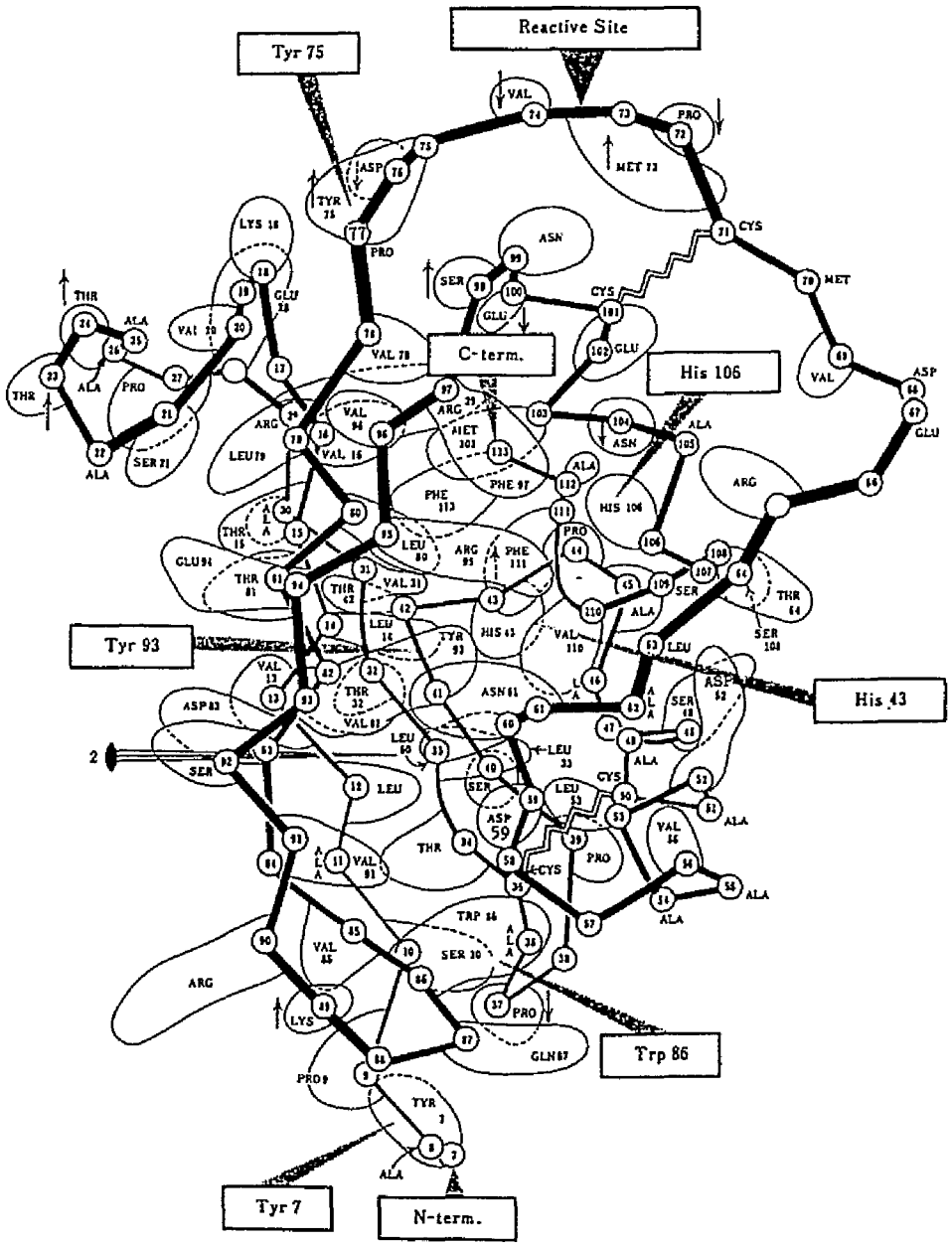

Fig. 2-b. A Schematic drawing of the SSI subunit. (11) The circles with residue numbers represent α-carbon atms. Disulfide bridges are denoted by zig-zag double lines.

Chapter 1
Interaction of Subtilisin BPN' and Recombinant *Streptomyces* Subtilisin Inhibitors with Substituted P_1 Site Residues

The interaction between proteinaceous proteinase inhibitors and proteinases is important for understanding the mechanisms of specific protein-protein interaction and of proteolysis. The most fundamental question about proteinaceous proteinase inhibitors concerns the nature of the structural requirements for a protein to be a proteinase inhibitor.

The three-dimensional structures of *Streptomyces* subtilisin inhibitor (SSI) (10-11) and SSI-subtilisin BPN' complex (12-13) have been resolved by X-ray crystallography. The SSI-subtilisin BPN' complex is in the form of a Michaelis complex (12-14) similar to those of bovine pancreatic trypsin inhibitor-trypsin complex (22), turkey ovomucoid third domain-*Streptomyces griseus* proteinase B complex (23), eglin-c-subtilisin Carlsberg complex, and barley chymotrypsin inhibitor-subtilisin complex (24). The term Michaelis complex here means one in which the carbonyl carbon of the scissile peptide bond of the inhibitor remains trigonal. The SSI gene has been isolated (15), and an expression system has been established in a heterologous host, *Streptomyces lividans* 66 (16). Accordingly, subtilisin BPN' and SSI can provide a suitable system for detailed analysis of the structure-function relationship of specific protein-protein interaction and of the reaction mechanism of serine proteinase.

In studies of the structure-function relationship of SSI, the role of the P_1 site residue (according to Schechter & Berger's nomenclature (25)) in the interaction with subtilisin BPN' was first analyzed. This was done with ovomucoid inhibitors (26) and barley chymotrypsin inhibitors (27). Recombinant SSIs in which a different amino acid was substituted for the P_1 residue, Met73 in the wild type, were prepared by site-directed mutagenesis, and their binding affinity with subtilisin BPN' was determined (28).

In the present chapter, the interaction of SSI with subtilisin BPN' was analyzed by kinetic methods. The simplest binding mechanism of an enzyme and an inhibitor is represented as Eq. 1-1:

$$E + I \underset{k_{off}}{\overset{k_{on}}{\rightleftharpoons}} EI \qquad (1\text{-}1)$$

and the inhibitor constant, K_i, is defined as Eq.1-2:

$$K_i = \frac{[E][I]}{[EI]} = \frac{k_{off}}{k_{on}} \qquad (1\text{-}2)$$

where [E], [I], and [EI] are the concentrations of free enzyme, free inhibitor, and EI complex, respectively. k_{on} and k_{off} are the bimolecular association rate constant and the unimolecular dissociation rate constant, respectively, and they are composite constants as shown in Results.

In this study I have derived equations with which one can obtain k_{on} and k_{off} simultaneously from a progress curve of peptide hydrolysis reaction. Application of these equations has enabled us to work with smaller amounts of precious samples. The rapid reaction kinetic studies with the stopped-flow method were made to clarify these binding processes.

MATERIALS AND METHODS

Proteins - SSI was purified from the culture filtrate of Streptomyces albogriseolus S-3253 essentially as described previously (7). A thrice crystallized and lyophilized subtilisin BPN' (EC 3.4.21.14) (lot No.7370935) was purchased from Nagase Sangyo Company Ltd., Osaka. The concentration of active enzyme was determined to be 75 % by the initial burst titration with N-trans-cinnamoylimidazole (29). The protein concentration was determined spectrophotometrically, from the absorbance at pH 7.0 by using A_{278}(1 mg/ml) = 0.829 for SSI and A_{278}(1 mg/ml) = 1.063 for subtilisin BPN' (17). The molecular weights were 11500 for SSI (subunit) (9,18) and 27500 for subtilisin BPN' (30). SSI concentration in the text, shown as [I], is represented as subunit concentration unless otherwise mentioned.

The site-directed mutagenesis of the SSI gene and its expression were carried out as previously described (16, 28). Mutant SSIs were purified from the culture media by the same method as used for the wild-type SSI (abbreviated to SSI(wt)) (7) except that DEAE-cellulose chromatography (10 mM borate buffer at pH 7.2) was changed to QAE-Toyopearl chromatography (25 mM borate-KCl buffer at pH 9.4). Mutant SSIs are named SSIM73X, where X represents the amino acid replacing Met at position 73.

Chemicals - Succinyl(Suc)-Ala-Ala-Pro-Phe *p*-nitroanilide (*p*-NA) and succinyl(Suc)-Ala-Ala-Pro-Phe-methyl-coumaryl-amide (MCA) were purchased from Boehringer-Mannheim Co. and Peptide Research Institute, Inc., Minoh, respectively, and dissolved in dimethylsulfoxide to prepare a stock solution of 8 mM and 10 mM, respectively. All other chemicals were

of the best grade commercially available.

Enzyme activity - Enzyme activity was measured by the initial rate of the hydrolysis of Suc-Ala-Ala-Pro-Phe-MCA as substrate. Reactions were carried out in 25 mM phosphate buffer, pH 7.0, I=0.1 M (NaCl), containing 0.005 % (w/v) Triton X-100 at 25 ℃. Triton X-100 was included in the buffer to prevent undesired protein adsorption to incubation vessels (26). The reaction was started by the addition of the substrate (final concentration 1.2 μM) to the enzyme (3 nM), and the release of 7-amino-4-methyl-coumarin (AMC) was followed by measuring fluorescence intensity at 440 nm with excitation at 350 nm. K_m and k_{cat} were respectively 3.7 X 10^{-5} M and 0.8 s^{-1} under these conditions.

Enzyme inhibition - The inhibition of subtilisin BPN' by SSI was measured as described in the previous section in the presence of various amounts of the inhibitor: 5～100 μl of inhibitor solution (0.13 μM) was added by use of a micro-syringe to 2 ml of the enzyme solution in a test tube, mixed and incubated for 30 min at 25℃ before addition of the substrate. The initial rate of enzyme reaction in the presence of the inhibitor was taken as the residual enzyme activity.

K_i determination - The residual enzyme activity was plotted against the inhibitor concentration. These data were fitted to a theoretical equation derived for the one-to-one binding of an enzyme and an inhibitor, with the aid of a computer program for the nonlinear least-squares analysis developed in the laboratory of Prof. M. Laskowski, Jr. (31). Since SSI is a competitive inhibitor, the K_i thus obtained was an apparent constant, K_{app}, and the intrinsic K_i was calculated by $K_i = K_{app}/(1+[S]_0/K_m)$

(32).

Estimation of the rate of enzyme-inhibitor interaction by enzyme activity - Suc-Ala-Ala-Pro-Phe *p*-NA was used as substrate of the enzyme. Assays were carried out in 25 mM phosphate buffer, pH 7.0 and 8.6, I=0.1 M (NaCl), containing 0.005 % (w/v) Triton X-100 at 25°C. The enzyme concentration was 0.3 nM except for the cases of SSIM73E and SSIM73D, for which it was 6 nM and 16 nM, respectively, so that the rate of inhibitor binding was in the time range of the steady-state enzyme activity measurement. Reactions were started by adding enzyme solution (1 ml) to a cuvette containing 50 µl of 4 mM substrate solution (final concentration 0.18 mM) and 50 µl of the inhibitor solution or the buffer solution. The inhibitor concentration was set such that $[I]_0 \geq 5[E]_0$. The release of *p*-nitroaniline was followed at 405 nm for 20 min. The progress curve was analyzed as described in Results to obtain the rate constants. The K_m was 0.22 mM and 0.17 mM at pH 7.0 and 8.6, respectively.

Dissociation Kinetics - Conventional determination of the dissociation rate constant, k_{off}, was made by diluting the preformed enzyme-inhibitor complex (EI) (33). That is, 50 µl of the substrate solution (final concentration 0.25 mM) and 2.5 ml of 25 mM phosphate buffer, pH 7.0, containing 0.005% (w/v) Triton X-100 were mixed in a cuvette and 50 µl of the EI complex solution (2 nM) was added to it (final concentration 0.04 nM). Increase in A_{405} was followed. The reaction kinetics was treated as first-order by assuming $k_{on}[E][I] \ll k_{off}[EI]$ under the conditions employed. The k_{off} was also obtained with the newly derived equations as described in Results.

Stopped-flow measurements - A Union Giken RA-1300 (gas pressure-driven) stopped-flow apparatus was used for the direct measurement of the interaction. The fluorescence change through a cutoff filter at 310 nm was detected perpendicular to the excitation beam at 280 nm. A cylindrical cell of optical path 2 mm was used, and the dead time of the apparatus was about 2 ms under the working conditions. The apparent first-order rate constant, k_{app}, was obtained by the Guggenheim plot (34) under the conditions of $[I]_0 \geqq 5[E]_0$, $[I]_0 = 20 \sim 340\ \mu M$, and pH 7.0 (25 mM phosphate buffer) at 25°C.

RESULTS

Inhibitor constant, K_i - Figure 1-1 shows the titration curves of the enzyme with the inhibitor as monitored by the residual activity. The inhibitor constants of SSI(wt) and recombinant SSIs against subtilisin BPN' at pH 7.0 are summarized in Table 1-1. These values show a general tendency similar to those obtained at pH 9.5 by Kojima et al. (28), except for the Asp and Glu mutants. Among the P_1 mutants examined, SSIM73I was the weakest inhibitor, K_i being 2.7 (±0.2) X 10^{-10} M, which is about 15 times larger than that of SSI(wt); SSIM73V, SSIM73E, and SSIM73D showed a little weaker inhibitory activity than SSI(wt). pH-Dependence of K_i values of SSI(wt), SSIM73K, SSIM73E, and SSIM73D were studied in the pH range from 7 to 10 (Fig. 1-2). SSIM73E and SSIM73D showed clear pH dependence, whereas SSIM73K and SSI(wt) exhibited little dependence. In the

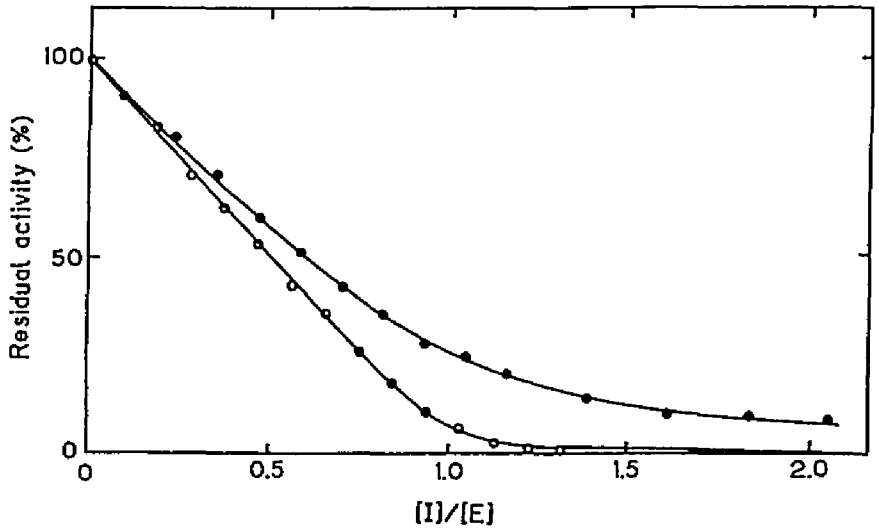

Fig. 1-1. Titration of subtilisin BPN' with SSI(wt) and SSIM73I at pH 7.0, 25 ℃. $[E]_0$=3.0 nM, $[S]_0$=1.23 μM. Substrate: Suc-Ala-Ala-Pro-Phe-MCA. ○: SSI(wt); ●: SSIM73I. The solid lines are the theoretical curves of K_i = 1.8 X10^{-11} M and 2.7 X10^{-10} for SSI(wt) and SSIM73I, respectively.

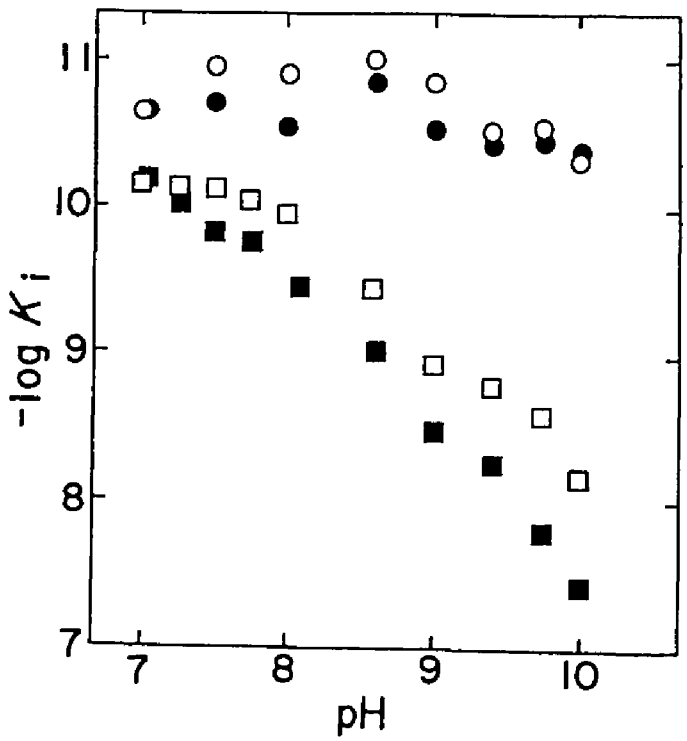

Fig. 1-2. Effect of pH on K_i of SSIs toward subtilisin-BPN' at 25℃. ○: SSI(wt), ●: SSIM73K, □: SSIM73E, ■: SSIM73D.

former two mutants, $-\log K_i$ values decreased as pH increased.

Estimation of the rate of enzyme-inhibitor interaction by enzyme activity - The reaction scheme is assumed to be as in Eq. 1-3, since SSI is a competitive inhibitor (18):

$$\begin{array}{ccccc} E + S & \rightleftharpoons & ES & \rightarrow & E + P \\ + & & & & \\ I & & & & \\ k_{on} \;||\; k_{off} & & & & \\ EI & & & & \end{array} \qquad (1\text{-}3)$$

where S, ES, and P are the substrate, enzyme-substrate complex, and the product, respectively. $[E]_0$, the initial enzyme concentration, and K_m, the Michaelis constant, are assumed to be as in Eqs. 1-4 and 1-5, respectively.

$$[E]_0=[E]+[EI]+[ES] \qquad (1\text{-}4)$$

$$K_m = \frac{[E][S]}{[ES]} \qquad (1\text{-}5)$$

A progress curve was obtained (Fig. 1-3, curve a) by following liberation of the product in the reaction. If it can be assumed that the association of the substrate with free enzyme is much faster than the inhibitor-enzyme association under the experimental conditions (the relationship between curves a and b of Fig. 1-3 supports the validity of the assumption), the slope of the contact line $(d[P]/dt)_t$ on the progress curve at time t will give the enzyme activity at time t, v_t (Eq. 1-6).

$$\frac{d[P]}{dt} = v_t \qquad (1\text{-}6)$$

Instead of drawing the contact line at $t = 0$ to estimate v_0, we carried out the reaction in the absence of the inhibitor and obtained v_0 from the slope of the straight progress line in the initial time range (Fig. 1-3, curve b).

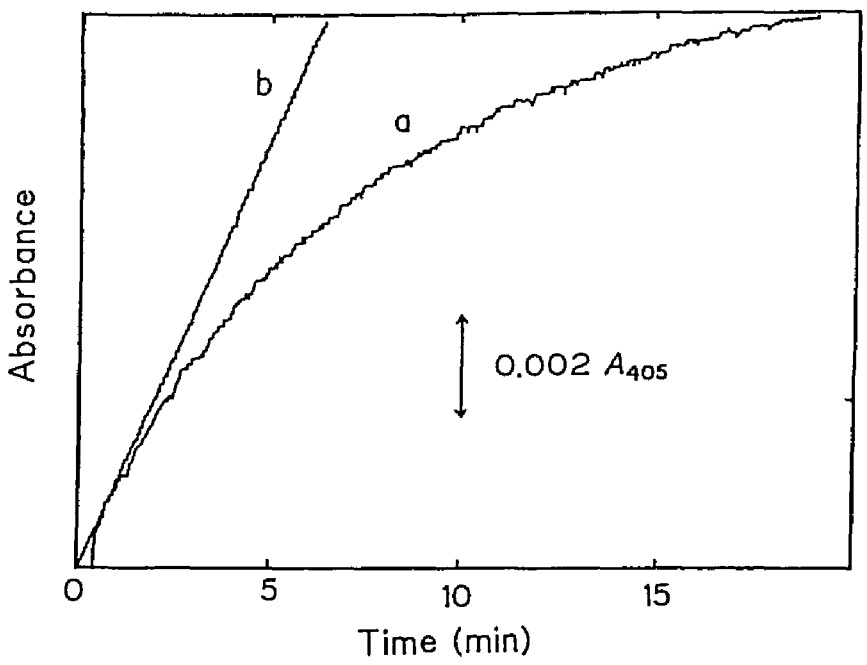

Fig. 1-3. Hydrolysis of Suc-Ala-Ala-Pro-Phe *p*-NA by subtilisin BPN' at pH 8.6, 25 ℃. $[E]_0$=0.3 nM, $[S]_0$=0.18 mM. a: progress curve with 1.5 nM SSI(wt); b: control without the inhibitor.

Thus, the concentration of EI at time t is given by Eq. 1-7.

$$[EI]=[E]_0 \times \left(1-\frac{v_t}{v_0}\right) \qquad (1\text{-}7)$$

Equations 1-8 and 1-9 are derived from Eqs. 1-3, 1-4, and 1-5 under the conditions of $[I]_0 \gg [E]_0$ and $[S]_0 \gg [E]_0$.

$$\frac{d[EI]}{dt} = k_{on}[I]_0[E]-k_{off}[EI]$$

$$= k_{on}\frac{[I]_0([E]_0-[EI])}{(1+[S]_0/K_m)}-k_{off}[EI] \qquad (1\text{-}8)$$

$$\frac{d[EI]/dt}{([E]_0-[EI])} = k_{on}\frac{[I]_0}{(1+[S]_0/K_m)}-k_{off}\frac{[EI]}{([E]_0-[EI])} \qquad (1\text{-}9)$$

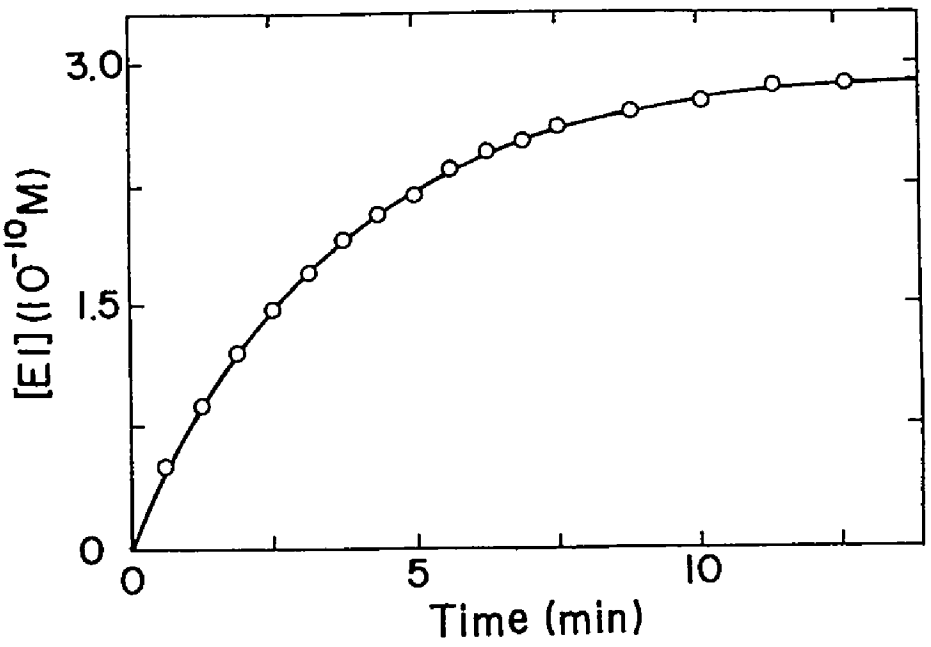

Fig. 1-4. Formation of subtilisin BPN'-SSI(wt) complex reconstructed with Eqs. 1-6 & 1-7 from the curves given in Fig. 3. The solid line is the theoretical curve drawn according to Eq. 1-10 with the values: k_{on}=4.8X10^{6} M^{-1}s^{-1}, k_{off}=1.0X10^{-4} s^{-1}. See the text for details.

The v_i value was obtained by graphical differentiation of the progress curve (Fig. 1-3, curve a); thus [EI] at time t calculated by Eq 1-7. is shown in Fig. 1-4. The value of d[EI]/dt was obtained by similarly differentiating [EI] with respect to time on Fig. 1-4. The plot of (d[EI]/dt)/([E]$_0$-[EI]) against [EI]/([E]$_0$-[EI]) gives a straight line, from which k_{on}[I]$_0$/(1+[S]$_0$/K_m) and k_{off} can be determined independently according to Eq. 1-9 (Fig. 1-5). Equation 1-8 was transformed to Eq. 1-10 by integration, which should give the time dependence of [EI].

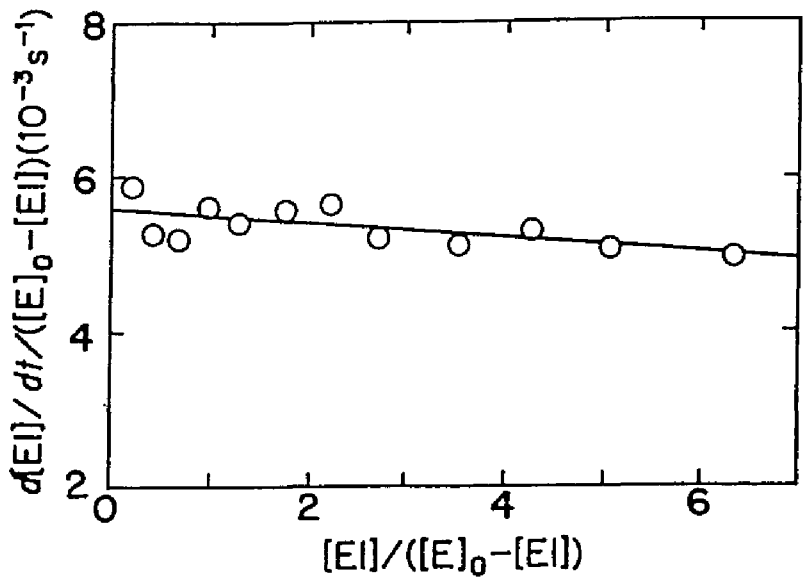

Fig. 1-5. Graphical determination of the association and dissociation rate constants. The plots are made according to Eq. 9 from the curve in Fig. 4. k_{on} and k_{off} were determined from the vertical intercept and the slope, respectively. The solid line is drawn by the least squares method. See the text for the details.

$$[EI] = \frac{k_{on}[I]_0[E]_0}{k_{on}[I]_0+k_{off}(1+S_0/K_m)} \times \left\{1- \exp\left\{- \left\{\frac{k_{on}[I]_0+k_{off}(1+S_0/K_m)}{1+S_0/K_m}\right\} \cdot t \right\}\right\} \quad (1-10)$$

On the other hand, k_{on} can be obtained conventionally by Eq. 1-11, which is derived from Eqs. 1-3, 1-4, and 1-5 by assuming $k_{off} \fallingdotseq 0$.

$$\ln \frac{v_0}{v_t} = \frac{k_{on}[I]_0}{(1+S_0/K_m)} t \quad (1-11)$$

The treatment of Eq. 1-11 has been employed for many years (35). The results of these analyses are presented in Table 1-1.

The association rate constant, k_{on}, of SSI(wt) with S-BPN' was obtained as $6.5(\pm0.1)\times10^{6}$ $M^{-1}s^{-1}$ and the dissociation rate constant, k_{off}, of SSI(wt) as $0.9(\pm0.2)\times10^{-4}$ s^{-1}. Accordingly, K_i calculated by Eq. 1-2 with the kinetic constants was $1.4(\pm0.3)\times10^{-11}$ M (Table 1-1, the right most column), which is in good agreement with the value obtained by the equilibrium method (Table 1-1, the second column from the left). The values of k_{on} at pH 7.0 of almost all the mutant SSI's treated are similar to that of SSI(wt), except for those of SSIM73E and SSIM73D, which are slightly smaller. The values of k_{off} are also almost the same as that of SSI(wt), except for SSIM73I, for which k_{off} was 1.7×10^{-3} s^{-1}, about 20 times larger than that of SSI(wt).

For SSIM73K and SSIM73R, K_i values were as same as that of SSI(wt) but the values of k_{on} obtained by Eq. 1-11 were smaller than that for SSI(wt). However, the plots of $(d[EI]/dt)/([E]_0-[EI])$ against $[EI]/([E]_0-[EI])$ did not give good straight lines due to some yet unknown reason. Accordingly, k_{on} and k_{off} for these mutants were not determined in the present analysis.

Kinetic analysis was also made at pH 8.6, 25 ℃ for SSI(wt), SSIM73E, and SSIM73D (Table 1-2), and the values of k_{on} were $4.8(\pm0.1)\times10^{6}$ $M^{-1}s^{-1}$, $5.9(\pm0.2)\times10^{5}$ $M^{-1}s^{-1}$, and $3.7(\pm0.1)\times10^{5}$ $M^{-1}s^{-1}$, respectively. These two mutants having an acidic residue at P_1 site showed much weaker affinity and considerably smaller k_{on} values than does the wild type, whereas their k_{off} values are larger, though the difference is less than 3-fold.

Direct measurement of enzyme-inhibitor interaction by stopped-flow method The apparent first-order rate constant,

TABLE 1-1: Equilibrium and kinetic parameters for the binding of subtilisin-BPN' and inhibitors, at pH 7.0, 25 ℃.

SSI species (shown by P_1)	K_i (10^{-11}M)	k'_{on}[a] (10^6/M·s)	k_{on}[b] (10^6/M·s)	k'_{off}[c] (10^{-4}/s)	k_{off}[b] (10^{-4}/s)	k_{off}/k_{on}[b] (10^{-11}M)
Met73(wt)	1.8(±0.3)	4.8(±0.1)	6.5(±0.1)	1.6(±0.1)	0.9(±0.2)	1.4(±0.3)
Met73Glu	6.9(±1.0)	1.8(±0.1)	1.9(±0.1)	-	1.1(±0.2)	5.7(±1.4)
Asp	6.4(±1.0)	1.4(±0.1)	1.8(±0.1)	-	2.6(±0.5)	14.0(±1.5)
His	2.6(±0.6)	3.3(±0.2)	4.4(±0.1)	-	4.1(±0.2)	9.4(±0.7)
Lys	1.8(±0.4)	1.5(±0.1)	ND	-	ND	ND
Arg	1.8(±0.6)	2.2(±0.2)	ND	-	ND	ND
Gly	2.3(±0.5)	4.0(±0.1)	4.5(±0.2)	-	1.3(±0.4)	2.8(±1.0)
Ala	2.6(±0.5)	3.3(±0.1)	3.7(±0.1)	-	1.4(±0.1)	3.6(±0.4)
Leu	1.2(±0.8)	3.2(±0.01)	4.2(±0.1)	-	2.1(±0.3)	5.0(±0.8)
Val	6.0(±0.8)	3.8(±0.1)	5.4(±0.6)	-	3.5(±0.2)	6.5(±1.1)
Ile	27.0(±2.2)	4.2(±0.3)	6.2(±0.6)	-	17.0(±2.6)	27.0(±5.9)

[a]calculated from Eq. 1-11. [b]calculated from Eq. 1-9. [c]determined by the conventional method (see text). ND: not determined. -: no data.

The association rate constant, k_{on}, of SSI(wt) with S-BPN' was obtained as $6.5(\pm0.1)\times10^{6}$ $M^{-1}s^{-1}$ and the dissociation rate constant, k_{off}, of SSI(wt) as $0.9(\pm0.2)\times10^{-4}$ s^{-1}. Accordingly, K_i calculated by Eq. 1-2 with the kinetic constants was $1.4(\pm0.3)\times10^{-11}$ M (Table 1-1, the right most column), which is in good agreement with the value obtained by the equilibrium method (Table 1-1, the second column from the left). The values of k_{on} at pH 7.0 of almost all the mutant SSI's treated are similar to that of SSI(wt), except for those of SSIM73E and SSIM73D, which are slightly smaller. The values of k_{off} are also almost the same as that of SSI(wt), except for SSIM73I, for which k_{off} was 1.7×10^{-3} s^{-1}, about 20 times larger than that of SSI(wt).

For SSIM73K and SSIM73R, K_i values were as same as that of SSI(wt) but the values of k_{on} obtained by Eq. 1-11 were smaller than that for SSI(wt). However, the plots of $(d[EI]/dt)/([E]_0-[EI])$ against $[EI]/([E]_0-[EI])$ did not give good straight lines due to some yet unknown reason. Accordingly, k_{on} and k_{off} for these mutants were not determined in the present analysis.

Kinetic analysis was also made at pH 8.6, 25 ℃ for SSI(wt), SSIM73E, and SSIM73D (Table 1-2), and the values of k_{on} were $4.8(\pm0.1)\times10^{6}$ $M^{-1}s^{-1}$, $5.9(\pm0.2)\times10^{5}$ $M^{-1}s^{-1}$, and $3.7(\pm0.1)\times10^{5}$ $M^{-1}s^{-1}$, respectively. These two mutants having an acidic residue at P_1 site showed much weaker affinity and considerably smaller k_{on} values than does the wild type, whereas their k_{off} values are larger, though the difference is less than 3-fold.

Direct measurement of enzyme-inhibitor interaction by stopped-flow method The apparent first-order rate constant,

k_{app}, for the association was obtained from the stopped-flow reaction curve (Fig. 1-6). When k_{app} was plotted against the inhibitor concentration (Fig. 1-7), a hyperbolic curve was observed. This concentration dependence of k_{app} is consistent with a two-step mechanism in which a fast bimolecular process for the formation of a loosely bound intermediate is followed by a slower unimolecular isomerization step (36):

$$E + I \underset{k_{-1}}{\overset{k_{+1}}{\rightleftharpoons}} (EI)_L \underset{k_{-2}}{\overset{k_{+2}}{\rightleftharpoons}} EI \qquad (1\text{-}12)$$

In Eq. 1-12, $(EI)_L$ and EI represent the loosely bound intermediate complex and the tightly bound complex, respectively; and k_{+1}, k_{-1}, k_{+2}, and k_{-2} are rate constants.

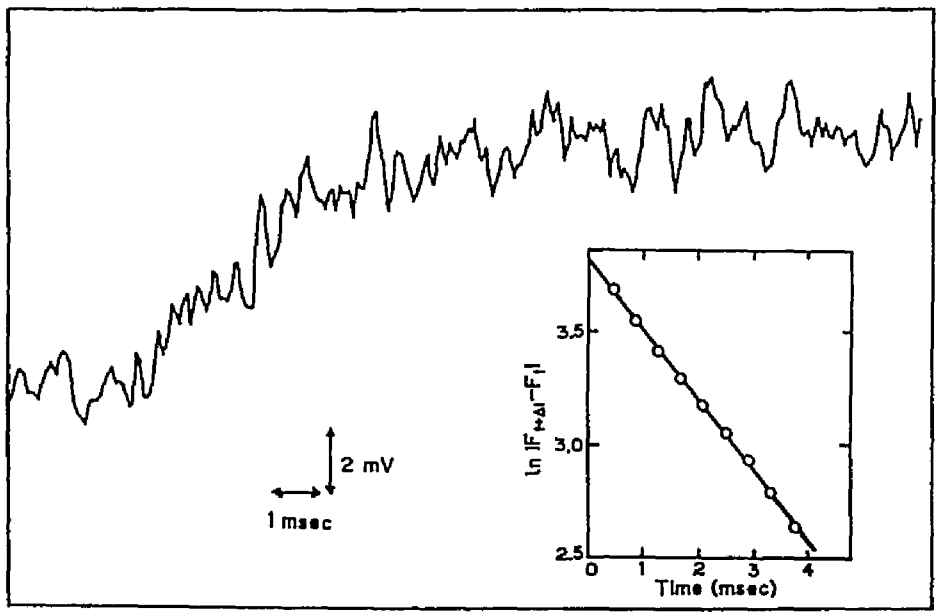

Fig. 1-6. A typical reaction curve for the EI complex formation under the apparent first-order condition, $[I]_0 \gg [E]_0$. Fluorescence change was monitored with a cutoff filter at 310 nm. Excitation wavelength at 280 nm, pH 7.0, 25 ℃. $[SSIM73I]_0$ = 70 μM; [subtilisin BPN']$_0$ = 15 μM. The curve was obtained by accumulation and averaging of 12 reaction curves. Inset: Guggenheim plot of the curve, Δt = 3.3 msec.

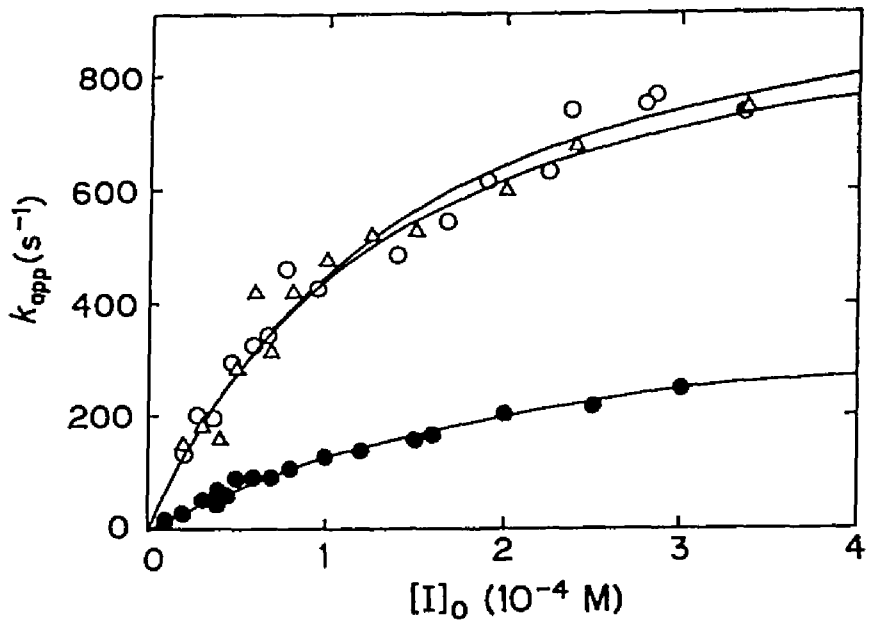

Fig. 1-7. Dependence of the apparent first-order rate constant on the initial concentrations of the inhibitors at pH 7.0, 25 ℃. ○: SSI(wt); △: SSIM73I; ●: SSIM73D. The solid lines are the theoretical curves drawn according to eq. 1-13 with K_L = 1.4X10^{-4} M, k_{+2} = 1100 s^{-1}, and k_{-2} = 0 for SSI(wt); with K_L = 1.3X10^{-4} M, k_{+2} = 1020 s^{-1}, and k_{-2} = 0 for SSIM73I; with K_L = 2.5X10^{-4} M, k_{+2} = 440 s^{-1}, and k_{-2} = 0 for SSIM73D.

Two relaxation times may be expected and the reciprocal of the slower relaxation time, designated by k_{app}, can be expressed under the condition that $[I]_0 \gg [E]_0$ as follows:

$$k_{app} = \frac{k_{+2}[I]_0}{[I]_0 + K_L} + k_{-2} \qquad (1\text{-}13)$$

where K_L is the dissociation constant of the loosely bound complex $(EI)_L$,

$$K_L = \frac{[E][I]}{[(EI)_L]} = \frac{k_{-1}}{k_{+1}} \qquad (1\text{-}14)$$

The concentration dependence of k_{app} shown in Fig. 1-7 is consistent with Eq. 1-13 with $k_{-2} \fallingdotseq 0$. K_L and k_{+2} were

calculated according to Eq. 1-13 by the nonlinear least-squares method. In the two-step mechanism like this, the overall dissociation constant (equal to the inhibitor constant, K_i) is expressed as Eq. 1-15:

$$K_i = K_L \times \frac{1}{1+(k_{+2}/k_{-2})} \qquad (1\text{-}15)$$

By using the values of K_L and k_{+2} calculated above and K_i values of Table 1-1, we estimated k_{-2} values. And k_{on} was also calculated from the equation $k_{on} = k_{+2}/K_L$ (1-16). All the values at pH 7.0, 25℃ obtained for SSI(wt), SSIM73I, and SSIM73D are listed in Table 1-3. There is no essential difference in K_L and k_{+2} between SSI(wt) and SSIM73I; however, k_{-2} of SSIM73I is 15 times larger than those of SSI(wt). On the other hand, for SSIM73D, K_L is about twice and k_{+2} is 40% of that of SSI(wt). The k_{on} values calculated by Eq. 1-16 show good agreement with that obtained under the slower binding conditions with the enzyme activity as probe (Table 1-1).

DISCUSSION

In measuring the interaction between an enzyme and a proteinaceous inhibitor, it is preferable to detect direct signals accompanying the binding such as difference absorption or fluorescence. However, the magnitude of these signals is usually small, and therefore measurement at high protein concentration is necessary. Under these conditions, the reaction is fast, and it has to be measured by a method with a rapid response, such as stopped-flow apparatus. On the other hand, the use of the more sensitive enzyme

TABLE 1-2: Equilibrium and kinetic parameters for the binding of S-BPN' and inhibitors, at pH 8.6, 25 ℃.

SSIs	K_i (10^{-11}M)	k_{on} (10^6/M·s)	k_{off} (10^{-4}/s)	k_{off}/k_{on} (10^{-11}M)
SSI(wt)	1.0(± 0.3)	4.8(±0.1)	1.0(±0.3)	2.0(± 0.7)
Met73Glu	37 (± 3.2)	0.59(±0.02)	1.9(±0.4)	32 (± 7.9)
Asp	95 (±11.7)	0.37(±0.01)	3.0(±0.6)	81 (±18.4)

activity as probe allows measurement at low enzyme concentration, in which the reaction is much slower. There have been many kinetic studies of tight binding inhibitors in which enzyme activity was used as probe (3,37,38). In addition, the treatment proposed in this paper has made it possible to determine the values of k_{on} and k_{off} independently from one reaction curve, and has facilitated the study of precious inhibitor samples.

The k_{on} value obtained by the present treatment for SSI(wt) and subtilisin BPN', 6.5(±0.1)X10^6 $M^{-1}s^{-1}$, is the same as that obtained by the stopped-flow method with fluorescence change as probe (39). All values of k_{on} (Table 1-1) are close to, but a little larger than, those (k'_{on} in Table 1-1) obtained conventionally with Eq. 1-11, in which k_{off} was neglected. The k_{off} value obtained by the present treatment for the wild type, 0.9(±0.2)X10^{-4} s^{-1}, is almost the same as that obtained by the conventional method (1.6(±0.1)X10^{-4} s^{-1}; k'_{off} in Table 1-1). The values of k_{off}/k_{on} are close to the K_i values obtained by the equilibrium analysis as in Fig. 1-1 except for the cases of Asp, His, and Leu mutants (Table 1-1), the reason for which is not clear.

SSIM73I exhibits the weakest inhibition at pH 7.0 among the P_1 mutants tested. This may be due to the steric

TABLE 1-3: Equilibrium and kinetic parameters for the two-step binding mechanism of S-BPN' and inhibitors, at pH 7.0, 25 ℃.

SSIs	K_L (10^{-4}M)	k_{+2} (/s)	k_{-2} (10^{-4}/s)	k_{on} (10^6/M·s)
SSI(wt)	1.4(±0.2)	1100(±70)	1.4(±0.3)	7.8(±1.9)
Met73Ile	1.3(±0.2)	1020(±85)	22.0(±0.5)	7.9(±2.2)
Asp	2.5(±0.2)	440(±30)	1.1(±0.2)	1.8(±0.2)

hindrance of the β-branched side chain of Ile with the P_1 binding pocket of subtilisin BPN'; the valine mutant also has weaker inhibitory activity. The difference in the K_i values between SSI(wt) and SSIM73I was found to be largely due to the difference in dissociation rate constant, k_{off} (Table 1-1). That the increase in K_i is accounted for by the increase of k_{off} was also reported for the binding of SSI with α-chymotrypsin and subtilisin BPN' (40); ovomucoid third domain with serine proteinases (26); and barley chymotrypsin inhibitor 2 with subtilisin BPN' and chymotrypsin (27).

SSIM73E and SSIM73D also have lower inhibitory activity (Table 1-1), and this effect of P_1 substitution by acidic residues is more pronounced in the basic pH region (Fig. 1-2). The isoelectric point, pI, of SSI(wt) is 4.3 (20), and glutamic and aspartic acid residues, must have a fully negative charge in this pH range. Therefore, the effect of pH the binding of these recombinant SSI's in this region is likely to be due to proton dissociation on the enzyme side. A model peptide substrate with Glu at the P_1 position was a poor substrate of subtilisin BPN', and electrostatic repulsion between Glu156 of the enzyme and the P_1 Glu residue was shown partly to account for its low preference

for this substrate (41). However, it is unlikely that the repulsion between these two Glu residues would cause the present pH dependence of K_i of SSIM73E in this pH range. On the other hand, the pI of subtilisin BPN' is 7.8 (42), and this may be partly related to the pH effect here in question. The differences in K_i values of SSIM73D and SSIM73E at pH 8.6 are found to be largely due to the difference in the association rate constant, k_{on} (Table 1-2), in contrast to the case of SSIM73I. Therefore, in the cases of SSIM73D and SSIM73E, repulsion between the like net charges of the two proteins may be a cause of the decrease in the binding rate constant, which results in the larger inhibitor constant, K_i, in the alkaline pH region. Between these two mutants, SSIM73D has lower affinity to subtilisin BPN' than does SSIM73E (Fig. 1-2), and the kinetic analysis shows that this difference stems from both k_{on} and k_{off} (Table 1-2).

The standard free energy change of binding of subtilisin BPN' and the inhibitors, ΔG^0 (= $2.303RT\log K_i$), where R is the gas constant and T the absolute temperature, are -14.7, -13.9, -13.9, and -13.1 kcal mol^{-1} for SSI(wt), SSIM73E, SSIM73D, and SSIM73I, respectively, at pH 7.0. The free energy level of the subtilisin BPN'-SSI complex is thus in the order of SSI(wt) < SSIM73E = SSIM73D < SSIM73I. These complexes are assumed to exist as Michaelis complexes, as has been elucidated for the wild-type complex by X-ray crystallographic analysis (12-13) and NMR study (14).

The free energy of activation for the association of subtilisin BPN' and the inhibitor, $\Delta G^{\ddagger}_i$ (= $2.303RT\{\log(k_BT/h) - \log k_{on}\}$), where k_B is Boltzmann's constant and h, Planck's constant, are 8.16,

8.89, 8.92, and 8.18 kcal mol^{-1} for SSI(wt), SSIM73E, SSIM73D, and SSIM73I, respectively. Therefore, it can be assumed that the free energy level of the transition state of association for subtilisin BPN' and SSIM73I is close to that of the wild-type complex, whereas those for SSIM73D and SSIM73E are higher than that of the wild type.

In this regard, it should be worth analyzing this binding process of the recombinant SSIs with rapid reaction kinetics. A two-step mechanism (Eq. 1-12) in which a fast bimolecular process for the formation of a loosely bound intermediate is followed by a slower unimolecular step has been proposed for the interaction of SSI(wt) and subtilisin BPN' (39). A similar plot of k_{app} against inhibitor concentration was obtained for SSIM73I and SSI(wt) (Fig. 1-7) indicating similar values of K_L and k_{+2} for the two SSIs (Table 1-3). The k_{-2} of SSIM73I was calculated to be 2.2×10^{-3} s^{-1} from Eq. 1-15, which is considerably larger than that of SSI(wt). These results suggest that, like SSI(wt), SSIM73I binds with subtilisin BPN' in the fast bimolecular process to make a loose complex, but that the tight complex of SSIM73I and subtilisin BPN' is less stable than that of SSI(wt). The β-branched side chain of Ile seems to prevent the residue from fitting tightly into the S_1 pocket of subtilisin BPN'. The relationship between k_{app} and SSIM73D concentration was different from that of SSI(wt) (Fig. 1-7). The larger value of K_L of SSIM73D represents the instability of the loose complex. There is also a difference in the slower unimolecular step: the smaller k_{+2} indicates difficulty in isomerization, and a possible explanation for this may be repulsion between the negative charges on Asp at the P_1 residue and Glu156 in the

S_1 pocket of subtilisin BPN'.

I have investigated the effects of replacement of the P_1 residue of a protein proteinase inhibitor, SSI, on its interaction with subtilisin BPN'. Kinetic analysis has revealed the significance of the P_1 side chain in the tight binding of SSI and subtilisin BPN' and given us a glimpse of the detailed mechanism of specific interaction between the two proteins.

Chapter 2

Identification of amino acid residues responsible for the changes of absorption and fluorescence spectra on the binding of subtilisin BPN' and *Streptomyces* Subtilisin Inhibitor

Streptomyces subtilisin inhibitor (SSI) is a proteinaceous proteinase inhibitor purified from the culture filtrate of *Streptomyces albogriseolus* S-3253, which strongly inhibits alkaline serine proteinases such as subtilisin BPN'. The specific interaction of subtilisin BPN' and SSI, is a suitable model not only of protein-protein interaction but also of enzyme-substrate interaction. SSI is a stable homodimer and one mole of SSI dimer binds with two moles of subtilisin BPN' to form a complex of molecular weight of 78000 (18). Crystallographic studies revealed that nine amino acid residues flanking the reactive site (Met73-Val74) of SSI make close contact with subtilisin BPN' (12). An ultraviolet absorption difference spectrum characteristic of protonation of tyrosyl residues was observed on the binding of subtilisin BPN' and SSI at alkaline pH (pH 9-10.2) (43). This difference spectrum provides a good probe for examining the specific interaction of these two proteins. The effect of pH on the magnitude of this difference spectrum implies that this change corresponds to the shift of pK_a of a tyrosyl residue from 9.7 to $\geqq$ 11.5; and the pK_a-shift is thought to result from an electrostatic interaction, because the characteristic spectrum was diminished at high ionic strength (0.6 M) (43). The interaction of tyrosyl

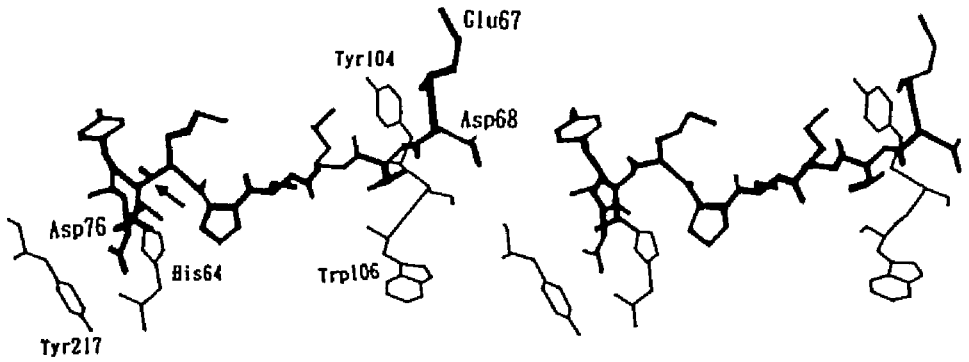

Fig. 2-1. The SSI-subtilisin BPN' interface. Chain segments of SSI are drawn in bold lines and marked by larger characters while those of subtilisin are drawn in thin lines. The scissile bond of SSI (between Met73 and Val74) is indicated by an arrow.

residue(s) of subtilisin BPN' and carboxyl group(s) of SSI was suggested by chemical modification study (43). From crystallographic study of the subtilisin BPN'-SSI complex (12), the interacting tyrosyl-carboxyl pair was suggested to be either Tyr217 (enzyme) and Asp76 (SSI) or Tyr104 (enzyme) and Asp68 (or Glu67) (SSI) (43) (Fig. 2-1). On the other hand, tryptophan fluorescence at 340 nm (excited at 280 nm) was found to increase on the binding of subtilisin BPN' and SSI, and the increase was pH-dependent at pH 7-11 (44). The tryptophan residue has been speculated to be Trp106 of subtilisin BPN' because no fluorescence change was observed on the binding of SSI and subtilisin Carlsberg, in which the amino acid residue corresponding to position 106 is Gly (45).

In this chapter, the interaction of subtilisin BPN' and SSI was studied to identify the residues causing the ultraviolet absorption difference spectrum and the fluorescence change on the formation of the enzyme-inhibitor complex by using natural and artificial mutants of SSI and an artificial mutant of subtilisin BPN' made by cassette and

site-directed mutagenesis.

MATERIALS AND METHODS

Materials - subtilisin BPN' (EC 3.4.21.14) (lot No. 7370935) (subtilisin BPN' wild type (S-BPN'(wt))) and SSI (SSI wild type (SSI(wt))) was prepared as described in Chapter 1. Mutant SSIs (SSIE67Q, SSID68N, SSIE67Q/D68N, and SSIE67G/D68G) were made by cassette mutagenesis as described below and purified from the culture media by the method described previously (28), except that DEAE-cellulose chromatography (20 mM Tris-HCl buffer at pH 7.2) was replaced by QAE-Toyopearl chromatography (25 mM borate KCl buffer at pH 9.4). A subtilisin BPN' mutant S-BPN'Y104F was made by site-directed mutagenesis as described below, and purified as follows. The Bacillus transformant was cultured for 24 h in LB medium with 20 μg/ml of tetracycline at 37°C. Culture supernatants were dialyzed against 10 mM acetate buffer, pH 5.0, containing 1 mM $CaCl_2$. The dialyzate was subjected to DEAE-cellulose column chromatography followed by CM-Cellulofine column chromatography. The enzyme was eluted with a linear concentration gradient of NaCl (0~0.4 M), dialyzed against distilled water, and lyophilized. The mutation was also confirmed by amino acid analysis of the products.

A mutant SSI, SSIW86H (46), in which Trp86 was replaced by His, was a gift from Prof. K. Akasaka of Kobe University. Plasminostreptin (47), API-2c' (48), and a mutant SSI, SSID76A, in which Asp76 was replaced by Ala were gifts from Prof. M. Kainosho of Tokyo Metropolitan University.

The protein concentration was determined

spectrophotometrically at pH 7.0 using A_{276}(1 mg/ml) = 0.829 for SSI and A_{278}(1 mg/ml) = 1.063 for subtilisin BPN' (18) and 1.014 for S-BPN'Y104F. Molecular weights of SSI (monomer) and subtilisin BPN' are 11500 (18-19) and 27500 (30), respectively. SSI concentration in the text is represented as monomer concentration unless otherwise mentioned. The concentration of active enzyme was determined to be 75% for S-BPN'(wt) by the initial burst titration with N-trans-cinnamoylimidazole (32), and 88.3% for S-BPN'Y104F from the titration with SSI. The enzyme activity (k_{cat}/K_m) of S-BPN'Y104F was 40% of that of S-BPN'(wt) at pH 9.8, 25℃. All enzyme solutions were prepared fresh before use.

Cassette mutagenesis of SSI gene - The SSI gene from Streptomyces albogriseolus S-3253 was cloned and expressed in S. lividans 66 as described previously (15-16). The mutations of Glu67 to Gln (SSIE67Q) and Asp68 to Asn (SSID68N), and the double mutations of Glu67 and Asp68 to Gln and Asn, respectively (SSIE67Q/D68N), and Glu67 and Asp68 to Gly (SSIE67G/D68G), were performed by cassette mutagenesis (50). Initially, a plasmid pSISXΔA was constructed by inserting a SmaI-XbaI fragment encoding a mature SSI into the SmaI-XbaI site of pUC18ΔA lacking an AatII site (51). The MluI site was created at the position Leu63 of SSI in the pSISXΔA by site-directed mutagenesis using a mutagenic primer, 5'TG-AAC-GCG-TTG*-ACG-CGG 3', where the asterisk indicates the mismatched base. The resulting plasmid pSISXΔA-M was digested with MluI and AatII, and a larger fragment was isolated. Two oligodeoxyribonucleotides, 5'C-GCG-CTG-ACG-CGG-GGC-(C,G)AG-(G,A)AC-GT

3' and 5'(C,T)-CT(G,C)-GCC-CCG-CGT-CAG 3', were designed to introduce the mutations Glu67 to Gln and Asp68 to Asn, and Glu67 and Asp68 to Gln and Asn, respectively. The oligodeoxyribonucleotides were annealed after phosphorylation of 5'-termini. The annealed DNA and the digested fragment were ligated and transferred into E. coli. The mutated plasmids were identified by colony hybridization using as probes 5'CG-CGG-GGC-CAG-GAC-GTC 3' for Glu67 to Gln, 5'GG-GGC-GAG-AAC-GTC-ATG 3' for Asp68 to Asn, and 5'G-CGG-GGC-CAG-AAC-GTC-AT 3' for Glu67 and Asp68 to Gln and Asn, respectively. For mutation of Glu67 and Asp68 to Gly, the Nsp I site was introduced at the position Val69 in the plasmid pSISXΔA-M by site-directed mutagenesis using a mutagenic primer 5'C-GAG-GAC-GAC-ATG-TGC-C 3', where the asterisk indicates the mismatched base. The mutated plasmid pSISXΔA-MN was digested with Nsp I and Xho I, followed by isolation of the fragment of 110 bp. A 2.9-kbp Mlu I-Xho I fragment was isolated from pSISXΔA-M after digestion with Mlu I and Xho I. Two oligodeoxyribonucleotides, 5' C-GCG-CTG-ACG-CGG-GGC-GGC-GGC-GTC-ATG 3' and 5' AC-GCC-GCC-GCC-CCG-CGT-CAG 3' were annealed after phosphorylation of 5'-termini, and ligated with two fragments isolated from the plasmids. Mutations were verified by dideoxy sequencing (52) of the mutated plasmid. After the construction of the mutated pSISXΔA, mutated SSI genes were inserted into a streptomycete plasmid pIJ702, followed by transformation of S. lividans 66 as described previously (28).

Site-directed mutagenesis of subtilisin BPN' gene - Subtilisin BPN' gene from Bacillus amyloliquefaciens was cloned as two fragments divided at the center of the gene,

based on the published sequences (53-54). The 1.5-kbp SmaI-ClaI fragment of the amino-terminal portion and the 1.1-kbp ClaI-HindIII fragment of the carboxy-terminal portion were inserted in the SmaI-AccI site and the AccI-HindIII site of pUC18 using 5'TCA-CAA-ATT-AAA-GCC-CCT-GC 3' and 5' ATC-GCA-AAC-AAT-ATG-GAC-GTT-ATT-AA 3' as probes, respectively. The ClaI site was regenerated at the AccI-ClaI junctions of these plasmids by site-directed mutagenesis to produce plasmid pSUB-N, which contains the amino-terminal portion, and pSUB-C, which contains the carboxyl-terminal portion. A 280-bp DraI fragment encoding Tyr104 was then isolated from pSUB-C and inserted into the SmaI site of pUC18 to obtain a plasmid pSUB-D. Amino acid substitution of Tyr104 to Phe (S-BPN'Y104F) was carried out by site-directed mutagenesis of the plasmid pSUB-D using a mutagenic primer, 5' C-GGC-CAA-TTC-AGC-TGG-A 3', where the asterisk indicates the mismatched base. After confirmation of the mutation, mutated pSUB-D was digested with NaeI and PvuII. The 110-bp NaeI-PvuII fragment containing the mutation was isolated and ligated with the 2.8-kbp NaeI-HindIII fragment of pSUB-C and the 0.8-kbp PvuII-HindIII fragment of pSUB-C to generate the mutated pSUB-C. The 1.1-kbp ClaI-HindIII fragment containing the mutation and the 1.6-kbp EcoRI-ClaI fragment were isolated from the plasmids and inserted into the EcoRI-HindIII site of a plasmid pHY300PLK (55), an E.coli-B.subtilis shuttle vector. The constructed plasmid was multimerized by E. coli JM101, and B. subtilis UOT0999 (his101, leuA8, nprE18, nprR2, sprEΔ3) was transformed with the resulting plasmid.

Ultraviolet absorption difference spectroscopy - The

ultraviolet absorption difference spectrum observed on the binding between SSI and subtilisin BPN' was examined at pH 9.8 (50 mM carbonate buffer of ionic strength 0.1 M (NaCl)) with a Shimadzu UV-240 or UV-2200 spectrophotometer at 25℃. Two pairs of matched cuvettes with 1.0-cm optical path were used.

K_i determination - The inhibitor constant was determined by the method as descrived in chapter 1.

Fluorescence study - Fluorescence intensity of the SSI-subtilisin BPN' complex was measured at 340 nm with excitation at 280 nm with a Hitachi fluorescence spectrophotometer 850 at 25℃. The following buffers were used for the study of pH dependence of the fluorescence intensity: 25 mM piperazine-N,N'-bis(2-ethnesulfonic acid) buffer for pH 6.0 - 7.5; 50 mM N,N-bis(2-hydroxyethyl) glycine buffer for pH 8.0 - 9.0; 50 mM 3-N-cyclohexylamino-2-hydroxypropane-sulfonic acid buffer for pH 9.4 - 10.7; and 50 mM carbonate for pH 11.0 - 11.3. Ionic strength of the buffer solutions was adjusted to 0.1 M with NaCl.

RESULTS

Ultraviolet absorption difference spectra - Ultraviolet absorption difference spectra were measured on the binding of S-BPN'(wt) with SSI(wt), API-2c', and plasminostreptin at pH 9.8 (Fig. 2-2). API-2c' and plasminostreptin are naturally occurring mutants of SSI, in which Asp68 or Glu67 of SSI are replaced by Gly, respectively (56). Absorbance differences at 245 nm (ΔA_{245}) observed with these inhibitors were smaller than the one obtained with SSI(wt).

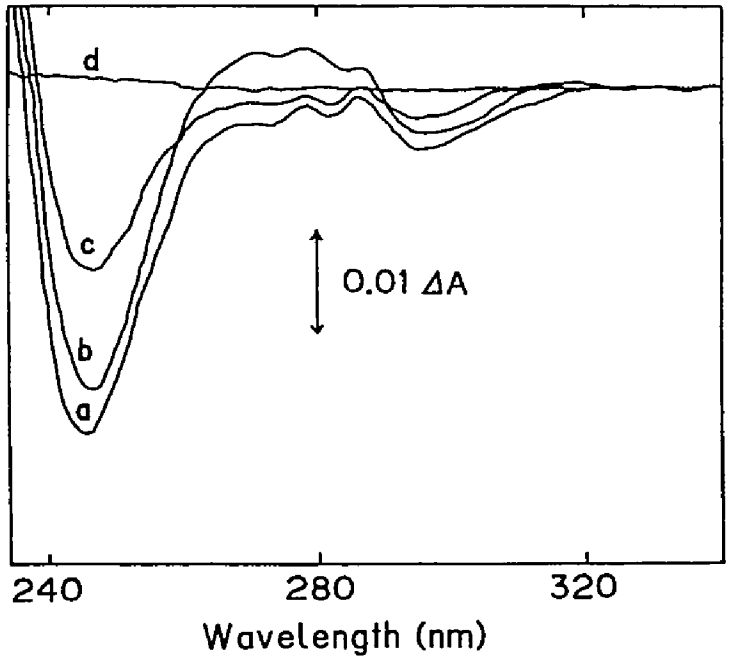

Fig. 2-2. Ultraviolet absorption difference spectra observed on the binding of subtilisin BPN' and SSI family inhibitors. a, SSI (wt); b, plasminostreptin; c, API-2c'; d, base line. Final concentrations of S-BPN'(wt), SSI, plasminostreptin, and API-2c' were 5.9 μM, in 50 mM carbonate buffer, pH 9.9, 24℃.

This suggested that the carboxyl groups of Glu67 and Asp68 participated in the appearance of the difference spectrum and that the tyrosyl residue in question was likely to be Tyr104 of subtilisin BPN'.

Accordingly, I prepared mutant SSIs by cassette mutagenesis in order to delete carboxyl charges on Asp68 and Glu67: SSIE67Q, SSID68N, double mutants SSIE67Q/D68N and SSIE67G/D68G. We also prepared a mutant subtilisin BPN' (S-BPN'Y104F) by site-directed mutagenesis to replace the tyrosyl residue. With the SSI mutants SSIE67Q, SSID68N, SSIE67Q/D68N, and SSIE67G/D68G, ΔA_{245} decreased (Fig. 2-3). In the case of SSIE67G/D68G, ΔA_{245} decreased significantly and the difference spectrum was similar to that obtained with an SSI of which carboxyl groups were

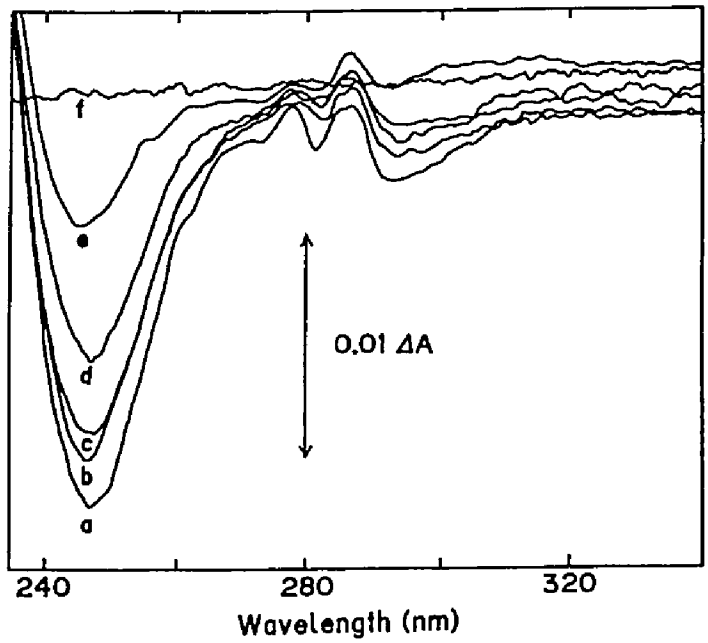

Fig. 2-3. Ultraviolet absorption difference spectra observed on the binding of subtilisin BPN' and mutant SSIs. a, SSI(wt); b, SSIE67Q; c, SSID68N; d, SSIE67Q/D68N; e, SSIE67G/D68G; f, base line. Final concentration of S-BPN'(wt) and SSI were 4 μM and 6 μM, respectively in 50 mM carbonate buffer, pH 9.8, 25°C.

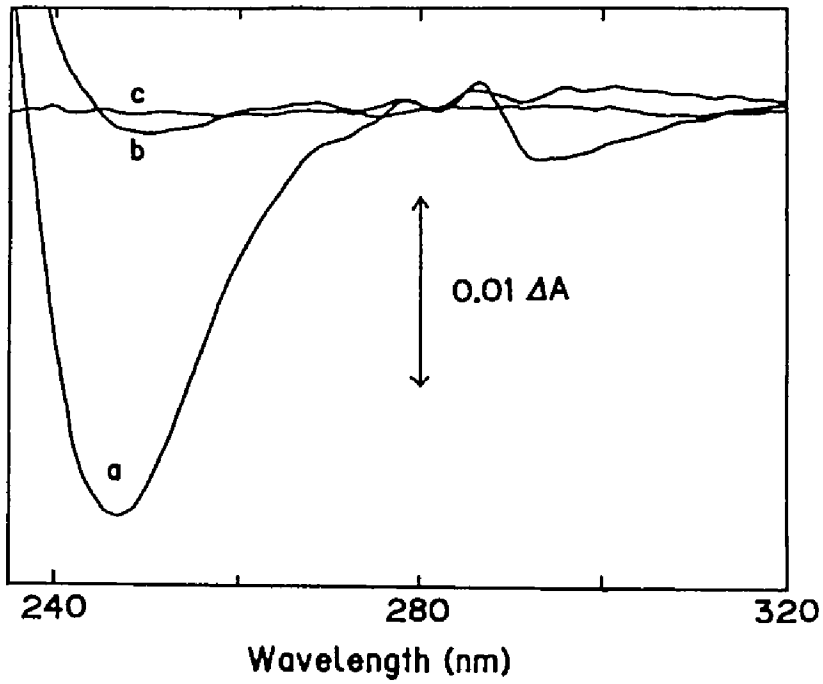

Fig. 2-4. Ultraviolet absorption difference spectra observed on the binding of SSI(wt) and mutant subtilisin BPN'. a, S-BPN'(wt); b, S-BPN'Y104F; c, base line. Final concentration of S-BPN' and S-BPN'Y104F were 4 μM; SSI(wt) was 7 μM in 50 mM carbonate buffer, pH 9.8, 25°C.

chemically modified with glycine methyl ester (43). Figure 2-4 shows the difference spectra on the binding of SSI(wt) with S-BPN'(wt) and S-BPN'Y104F at pH 9.8. The difference spectra completely disappeared on the binding of SSI(wt) and S-BPN'Y104F. It is evident, therefore, that Tyr104 of subtilisin BPN' causes the difference spectrum in the interaction with Glu67 and Asp68 of SSI. The difference spectrum was also examined on the binding of SSID76A and S-BPN'(wt) to elucidate the effect of the interaction of Tyr217 of subtilisin BPN' and Asp76 of SSI. The difference spectrum obtained was the same as that obtained with SSI(wt) and S-BPN'(wt) (data not shown). Accordingly, the possibility of the pK_a-shift of Tyr217 (enzyme) on the interaction with SSI can be ruled out.

Inhibitory activities - The inhibitor constants (K_i) of mutant SSIs toward S-BPN'(wt) and of SSI(wt) toward S-BPN'Y104F at pH 7.0, 25℃ are listed in Table 2-1. Similar K_i values were obtained in all cases. These mutant proteins bind strongly under the conditions of difference spectra measurements, and the interaction between Tyr104 of subtilisin BPN' and carboxyl groups of SSI seems to make little contribution to the intensity of SSI-subtilisin BPN' interaction.

Fluorescence spectra - A fluorescence increase (about 6% at pH 7.0) was observed on the binding of SSI(wt) and S-BPN'Y104F, similar to that on the binding of SSI(wt) and S-BPN'(wt) (data not shown). The effect of pH on the magnitude of the fluorescence increase was studied in the pH range 6.0-11.0 (Fig. 2-5). For the binding of SSI(wt) and S-BPN'(wt), the fluorescence increase was pH-dependent with pK_{app} 9.3, confirming the previous results (44), whereas

TABLE 2-1 Inhibitor constants of subtilisin BPN' and SSI family inhibitors at pH 7.0, 25℃.

Enzyme	Inhibitor	K_i (10^{-11} M)
S-BPN'(wt)	SSI(wt)	1.8(±0.3)
	Plasminostreptin	2.8(±0.8)
	SSIE67Q	3.0(±0.6)
	SSID68N	4.0(±0.5)
	SSID67Q/E68N	2.7(±0.6)
	SSID67G/E68G	1.9(±0.9)
	SSID76A	1.7(±0.7)
	SSIW86H	2.7(±0.9)
S-BPN'Y104F	SSI(wt)	2.6(±0.6)

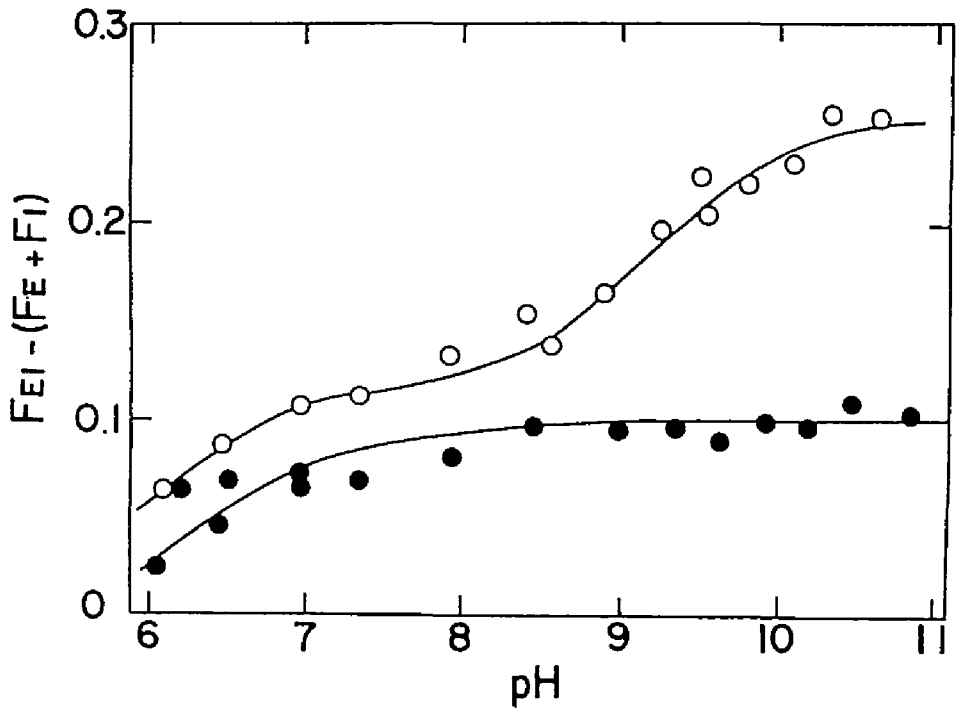

Fig. 2-5. Effect of pH on the fluorescence change observed on the binding of SSI(wt) and mutant subtilisin BPN'. (○), S-BPN'(wt); (●), S-BPN'Y104F. Emission at 340 nm with excitation at 280 nm at 25℃. Final concentration of all protein species employed was 0.4 μM. The solid lines are theoretical curves calculated with pK_{app} values of 6.0 and 9.3 for S-BPN'(wt) and 6.4 for S-BPN'Y104F. The vertical axis shows the direct reading of the instrument, and 0.1 corresponded to the fluorescence intensity of 0.4 μM acetyl-L-tryptophan-methyl-ester at pH 7.0, 25℃

the pH-dependence disappeared almost completely in the case of SSI(wt) and S-BPN'Y104F.

SSI has only one tryptophan residue in the subunit, Trp86, and it has been reported that its fluorescence is quenched under normal conditions (57). To examine the possibility that the fluorescence increase observed on the interaction of SSI and S-BPN' might be caused by Trp86 of SSI, the fluorescence change was measured with an SSI mutant, SSIW86H, in which Trp86 was replaced by His. A similar fluorescence increase was observed to that with SSI(wt) (data not shown). These results indicate that the tryptophan residue responsible for the increase is in the subtilisin BPN' molecule and not Trp86 of SSI.

DISCUSSION

Ultraviolet absorption difference spectra - The ultraviolet absorption difference spectrum observed on the binding of SSI and subtilisin BPN' at alkaline pH (Fig. 2-2 a) is typical of a change in ionization state of a tyrosyl residue (43). The amino acid residues responsible for the difference absorption were sought by using mutant proteins.

The possibility that the interacting amino acid pair consisted of either Tyr217 (enzyme) and Asp76 (SSI) or Tyr104 (enzyme) and Asp68 (or Glu67) (SSI) was suggested by chemical modification study (43) and crystallographic study of the subtilisin BPN'-SSI complex (12). The ultraviolet absorption difference disappeared on the binding of S-BPN'Y104F and SSI(wt) (Fig. 2-4), which clearly indicates the latter pair. This indication is supported by the

evidence that the difference spectra observed on the interaction of subtilisin Carlsberg (in which Tyr217 of subtilisin BPN' is replaced by Leu) with SSI (58) and on the binding of S-BPN'(wt) with SSID76N were almost identical with that of S-BPN'(wt) and SSI.

This led me to wonder which residue of SSI would cause the pK_a shift of Tyr104 of subtilisin BPN'. There are two naturally occurring mutants of SSI, API-2c' and plasminostreptin, whose sequence homology to SSI is 90% and 68%, respectively, and in which Asp68 and Glu67 of SSI are respectively replaced by Gly (56). The smaller difference absorption spectra observed on the binding of these mutants and S-BPN'(wt) (Fig. 2-2) suggested that these acidic residues of SSI are both responsible for the difference spectra.

That the absorbance difference decreased but did not completely disappear on the binding of S-BPN'(wt) with SSIs with a single mutation at position 67 or 68 (Fig. 2-3), also suggested the participation of both Glu67 and Asp68. However, the difference spectrum was also observed on the binding of S-BPN'(wt) and the doubly mutated SSIE67Q/D68N (Fig. 2-3, d). It was revealed that the presence of a negatively charged residue was not essential to cause the pK_a shift of Tyr104 (enzyme). The smaller ΔA_{245} values obtained with these mutant SSIs would mean smaller pK_a shifts than with SSI(wt). These difference spectra may be due to hydrogen bonding between the amide group(s) of glutamine and asparagine of mutant SSI and phenolic group of Tyr104 of subtilisin BPN'.

The difference spectrum was observed even on the binding of S-BPN'(wt) and SSIE67G/D68G, although ΔA_{245} was only

34% of that obtained with SSI(wt) (Fig. 2-3 e). The formation of a hydrogen bond with an H_2O molecule in the hydrophobic environment, and an effect of distant charged group(s) of SSI could be the cause of this pK_a shift of Tyr104. Tyr104 is located at the hydrophobic S_4 pocket of S-BPN' and moves with binding of a substrate (59) or SSI (12-13). The phenolic hydroxyl group would be unstable in the deprotonated form in the hydrophobic S_4 pocket at the interface of the enzyme-inhibitor complex. It was reported that Tyr104 of subtilisin Carlsberg formed a hydrogen bond with the carbonyl oxygen of the main chain of a proteinase inhibitor, eglin C (24). However, X-ray crystallographic analysis (12-13) suggests that such hydrogen bonding is very unlikely in the case of S-BPN'(wt) and SSI(wt).

Fluorescence spectra - A small increase (about 6% at pH 7.0) in fluorescence intensity was detected at 340 nm with excitation at 280 nm on the binding of subtilisin BPN' and SSI, and this change originated from tryptophan residue(s) (44). No fluorescence change was observed on the binding of SSI and subtilisin Carlsberg, which has Gly at position 106 as compared with Trp in subtilisin BPN' (44). Therefore, the Trp in question is in the enzyme molecule, and it is probably Trp106 of subtilisin BPN' (45). The observation of a similar fluorescence change on the binding of SSIW86H and S-BPN'(wt) supports this interpretation.

The fluorescence change was also observed on the binding of SSI(wt) and S-BPN'Y104F at neutral pH (Fig. 2-5). However, the pH-dependence of the fluorescence increase in the alkaline region disappeared in this case, suggesting the effect of the electrostatic charge of Tyr104 on the fluorescence. The fluorescence intensity of free subtilisin

BPN' (F_E) decreased at alkaline pH with an apparent pK_a of 9.3, probably because of the effect of the tyrosyl residue; but Tyr104 was protonated in this pH range in the subtilisin BPN'-SSI complex because of the pK_a-shift described above, and the fluorescence intensity of the complex (F_{EI}) did not change. The apparent increase of fluorescence shown in Fig. 2-5 is the difference between the fluorescence intensity of subtilisin BPN'-SSI complex and those of free subtilisin BPN' and free SSI [$F_{EI} - (F_E + F_I)$]. We observed that the fluorescence of free SSI (F_I) was pH-independent in this pH region. Accordingly, the pH-dependence of the apparent fluorescence increase with pK_a 9.3 was obtained.

The specific interaction between SSI(wt) and subtilisin BPN'(wt) was studied by using the difference absorption spectrum and the fluorescence increase as probes. The dissociation constant was determined by directly measuring the fluorescence change on the binding of SSI and subtilisin BPN' (44). These spectroscopic probes were also useful in kinetic analysis by the stopped-flow method. The association rate constant of SSI(wt) with subtilisin BPN' was determined to be about 3×10^6 $M^{-1}\cdot s^{-1}$ by monitoring directly the difference spectrum ΔA_{245} or the fluorescence change at alkaline pH (39,58). These results suggested that the changes of state of both the tyrosine and the tryptophan residue occur at the same stage of the binding of SSI and subtilisin BPN'. Now, I have assigned the tyrosyl residue to Tyr104 and the tryptophanyl residue probably to Trp106 of subtilisin BPN'. This enables us to interpret more clearly the fluorescence behavior. These spectroscopic signals reflect the specific, local structural changes on the binding of the inhibitor and the enzyme. They should be

useful for the detailed interpretation of the mechanism of interaction between SSI and subtilisin BPN'.

Chapter 3

Equilibrium constants K_{hyd} for the hydrolysis of the reactive-site peptide bond of Streptomyces subtilisin inhibitor (SSI)

Proteinaceous proteinase inhibitors inhibit target proteinase although it is protein itself. The interaction between a protein proteinase inhibitor and a proteinase has drawn much attention as a model of the mechanism of proteolysis as well as protein-protein interaction. Most of the well studied serine proteinase inhibitors are proposed to obey "the standard mechanism" (3) represented as Eq. 3-1:

$$E + I \rightleftharpoons C \rightleftharpoons E + I^* \qquad (3\text{-}1)$$

where E is the enzyme and C is the stable complex between enzyme and inhibitor. I is the intact inhibitor and I* is the modified inhibitor whose reactive site peptide bond is hydrolyzed. The incubation of inhibitors with catalytic amounts of proteinases which have a mutual affinity leads to the equilibrium of hydrolysis of the reactive site, which can be characterized by the equilibrium constant K_{hyd}:

$$K_{hyd} = \frac{[I^*]}{[I]} \qquad (3\text{-}2)$$

where [I] and [I*] are the moler concentrations of free intact inhibitor and free modified inhibitor, respectively. Since Niekamp et al. (60) reported the equilibrium of hydrolysis of soybean trypsin inhibitor, this constant has been studied for several protein serine proteinase inhibitors (61-65).

Streptomyces subtilisin inhibitor (SSI) inhibits strongly bacterial alkaline serine proteinases such as subtilisin BPN'. It has been suspected that the interaction between SSI and subtilisin BPN' corresponds to the Eq. 3-1. In the

present chapter the equilibrium of hydrolysis of SSI with catalytic amount of subtilisin BPN' and the pH dependence of K_{hyd} were investigated.

MATERIALS AND METHODS

Proteins - SSI and subtilisin BPN' (EC 3.4.21.14) (lot No.7370935) were prepared as described in Chapter 1. Modified SSI, designated as SSI*, in which the reactive site bond, Met73-Val74, was cleaved enzymatically was prepared by the method of Tonomura (66): A complex of subtilisin BPN' and SSI isolated by gel filtration at pH 7.0 was subjected to pH jump to pH 2.7 at 0°C. After incubation at pH 2.7, 0°C for 2 h, the pH of the solution was brought to neutral and SSI* was isolated by QAE-Toyopearl chromatography at pH 9.4 with following lyophilization.

The protein concentration was determined spectrophotometrically as described in Chapter 1. All SSI concentration in the text is represented as subunit concentration unless otherwise mentioned.

K_{hyd} determination - In order to examine the effect of enzyme amount, SSI or SSI*, each concentration 60 μM, were incubated with 20 ~ 60 mol% enzyme in 50 mM citrate buffer containing 0.02% NaN_3, I = 0.1 (NaCl) at pH 7.5, room temperature. 10 μl of the incubation mixture at appropriate time was subjected to PAGE.

The K_{hyd} values were obtained at various pH under the conditions as follows: $[I]_0$ = 83 μM, $[E]_0$ = 41.5 μM at pH 3.0, 3.2, and 3.5; $[I]_0$ = 100 μM, $[E]_0$ = 50 μM at pH 3.1, 3.3, 3.4 ,3.8, and 4.2; $[I]_0$ = 100 μM, $[E]_0$ = 30 μM at pH 4.1; $[I]_0$ = 40 μM, $[E]_0$ = 4 μM at pH 5.0, 5.5, 6.5, 7.5, 8.5, and 8.5; $[I]_0$ = 43.5 μM, $[E]_0$ = 4.4 μM at pH 4.65 and

7.0; $[I]_0$ = 40 μM, $[E]_0$ = 2 μM at pH 6.0 and 8.0. Buffer was used as follows: 50 mM citrate at pH 3.0 ~ 6.5, and 7.5, 50 mM phosphate buffer at pH 7.0, 50 mM Tris-HCl buffer at pH 8.0, and 50 mM H_3BO_3 buffer at pH 8.5 ~ 9.5. Each buffer contains 0.02% NaN_3 and I = 0.1 M (NaCl). SSI, SSI*, and the mixture of SSI and SSI* were incubated at room temperature, then subjected to PAGE.

PAGE was carried out with a RESOLMAX-SLAB (ATTO Corporation, Tokyo) system on slab gel (11.2 %) at pH 9.4 and 0 ℃ in ice water (67). Proteins were stained with Coomassie Brilliant Blue R-250 and the density of the bands were measured at 590 nm with a Shimadzu dual-wavelength TLC scanner CS-900. The density of bands was proportional to protein concentration up to 9 μg/band.

RESULTS

Effect of enzyme amount on the equilibrium point - A typical PAGE pattern was shown on Fig. 3-1. There are 6 bands in one lane on PAGE and each bands has been assigned from the top to be E_2I_2 complex, EI_2 complex, EII* complex, SSI dimer, SSI-SSI* hybrid dimer, and SSI* dimer, respectively. Because SSI exists as dimer protein, the PAGE pattern becomes complicated; however, enzyme-inhibitor complexs (E_2I_2, EI_2, and EII*) are ignored to obtain the K_{hyd} value, and the density of lower three inhibitor bands were measured and one half of the middle band (SSI-SSI* hybrid) was regarded as SSI and the other half of that was SSI*.

Figure 3-2 shows the time course of the fraction of SSI* ($\alpha = [I^*]/([I]+[I^*])$), at pH 7.5 under the different enzyme concentration from 20 ~ 60 mol% of inhibitor concentration.

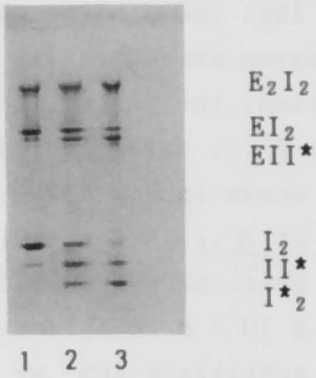

Fig. 3-1. The PAGE profile of the reaction mixture at pH 9.4. Inhibitor solution (40 μM) with 30 mol% of subtilisin-BPN' was incubated for 5 days at pH 8.0, room temperature. The reactions were started at the condition as follows: Lanes a, SSI; b, the mixture of SSI and SSI*; c, SSI*.

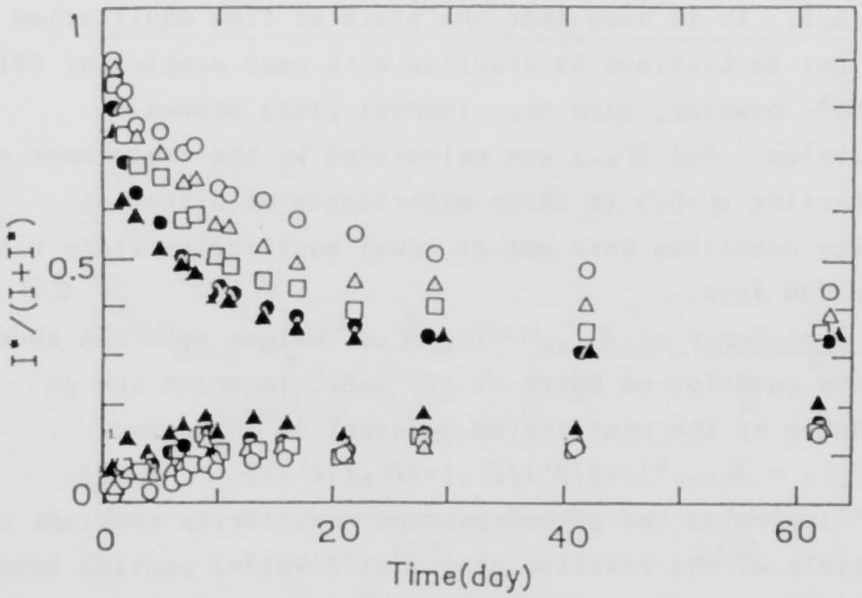

Fig. 3-2 Time course of the fraction α of SSI* at various subtilisin BPN' concentration, at pH 7.5, room temperature. Inhibitor concentration was 60 μM. Starting conditions: α = 0 and 1. ○, [E]/[I] = 0.2; △, [E]/[I] = 0.3; □, [E]/[I] = 0.4; ●, [E]/[I] = 0.5; ▲, [E]/[I] = 0.6.

It could be seen that the similar equilibrium was obtained with different enzyme concentration and that the higher the enzyme concentration, the faster the rate to reach the equilibrium. The K_{hyd} value is independent on the enzyme concentration as shown in Eq. 3-2.

Determination of K_{hyd} - The equilibrium constant K_{hyd} was investigated over the pH range 3.0 ~ 9.5. For this purpose, about 4 X 10^{-5} M inhibitor solutions were incubated with 5 ~ 10 mol% subtilisin BPN' at neutral and alkaline pH, and higher inhibitor concentration and higher enzyme concentration percentage (up to 50%) was chosen at acidic pH because of the unstability of these proteins. Starting conditions were α=0, α=0.5, and α=1.

The principle underlying the investigation of the state of equilibrium is shown in Fig. 3-3. This shows the time course of α at pH 3.3. It took 500 min to reach the equilibrium state. Figure 3-4 shows the time course of α at pH 6.5. It is seen that the state of time equilibrium could not be attained by starting with pure samples of SSI and SSI*, however, each experimental plots showed equilibrium. And K_{hyd} was calculated by the experiment of the starting α=0.5 if three experiments of different starting condition were not at equal equilibrium state with in the 200 days.

pH dependence of K_{hyd} - The K_{hyd} values obtained should obey the equation of Dobry et al. (68), in which the pH dependence of the equilibrium constant is expressed:

$$K_{hyd} = K_{hyd}^{0}\{1+([H^+]/K_1)+(K_2/[H^+])\} \qquad (3\text{-}3)$$

K_{hyd}^{0} indicates the pH-independent equilibrium constant for hydrolysis of the reactive site (Met73-Val74) peptide bond of the SSI, and K_1 and K_2 are the corresponding ionization constants of the carboxyl group of Met73 and the amino group of Val74, respectively.

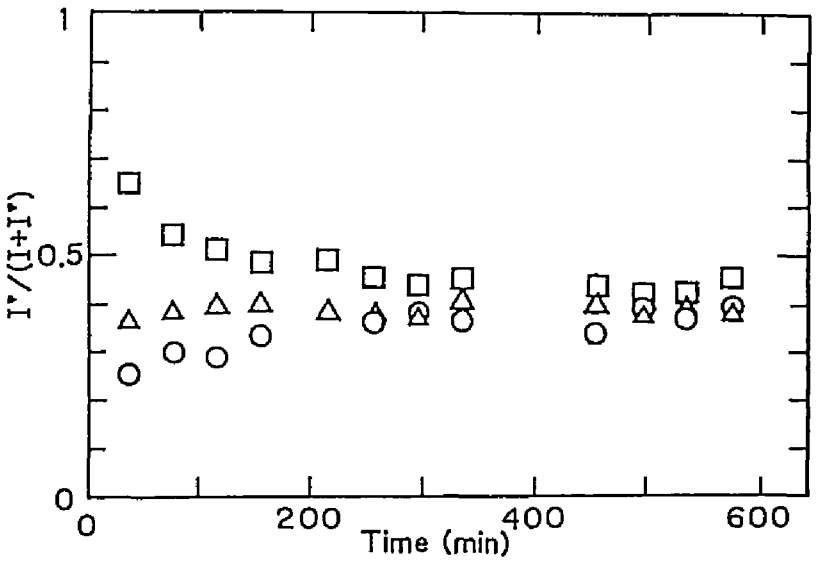

Fig. 3-3. Time course of the fraction α of SSI* at pH 3.5, room temperature. [I] = 42 μM, [E]/[I] = 0.5. Starting conditions: □, α = 1; △, α = 0.5; ○, α = 0.

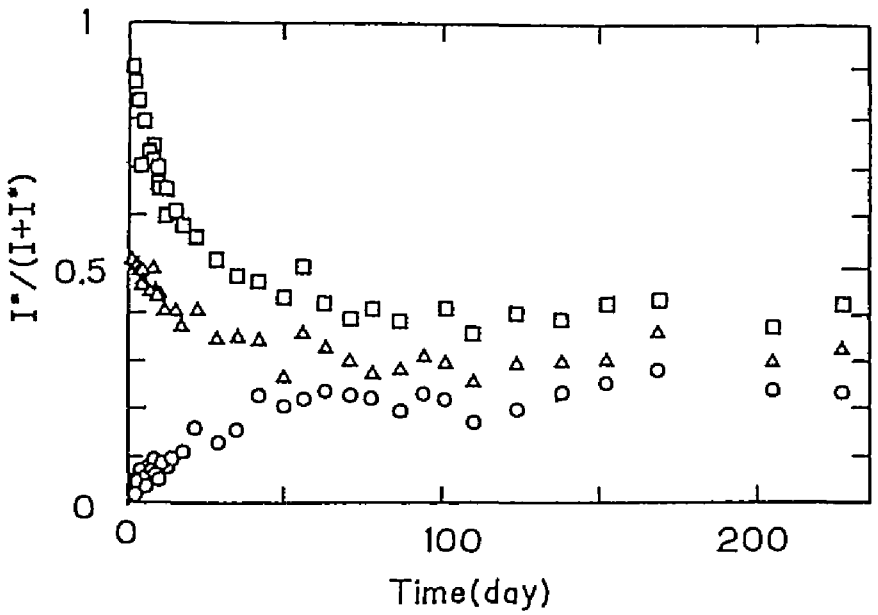

Fig. 3-4. Time course of the fraction α of SSI* at pH 6.5, room temperature. [I] = 44 μM, [E]/[I] = 0.1. Starting conditions: □, α = 1; △, α = 0.5; ○, α = 0.

The K_{hyd} values obtained were fitted to this equation by using non-linear least squares analysis. Figure 3-5 shows the pH dependence of K_{hyd} and the theoretical curve, and fitting parameters were obtained to be K_{hyd}^0 = 0.37; pK_1 = 3.6; pK_2 = 9.0.

Discussion

Protein proteinase inhibitor which obey "the standard mechanism" could still inhibit the enzyme when the reactive site peptide bond has been cleaved. Then the equilibrium constant K_{hyd} is characterized in Eq. 3-2 and includes no item of enzyme. The experiment at several enzyme concentration up to 60 mol% proves that. Smaller proportion of enzyme used may be desirable because the amount of enzyme-inhibitor complex (E_2I_2, EI_2, and EII*) are neglected in the experiment. However, it was difficult to obtain the K_{hyd} value at acidic pH under pH 4.0 because of the unstability of both proteins, and therefore, high proportion of enzyme were used. It took very long time to reach the equilibrium at neutral or alkaline range where subtilisin BPN' has higher activity, whereas it took shorter time at acidic pH, and the reason has not been made clear.

The value of K_{hyd}^0 of SSI is 0.37, that means the intact form is thermodynamically more stable than modified form in the solution at neutral pH. This is an even more dramatic exception to the common facile assumption that hydrolysis of all peptide bonds in proteins proceeds to completion. The value of K_{hyd}^0 STI (Kunitz) and BPTI (Kunitz) are 1.56 (61) and 0.95 (63), respectively and it was regarded that the K_{hyd}^0 value was around unity or larger. That means the modified form is equal to or more stable than the intact

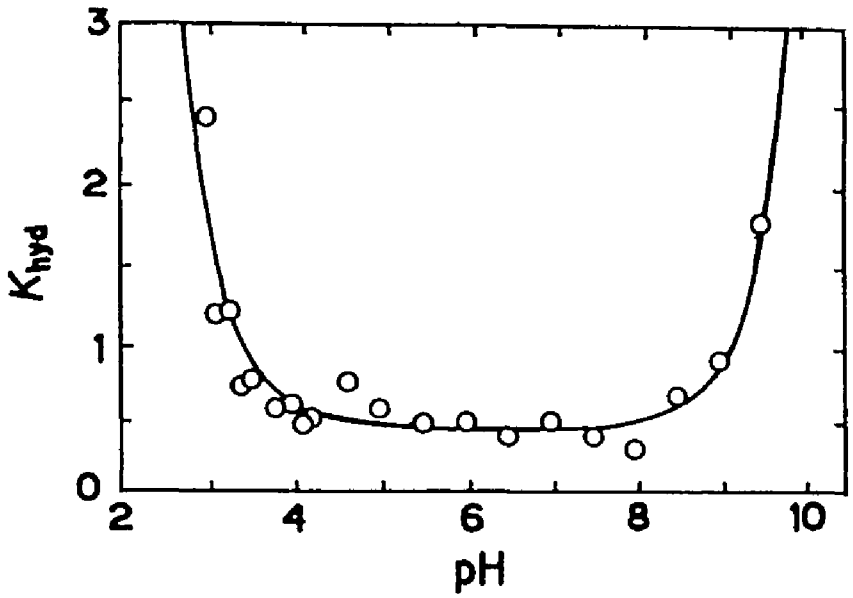

Fig. 3-5. The pH dependence of the equilibrium constant K_{hyd}. The solid line is the theoretical curve drawn according to Eq. 2 with the values: K_{hyd}^0 = 0.37, pK_1 = 3.6, pK_2 = 9.0.

form. However, the low K_{hyd}^0 value has reported about BPSTI (K_{hyd}^0 = 0.25) (62), OMADR3 (K_{hyd}^0 = 0.45), and OMJPQ3 (K_{hyd}^0 = 0.40) (65) which are all classified to Kazal type serine proteinase inhibitor, therefore, smaller K_{hyd} value may be characteristic of Kazal type serine proteinase inhibitor, although Ardelt and Laskowski, Jr. reported that the K_{hyd} value of avian ovomucoid 3rd domain which is classified into Kazal family have wide range from 0.4 to 35 (65). The amino acid sequence around the reactive site of SSI shows good homology (9) to the Kazal type. The reactive site peptide loop is linked by disulfied bond (Cys71 (P_3) - Cys101) to the core and Pro residue (P_4') is also conserved (69). The mutated SSI which does not have this disulfide bond because of the replacement of Cys71 and Cys101 to Ser is digested by subtilisin BPN' (Kojima et al. personal communication), that means the K_{hyd}^0 value is ∞. And the K_{hyd}^0 value of the other mutated SSI in which Pro72 and Pro77 are replaced by Ala was 1.9 as described in

Chapter 5. These results support that these residues contribute to the rigidity of the reactive site peptide loop and low K_{hyd}^0 value. Niekamp et al. (60) have suggested that the value of K_{hyd}^0 will depend upon the extent to which the peptide chain gains freedom and hence rotational entropy upon hydrolysis. Then as for Sealock and Laskowski Jr. surmised about BPSTI (62), small rotational freedom gained with the hydrolysis may cause the low K_{hyd}^0 value of SSI.

It was surmised that in all modified inhibitors obeying the reactive site model the P_1' residue is rigidly held to the inhibitor molecule (14). It is reported that the NH of the P_1' residue Val74 of SSI is directed inward as judged by hydrogen-deuterium exchange rate and solvent accessibility calculations (70) and that this conformation may be persist even after the reactive site peptide bond had been cleaved.

It was surmised that the newly formed α-amino group of P_1' and the carboxylate of P_1 might be relatively close on the average and thus subjected to mutual electrostatic interaction in the modified BPSTI (62) because of the low K_{hyd}^0 and the low pK_1 value of the P_1 residue COOH. The pK_1 value of Met73 COOH of SSI obtained to be 3.6 is higher than that of BPSTI (pK_1 = 3.17) (62) and OMTKY3 (pK_1 = 3.27) (71) and is similar to the STI (pK_1 = 3.56) (61), but it may be difficult to compare because of the different P_1 amino acid. However, the pK_2 value of Val74 NH_2 of SSI obtained to be 9.0 is clearly higher than that obtained for all inhibitors (7.8 ~ 8.3). That would be explained by the interaction between newly formed amino group and carboxylate.

The three dimensional structure of the reactive site of SSI is similar to the reactive site of OMJPQ3 (56). Recently, X-ray crystallographic structures of modified

OMJPQ3 (K_{hyd}^0 = 0.45) and OMSVP3 (K_{hyd}^0 = 1.6) were solved and the structure of both intact and modified inhibitors had no serious change (72). Unfortunately the X-ray crystallographic study have not been done with SSI*, spectroscopic study of SSI* shows no serious change depending upon the modification (unpublished data). This may be the reason is why the modified inhibitor could inhibit the enzyme and these inhibitors shows the low K_{hyd}^0 value. In the interaction between SSI and subtilisin BPN' (Eq. 3-1), it was reported that the most stable form was the Michaelis complex by the X-ray crystallographic study and NMR study (12-14). Further this K_{hyd}^0 value is very important to investigate the equilibrium of reaction.

Chapter 4
Resynthesis of the cleaved reactive site of Streptomyces subtilisin inhibitor (SSI) by subtilisin BPN'

The interaction of proteinaceous proteinase inhibitor with the target enzyme constitutes a well defined example of protein-protein interaction. Furthermore, the mechanism of interaction resembles the catalytic process in the reactive site peptide bond (3-4). The standard mechanism of interaction of serine proteinase with inhibitor has been proposed as eq. 4-1:

$$E + I \underset{k_{off}}{\overset{k_{on}}{\rightleftharpoons}} EI \underset{k_{-c}}{\overset{k_{+c}}{\rightleftharpoons}} EI^* \underset{k_{on}^*}{\overset{k_{off}^*}{\rightleftharpoons}} E + I^* \qquad (4\text{-}1)$$

where E, I, I*, EI, and EI* represent an enzyme, an inhibitor, a modified inhibitor in which the reactive site peptide bond was cleaved, an enzyme-inhibitor complex, and an enzyme-modified inhibitor complex, respectively; and k_{on} and k_{on}^* are the association rate constants, k_{off} and k_{off}^* are dissociation rate constant, respectively. The rate constants of cleavage and resynthesis are represented by k_{+c} and k_{-c}, respectively. The resynthesis of EI* $\rightarrow$ EI is the reverse reaction of proteinase. The stable complex is generally in the form of Michaelis complex (EI), in which the inhibitor and the target enzyme binds noncovalently (22-24).

The scissile bond of Streptomyces subtilisin inhibitor (SSI) toward subtilisin BPN' is the peptide bond Met73-Val74 (21). The three-dimensional structures of SSI and SSI-subtilisin BPN' complex have been dissolved by X-ray crystallography (11-13). SSI is a dimeric protein which consists of two identical subunits of molecular weight

11500, and the SSI-subtilisin BPN' complex, the Michaelis complex (12-14), is a tetrameric protein forming E_2I_2; however, the author will deal SSI and SSI-subtilisin BPN' complex as monomer, I, and dimer, EI, in the text. EI complex is very stable at neutral pH and normal condition; however, the reactive site was cleaved by the enzyme to be SSI* at acidic pH (around pH 2.7) (66). SSI* also has an inhibitory activity and EI* complex which is made by the binding of SSI* and subtilisin BPN' acts as EI same as complex in spectrophotometrical view (73). These results indicate that the scissile bond seems to be resynthesized and become a stable EI complex. NMR study revealed that the scissile bond was resynthesized within a measuring time (about 3 hours) (74).

In this chapter, the author determined the apparent rate constant of the resynthesis of the reactive site of SSI, k_{app}, by investigating the time course of the ratio of [EI*] to [EI]. Because the EI complex is far stable than the EI* complex, it can be assumed to be $k_{-c} \gg k_{+c}$. Accordingly, it can be regarded as first-order reaction as Eq. 4-2.

$$EI^* \xrightarrow{k_{app}} EI \qquad (4\text{-}2)$$

This reaction was obtained by using pulse moter driven pumps for rapid quenching and polyacrylamide gel electrophoresis. Effect of reactant concentration on the apparent rate of resynthesis was studied to obtain K_i^* ($=([E][I^*])/[EI^*] = k_{off}^*/k_{on}^*$).

MATERIALS AND METHODS

Proteins SSI and subtilisin BPN' (EC 3.4.21.14) (lot No.7370935) was prepared as described in Chapter 1. SSI*

was purified by the method of Tonomura (66) and described in Chapter 3. The protein concentration was determined spectrophotometrically, from the absorbance at pH 7.0 by using A_{276}(1 mg/ml) = 0.829 for SSI and SSI*, and A_{278}(1 mg/ml) = 1.063 for subtilisin BPN' (17). The molecular weights were 11500 for SSI (subunit) (18) and SSI*, and 27500 for subtilisin BPN' (30). All SSI concentration in the text, shown as [I], is represented as subunit concentration unless otherwise mentioned.

Measurement of the resynthesis reaction - An apparatus was designed and constructed in which subtilisin BPN' and SSI* (pumps 1 & 2) could be mixed together to form the complex and then quenched by the automatic addition of acid (pump 3) at precisely controlled time intervals after mixing. The apparatus (Fig. 4-1) consisted of three microliter cylinges driven by pulse motor, and the sample volume could be controlled by the puls number and the cylinge size. Equimolar (1.25×10^{-4} M) subtilisin BPN' and SSI* solutions in 25 mM phosphate buffer pH 7.0 were mixed (15 μl each) at 25℃, and after desired delay time, the reaction was stopped by adding 0.4 M Gly-HCl buffer (45 μl) pH 1.5 at 0℃. All reactions was done in the mini tube which was vibrated by a mixer. 0.4 M Tris (60 μl) was added to the mini tube to be neutral pH after 90 sec of acid-treatment at 0℃. Both SSI and SSI* were alive and the enzyme denatured under this condition. The solution was subjected to PAGE at pH 9.4 as described in Chapter 3. The relative amounts of SSI and SSI* was calculated from these density.

These results were dealt with first-order reaction from eq. 4-2.

$$-d[EI^*]/dt = k_{app} \cdot [EI^*] \qquad (4\text{-}3)$$

The value of k_{app} was obtained with non-linear least

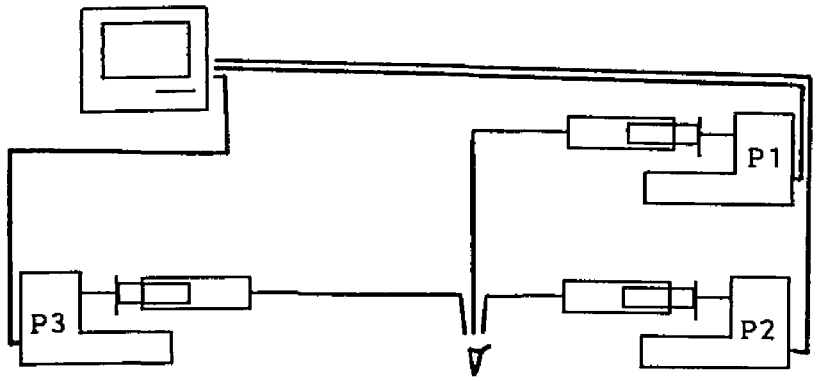

Fig. 4-1. Schematic diagram of pulse-motor driven pumps for rapid quenching.

squares method.

Apparent rate constant of resynthesis was also obtained under the conditions of $[E]_0 \geqq 5[I]_0$, $[E]_0 = 2 \sim 625\ \mu M$.

RESULTS

Figure 4-2 shows the standards of PAGE profile. Since electric charge of SSI* is more negative than that of SSI at pH 9.4, the band of SSI* has migrated further on the PAGE (lanes 1 & 2), The migrations on PAGE of both SSI* and SSI were not disturbed by acid-treatment (lanes 3 & 4). SSI has sub-band due to the uneven amino-terminal but that has no connection with its inhibitory activity, and the amino-terminal has become homogenous by mixing with subtilisin BPN'. The bands of EI* complex made by mixing equimoler

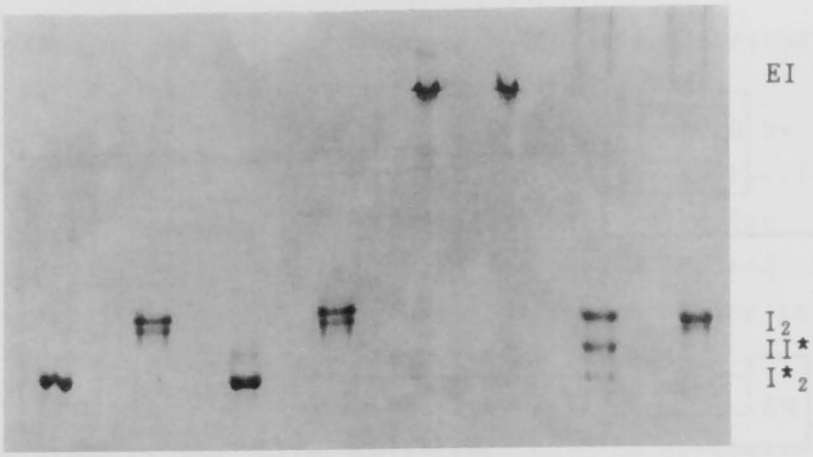

Fig. 4-2. PAGE patterns of proteins. Lane 1, SSI*; lane 2, SSI; lane 3, acid treated SSI*; lane 4, acid treated SSI; lane 5, enzyme-inhibitor complex made from subtilisin BPN' and SSI* (EI*); lane 6, enzyme-inhibitor complex made from subtilisin BPN' and SSI (EI); lane 7, acid treated EI*; lane 8, acid treated EI.

SSI* and subtilisin BPN' and EI complex show the same migration (lanes 5 & 6). They are indistinguishable on PAGE profile. So that complexs were dissociated into the enzyme and the inhibitor by acid-treatment to differentiate SSI* and SSI. EI* and EI complexes both of which were treated with acid are subjected (lanes 7 & 8). SSI* which has remained without the resynthesis by the enzyme and SSI which has been resynthesized by the enzyme on lane 7. Lane 8 shows the only SSI band. During the acid-treatment the EI* complex which had remained without the resynthesis of the scissile bond by the enzyme must have dissociated into free enzyme and free modified inhibitor, and the EI complex in which the inhibitor had been resynthesized at the scissile bond by the enzyme before the addition of acid into free enzyme and free intact inhibitor. At that time free enzyme in the solution was denatured irreversibly and inactivated, so that it could not form EI or EI* complex after neutralization. The middle band between the bands of SSI (top band) and SSI* (bottom band) has been regarded as the

hybrid species of SSI and SSI* because of the dimeric form (75, Chapter 5), so that one half of the middle band is calculated as SSI and the other half of it is as SSI*. The ratio of the SSI and SSI* after acid-treatment regarded as the ratio of the population of EI complex and EI* complex because it is impossible to distinguish between EI and EI* complex directly.

Figure 4-3 shows one of the PAGE profiles to determine the resynthesis rate, which shows the time course of the conversion of SSI* to SSI. The reaction time is from 0.03 s to 2.1 s with every 0.3 s interval. As the incubation time is longer, the bottom of the three bands which is SSI* becomes thinner and the top which is SSI becomes thicker. The time course of the ratio of SSI* against the total inhibitor amount, [SSI*]/([SSI]+[SSI*]), is shown in Fig. 4-4, which were obtained by the ratio of the density of the bands on PAGE. The curves of fraction of intact inhibitor obtained plotted against time could be fitted reasonably well to first order curves (eq. 4-3), and the apparent first-order reaction rate constant of resynthesis of the scissile bond of SSI, k_{app}, was determined to be 0.45 s^{-1} at pH 7.0, 25℃. The half-life period of this reaction, $t_{1/2}$, is calculated to be 1.5 sec, and modified inhibitor predominantly converted into intact inhibitor.

Because the scissile bond is almost resynthesized in 15 sec, one can not separate the EI* complex. Then the author regarded the formation of EI complex from S-BPN' and SSI* as two step mechanism, in which a fast bimolecular process for the formation of EI* as intermediate is followed by a slower unimolecular step.

$$E + I^* \underset{k_{off}^*}{\overset{\text{fast}\ k_{on}^*}{\rightleftharpoons}} EI^* \underset{k_{+c}}{\overset{\text{slow}\ k_{-c}}{\rightleftharpoons}} EI \qquad (4\text{-}4)$$

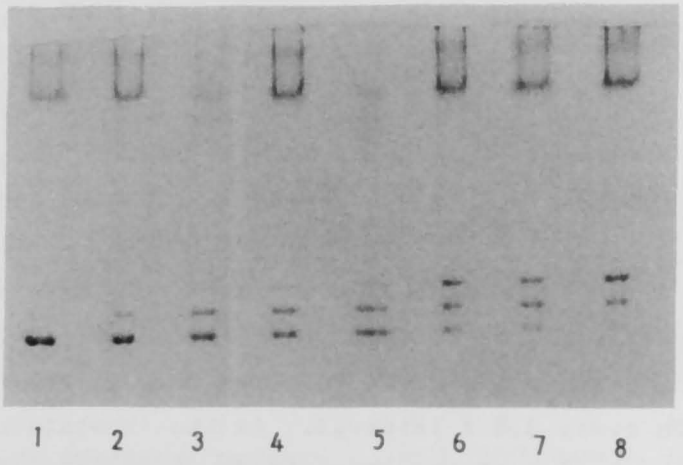

Fig. 4-3. PAGE patterns obtained on aliquots of the rapid mix quencher dissociation products of reaction in Fig. 4-4. $[E]_0 = [I^*]_0 = 1.25 \times 10^{-4}$ M at pH 7.0, 25°C. Time shown represent the interval between initial mixing of the protein solution and addition of acid to dissociate any complex formed. Lanes 1-8, 0.03, 0.3, 0.6, 0.9, 1.2, 1.5, 1.8, and 2.1 sec, respectively.

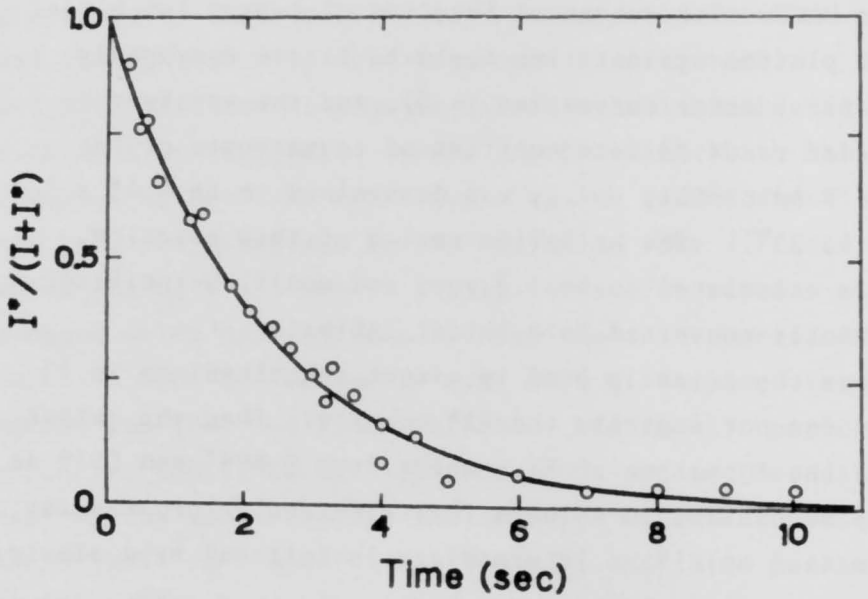

Fig. 4-4. Time course of the ratio of SSI* to (SSI + SSI*). $[E]_0 = [I^*]_0 = 1.25 \times 10^{-4}$ M at pH 7.0, 25°C. The solid line is the theoretical curve drawn according to Eq. 4-3 with $k_{app} = 0.45\ s^{-1}$.

The apparent rate of resynthesis, k_{app}, can be expressed under the condition that $[E]_0 \gg [I]_0$ as follows:

$$k_{app} = \frac{k_{-c} \cdot [E]_0}{[E]_0 + K_i^*} + k_{+c} \qquad (4\text{-}5)$$

The concentration dependence of k_{app} shows hyperbolic curve (Fig. 4-5) and is consistent with Eq. 4-5 with $k_{+c} \fallingdotseq 0$. K_i^* and k_{-c} were calculated according to Eq. 4-5 by nonlinear least-squares method. The over all dissociation constant of EI to E and I* is expressed as Eq. 4-6:

$$K_i \times K_{hyd} = K_i^* \times \frac{1}{1 + (k_{-c}/k_{+c})} \qquad (4\text{-}6)$$

where $K_i = ([E][I])/[EI])$ and $K_{hyd} = [I^*]/[I]$ are the dissociation constant of EI to E and I, and the equilibrium constant of peptide bond hydrolysis, respectively. These constants have already been obtained to be 1.8×10^{-11} M and 0.37, respectively (Chapter 1 and 3 in this thesis). By using the values obtained, the author estimated k_{+c} values to be 1.2×10^{-6} s^{-1}. The value of k_{off}^* was also calculated from the equation; $K_i^* = k_{off}^*/k_{on}^*$ (4-7). The value of k_{on}^* was obtained to be 3.0×10^6 $M^{-1} \cdot s^{-1}$ monitoring the protein fluorescence change on binding of subtilisin BPN' and SSI* (73), or the remaining enzyme activity so that the value of k_{off}^* was 7.5 s^{-1}. All the parameters of the interaction of subtilisin BPN' and SSI are listed in Table 4-1.

DISCUSSION

SSI* also strongly inhibits subtilisin BPN' activity and SSI*-subtilisin BPN' complex has similar spectoroscopic properties to SSI-subtilisin BPN' complex as shown by ultraviolet absorption difference spectrum and fluorescence

TABLE 4-1.
Equilibrium and kinetic constants in the interaction of S-BPN' and SSI at pH 7.0, 25℃.

K_i	(M)	1.8×10^{-11}
k_{on}	($M^{-1}s^{-1}$)	6.5×10^{6}
k_{off}	(s^{-1})	0.9×10^{-4}
k_{+c}	(s^{-1})	1.2×10^{-6}
k_{-c}	(s^{-1})	0.45
K_i^*	(M)	2.5×10^{-6}
k_{on}^*	($M^{-1}s^{-1}$)	3.0×10^{6}
k_{off}^*	(s^{-1})	7.5
K_{hyd}		0.37

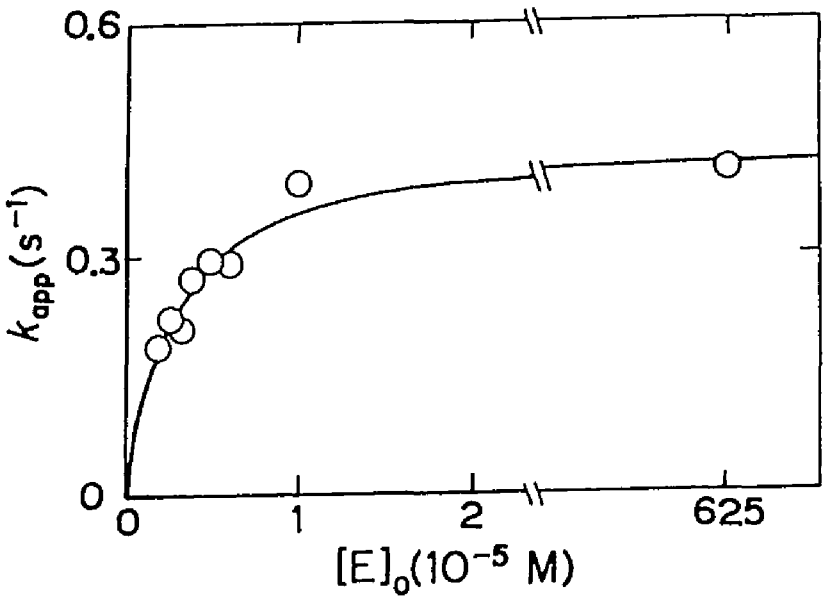

Fig. 4-5. Dependence of the apparent rate constant of resynthesis on the initial concentrations of the enzyme at pH 7.0, 25℃. The solid line is the theoretical curves drawn according to Eq. 4-5 with $K_i^* = 2.5\times10^{-6}$ M, $k_{-c} = 0.45\ s^{-1}$, $k_{+c} = 0$.

spectrum (73); therefore, the most stable complex formed by SSI* and subtilisin BPN' has been expected to be same as that formed by SSI and subtilisin BPN' by way of the resynthesis of the reactive site peptide bond in the complex. In 1988 Kainosho and Miyake reported that the reactive site peptide bond of SSI* was resynthesized in the complex made by SSI* and subtilisin BPN' within 3 hours which was the required time for NMR study (74). Furthermore the reaction rate constant of the resynthesis is determined to be 0.45 s^{-1} in the present study. The half life of this reaction is 1.5 s and the reaction will end within 15 s up to 99.9 %.

The reaction of the binding process of SSI* and subtilisin BPN' or the dissociation process of the complex in acid-treatment seem not to be the rate-determining step. According to the the second-order rate constant for the binding of SSI* and subtilisin BPN' obtained previously to be 3.0×10^6 $M^{-1} \cdot s^{-1}$ at pH 7.0 (73) and the present experimental conditions ($[E]_0 = 1.25 \times 10^{-4}$ M), the apparent first-order rate constant of association would be 3.5×10^2 s^{-1} ($t_{1/2} = 2.0 \times 10^{-3}$ s), which is 670-fold larger than the resynthesis rate constant obtained in this study. On the other hand, according to the pH dependence of the first-order rate constant for the dissociation of subtilisin BPN' complex at pH 1.5, 0℃ is presumed to be 5.0 s^{-1} ($t_{1/2} =$ 0.14 s) (Tonomura et al., unpublished data), that is 10-fold larger than k_{app}.

Further the dissociation constant of subtilisin BPN' to subtilisin BPN' and SSI*, K_1*, were obtained to be 2.5×10^{-6} M by the reactant concentration dependence of apparent rate constant of resynthesis. Two rate constants, k_{off}* and k_{+c}, were impossible to be measure directly, and they were calculated using other rate constants and equilibrium

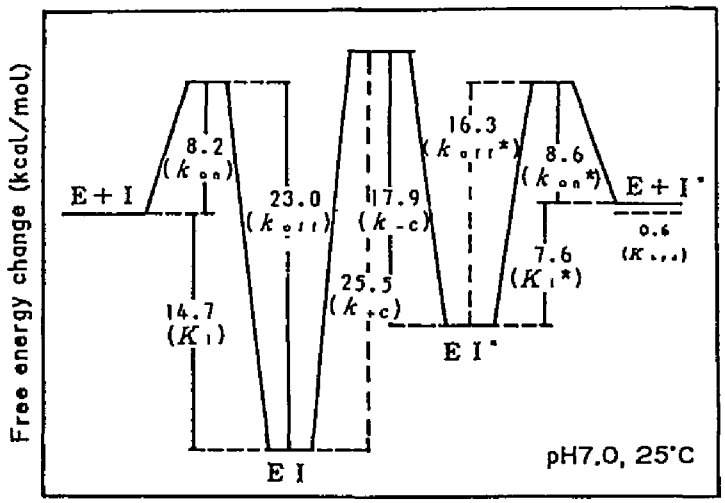

Fig. 4-6. Free energy profile for the interaction of subtilisin BPN' and SSI.

constants obtained already. Free energy profile of the interaction of subtilisin BPN' and SSI is drawn in Fig. 4-6. The EI complex which is the Michaelis complex is thermodynamically most stable with a large energy barrier preventing hydrolysis. The association rate constants of SSI and SSI* to subtilisin BPN' are almost same, and the large difference between K_1 and K_1* was due to the difference of dissociation rate constants.

Hixon and Laskowski reported the resynthesis of modified soybean trypsin inhibitor by trypsin by the essentially same method of this study, and the reaction of resynthesis was first-order and its rate constant was measured to be ~ 2 s^{-1} at pH 5.7 (76). As for bovine pancreas trypsin kallikrein inhibitor (BPTI) (Kunitz) (77), reaction rate constant of the presumable resynthesis by β-trypsin was 1×10^{-2} s^{-1} at pH 7.5, 23℃ which is about 50-fold smaller than that of SSI. When these were reported, the most stable complex of

serine proteinase and proteinaceous proteinase inhibitor was regarded as the tetrahedral intermediate, so that the interpretation of the rate constant was different; nevertheless, the value of K_i^* for BPTI and β-trypsin was estimated to be 3.5×10^{-6} M (77), which is similar to the value obtained for SSI and subtilisin BPN'.

It has been reported in this study that the rate determining step is the hydrolysis (k_{+c}), and this step should have tetrahedral intermediate and acyl enzyme (Fig. 4-6). It is very interesting to investigate the rate of each step and the difference between inhibitor and substrate.

Chapter 5

Kinetic and thermodynamic studies on the dissociation of a dimeric protein, Streptomyces Subtilisin Inhibitor (SSI)

There are many stable dimer proteins consisting of non-covalently bound subunits. Since detecting those subunits in an equilibrium state is usually difficult, there have been rather few kinetic studies on the dissociation of those stable dimers under the non-denaturing condition, except for the cases of enzyme-proteinaceous inhibitor complexes, for which the dissociation can be followed sensitivity by the appearance of enzyme activity. Streptomyces subtilisin inhibitor (abbreviated to SSI or I_2), a protein proteinase inhibitor produced by Streptomyces albogriseolus S-3253, is a stable homodimer of molecular weight 23000 consisting of subunit which contains 113 amino acid residues (7-9,17). The dissociation equilibrium constant of the dimer into the subunits was assumed to be much less than 0.5 μM by sedimentation study (17). A monomer SSI has been detected only under the denaturing conditions: presence of sodium dodecyl sulfate (SDS) (78), heat (79), or acidic pH (80). The three dimensional structure of SSI resolved by X-ray crystallography (10) revealed that a subunit contains a five-stranded anti-parallel β-sheet structure, two α-helices, and two disulfide bonds and that the β-sheets of two subunits faces each other constructing the subunit-subunit interface (Fig. 5-1). The double β-sheets at the interface constitute the core of globular dimer SSI. A modified SSI (represented as SSI* or I^*_2 hereafter) in which the reactive site peptide bond was cleaved enzymatically also has strong inhibitory activity, and can be separated from SSI on PAGE. When I_2 and I^*_2 were mixed, the hybrid

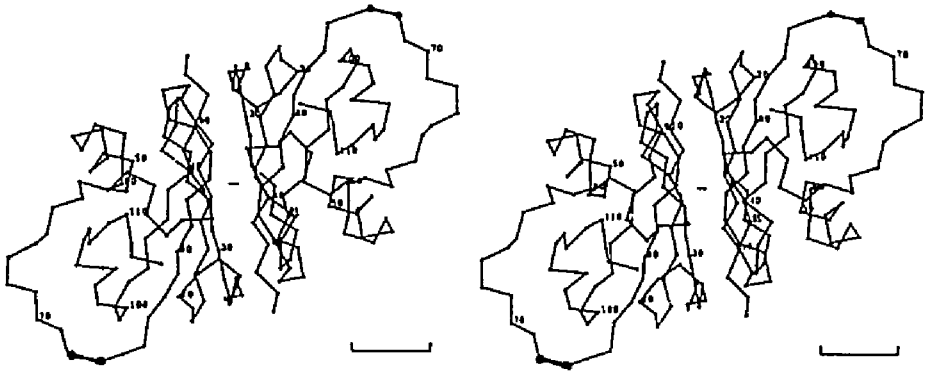

Fig. 5-1. Three dimensional structure of SSI dimer (11).

species, II*, was clearly detected on PAGE, and this provides us with a good prove for studying the dissociation of the SSI dimer. Characterization of the dimer structure is indispensable for understanding the structure-function relationship of SSI.

In this chapter, the author report the rates of dissociation of the SSI dimer and activation energy of dissociation.

Materials and Methods

Proteins SSI and modified SSI (SSI*) were prepared as described in Chapter 1 and 3, respectively. A mutant SSI, SSID68N in which Asp68 was replaced by Asn was prepared by the method described in Chapter 2. The protein concentration was determined spectrophotometrically from the absorbance at pH 7.0 by using A_{276} (1 mg/ml) = 0.829 for SSI and SSI* and the molecular weights of 11500 was used for SSI (monomer) (18) and SSI* (monomer), and the molar concentration is expressed as the concentration of monomer unless otherwise noticed.

Determination of dissociation rate constant - The ratio

of I_2:II*:I^*_2 was determined by PAGE described in Chapter 3.

The equilibria between monomer and dimer are shown as follows:

$$\begin{array}{ccccccc} & I_2 & & & I^*_2 & & \\ k_1 & \| & k_{-1} & k_1' & \| & k_{-1}' & k_1'' \\ & 2I & + & & 2I^* & \rightleftharpoons & 2II^* \\ & & & & & & k_{-1}'' \end{array} \qquad (5\text{-}1)$$

where I_2, I^*_2, II*, I, and I* indicate SSI dimer, SSI* dimer, hybrid dimer of SSI and SSI*, SSI monomer, and SSI* monomer, respectively; k_1, k_1', and k_1'' are the association rate constants and k_{-1}, k_{-1}', and k_{-1}'' are the dissociation rate constants at the respective steps indicated. The velocity of change of the three species can be expressed in the linear differential equations:

$$\begin{aligned} d[I_2]/dt &= k_1[I]^2 - k_{-1}[I_2], \\ d[I^*_2]/dt &= k_1'[I^*]^2 - k_{-1}'[I^*_2], \\ d[II^*]/dt &= 2k_1''[I][I^*] - k_{-1}''[II^*]. \end{aligned} \qquad (5\text{-}2)$$

And $[I_2]_0=[I_2]+[I]+\frac{[II^*]}{2}$, $[I^*_2]_0=[I^*_2]+[I^*]+\frac{[II^*]}{2}$, where $[I_2]_0$ and $[I^*_2]_0$ represent the initial concentration of those species. Since the equilibria shown in Eq. 5-1 are very much in favor for the dimeric species under the conditions of present experiment, the concentration of monomer, [I] and [I*], can be regarded negligibly small compared with those of dimeric species. Accordingly, the author have $[I_2] + [I^*_2] + [II^*] \fallingdotseq [I_2]_0 + [I^*_2]_0$. The author also assume that the rate constants are same for I_2, I_2^*, and II*, namely, $k_1 = k_1' = k''$ and $k_{-1} = k_{-1}' = k_{-1}''$. The validity of this assumption will be shown in Discussion. Solution of the above equations under the initial condition, $[I_2]_0 = [I^*_2]_0$ yields,

$$[II^*] = [I_2]_0(1 - \exp(-k_{-1}t)) \qquad (5\text{-}3)$$

$$[I_2] = ([I_2]_0/2)(1 + \exp(-k_{-1}t)). \qquad (5\text{-}4)$$

A normalized value of [II*] (%) (= [II*] × 100 / ([I_2] + [I^*_2] + [II*])) was fitted to Eq. 5-3 by the nonlinear least squares method and the rate constant k_{-1} was obtained.

Determination of activation parameters

The free energy of activation for the dissociation of SSI dimer ΔG^* was calculated from the dissociation rate constant

$$\Delta G^* = 2.303RT\{\log(k_B T/h) - \log k_{-1}\} \quad (5\text{-}5)$$

where k_B is Boltzmann's constant and h, Planck's constant.

$$\Delta S^* = (\Delta H^* - \Delta G^*)/T \quad (5\text{-}6)$$

The ΔH^* values were derived from the Arrhenius plots.

Results

Assignment of II* an hybrid dimer SSI on PAGE - When equal amount of SSI (I_2) and SSI* (I^*_2) (12 μM each as monomer) were mixed at pH 7.0 and after 1 h incubation at room temperature the mixture was applied to PAGE at pH 9.4, three bands were detected (Fig. 5-2, lane 3). The top and the bottom bands are I_2 and I^*_2, respectively, but the central band appeared newly by the mixing. Protein of the central band was extracted from the gel, and subjected to PAGE again. It yielded similar three bands (Fig. 5-2, lane 4). Their mobilities corresponded exactly to those observed for the original mixture (Lane 3). The proteins of these three bands in Lane 4 were extracted separately from the gel, and they were applied separately to the PAGE; the top band gave I_2 (lane 5), the central band three bands again (lane 6), and the bottom band I^*_2 (lane 7). These results suggested that the central band was the hybrid species of I_2 and I^*_2, namely II*. Detection of II* on PAGE indicates that the dimeric forms of I_2 and I^*_2 dissociate into the

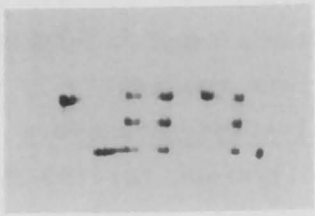

Fig. 5-2. PAGE of I_2, II*, and I^*_2 at pH 9.4. lane 1, I_2; lane 2, I^*_2; lane 3, mixture of I_2 and I^*_2; lane 4, Protein extracted from the central band of Lane 3; lane 5, Protein extracted from the top band of Lane 4; lane 6, Protein extracted from the central band of Lane 4; lane 7, Protein extracted from the bottom band of Lane 4.

monomers under the ordinary conditions and that the respective subunits are exchanged.

Dissociation rate constant of SSI dimer - Equimolar concentration of I_2 and I^*_2 (13 μM each as monomer) were mixed in 25 mM phosphate buffer, pH 7.0 at 1 ~ 25 ℃, and after appropriate incubation time the mixture was applied to PAGE at pH 9.4, 0 ℃. I_2, I^*_2, and II* were separated (Fig. 5-3a), and time dependent increase of II* and decrease of I_2 and I^*_2 were observable. Figure 5-3b shows the time course of the normalized value of [II*], which was fitted to Eq. 5-3 by the non-linear least squares method. The value of the dissociation rate constant k_{-1} was determined to be 1.63×10^{-4} s^{-1} at 4.3 ℃, pH 7.0 from this curve, and accordingly, the half-life time of this reaction was 71 min. To validate the assumption that the same rate constants can be used for I_2 and I^*_2, an artificial mutant SSI species, SSID68N, in which Asp68 was replaced by Asn and the reactive site was intact, was used instead of SSI*. SSID68N can be separated from the native SSI on PAGE because the former has lost a negative charge. Asp68 locates near the reactive site and is not involved in the subunit-subunit interaction (12-13), and SSID68N had high affinity to subtilisin BPN' as described in Chapter 2. The concentration of a hybrid

(a)

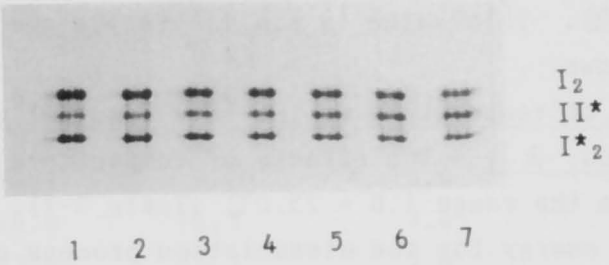

(b)

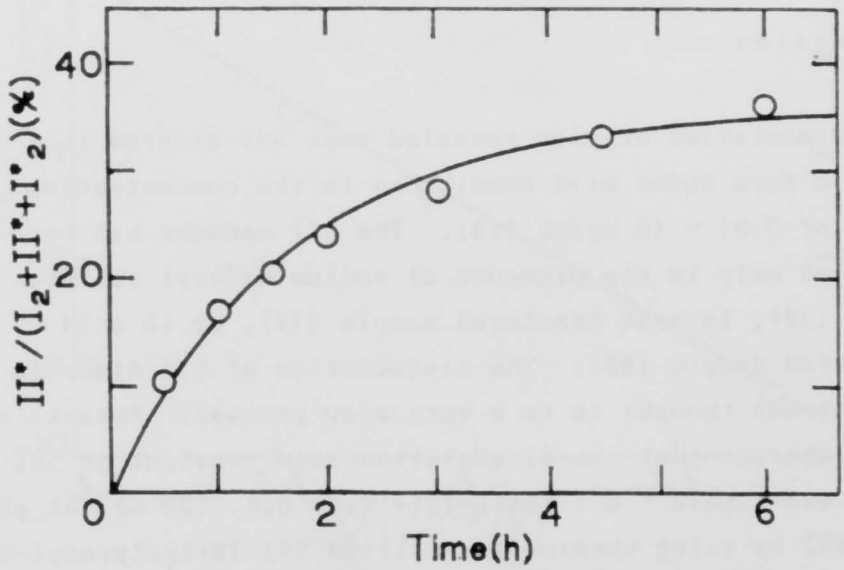

Fig. 5-3. Time course of the exchange of the subunits after mixing of I_2 and I^*_2, at 4.3 ℃ and pH 7.0. (a) PAGE at pH 9.4. The mixture of equal concentration of SSI and SSI* (13 μM as monomer) were incubated at 4.3 ℃, pH 7.0, and after various incubation time the mixture was applied to PAGE; for lanes 1-7, the incubation times were 0.5, 1.0, 1.5, 2.0, 3.0, 4.5, and 6.0 h, respectively. 4.2 μg protein /lane was applied. (b) The ratio of the II* density to total inhibitor density of PAGE (panel (a)) plotted vs. incubation time. The solid line is the theoretical curve drawn based on eq. 5-3 with $k_{-1} = 1.63 \times 10^{-4}$ s^{-1}.

species of SSI(wt) and SSID68N was fitted to Eq. 5-3. The dissociation rate constant was obtained as 4.5×10^{-4} s^{-1} at pH 7.0, 15℃. This value is similar to the one for I^*_2 at 15℃ as shown.

Effects of temperature on the rate constant of SSI dimer dissociation, k_{-1} - The effects of temperature on k_{-1} was examined in the range 1.0 ~ 25.0℃ (Table 5-1). The activation energy for the dissociation process of I_2 to 2I, E_A, obtained from the Arrhenius plots (Fig. 5-4) was 23.8 kcal/mol (99.5 kJ/mol). Other activation parameters for the dissociation at 25℃ was calculated. Gibbs' free energy of activation ($\Delta G^{\ddagger}$), the enthalpy of activation ($\Delta H^{\ddagger}$), and the entropy of activation ($\Delta S^{\ddagger}$) were 20.9 kcal/mol, 23.2 kcal/mol, and 7.7 *e.u.*, respectively (Table 5-2).

Discussion

Sedimentation studies revealed that SSI existed in a dimeric form under mild conditions in the concentration range of 0.01 ~ 10 mg/mL (18). The SSI monomer has been observed only in the presence of sodium dodecyl sulfate (SDS) (78), in heat denatured sample (79), or in acid denatured sample (80). The dissociation of SSI dimer to monomer was thought to be a very slow process. Akasaka et al., reported that the dissociation rate constant of SSI dimer was 1.6×10^{-6} s^{-1} (half-life time c.a. 120 h☆) at pH 8.7, 4℃ by using chemically modified SSI (Nitrotyrosyl-SSI) with high performance liquid chromatography (81). However, when the author mixed I_2 and I^*_2 at room temperature, the hybrid species II^* was detected easily on PAGE suggesting faster dissociation of the dimer. In the present study, the rate constant of dissociation, k_{-1}, was determined to be

Table 5-1: Effect of temperature on the dissociation rate constant of SSI dimer, k_{-1} at pH 7.0.

T (℃)	k_{-1} (10^{-4} s^{-1})	$t_{1/2}$ (min)
1	0.83	139
4.3	1.63	70.8
9.5	3.76	30.7
14.1	6.20	18.6
20.0	16.5	7.0
25.0	31.5	3.6

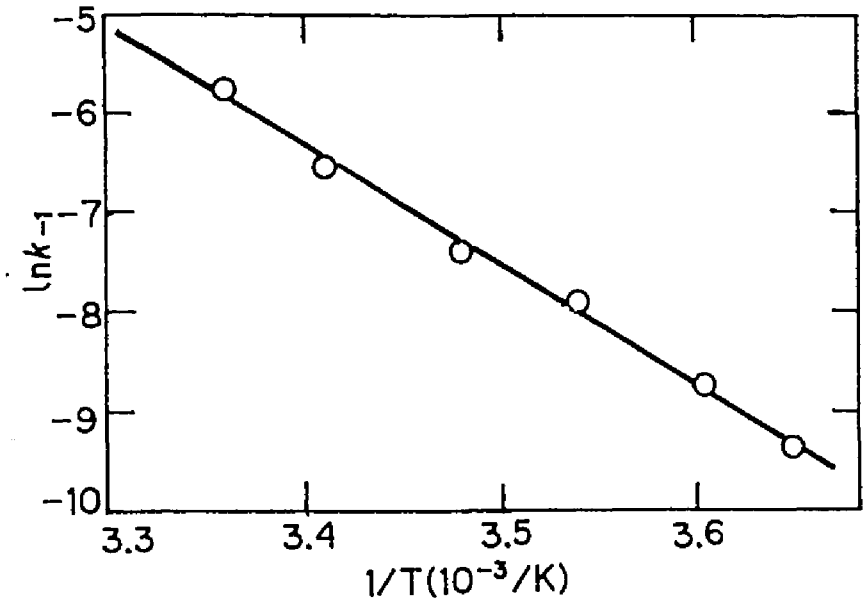

Fig. 5-4. Arrhenius plots of the dissociation rate constant of SSI dimer, k_{-1}, at pH 7.0. Activation energy E_A is calculated for the slope to be 23.8 kcal/mol.

1.6×10^{-4} s^{-1} at pH 7.0, 4.3℃ and 3.2×10^{-3} s^{-1} (a half-life time $t_{1/2}$ = 3.8 min) at pH 7.0, 25℃ (Table 5-2). The association rate constant, k_1, of SSI monomer to SSI dimer ($2I \rightarrow I_2$) can not been obtained experimentally, and it may be estimated by assuming a diffusion controlled association (82). The encounter rate constant for this size of proteins can be assumed as 6×10^9 $M^{-1}s^{-1}$. The steric factor which determines the probability of occurrence of specific association among random encounter of two subunits is assumed to be 10^{-2}, based on the consideration that about 10% of whole the surface of the monomer is covered by the dimer formation (83). Thus, the rate constant for the diffusion-controlled association of SSI monomer, k_1, would be 6×10^7 $M^{-1}s^{-1}$. Accordingly, the dissociation equilibrium constant of the dimeric SSI, $K_d = k_{-1}/k_1$, would be of the order of 10^{-12} M, which is close to that of SSI-subtilisin BPN' complex described in Chapter 1.

The experimental conditions were so chosen that further reaction during electrophoresis could be avoided as possible by setting the temperature at 0 ℃, at which the rate constant for dissociation was expected to be small enough because of the large activation energy of the dissociation (23.8 kcal/mol, Table 5-2). Though it took 90 min to run the electrophoresis, the facts that clear band of each moleculer species was obtained on PAGE and that the reaction curve well fitted to the theoretical first-order reaction curve indicate that such further reaction was successfully avoided.

The assumption that the dimeric dissociation rate constants of SSI and SSI* are equal is considered reasonable because a nick of SSI* at the reactive site (Met73-Val74 bond) locates outside of this globular dimeric molecule (10) (Fig. 5-1), and there is no significant structural change at

the monomer-monomer-interface (74). Furthermore, the experiment of mixing SSI with SSID68N, and E_2I_2 with I_2 and I^*_2 described in Appendix of this chapter gave the similar rate constants suggesting the validity of this assumption. Though the ratio of I_2: II^*: I^*_2 should be 1: 2: 1 at equilibrium under the initial condition of $[I_2]_0 = [I^*_2]_0$ the maximum values of the ratio of $[II^*]$ to the total inhibitor concentration obtained in this experiments were between 35 ~ 40% against the theoretical value of 50%. This difference may reflect the difference of the dissociation rate between SSI and SSI^*. However, the final ratio of the hybrid species of SSI and SSID68N to total inhibitor was also about 41 %.

The author can not explain the large difference between the rate constants obtained by Akasaka et al. and that by me. There are three different points in their study from mine: First, the reaction pH was different; secondly, SSI molecule was chemically modified at Tyr residue; thirdly, the reaction was analyzed with ion exchange column chromatography.

Koren and Hammes (84) reported the rate constant of dimer formation and dissociation of insulin, β-lactoglobulin, and α-chymotrypsin by pH jump and temperature jump. The order of magnitude of dissociation rate constant of these proteins, 10^3~10^4 s^{-1}, was larger than that of SSI dimer. And the dissociation equilibrium constants of these proteins were 10^{-4} M; the binding is much weaker here than the case of SSI.

The activation energy for the dissociation of dimeric SSI into monomer, 23.8 kcal/mol, is larger than the activation energy (14.2 kcal/mol) for dissociation of SSI-subtilisin BPN' complex into enzyme and inhibitor previously reported (39) (Table 5-2).

Table 5-2: Activation parameters for the dissociation at 25℃, pH 7.0

	k_{-1} (s^{-1})	E_A (kcal/mol)	$\Delta G^{\ddagger}$ (kcal/mol)	$\Delta H^{\ddagger}$ (kcal/mol)	$\Delta S^{\ddagger}$ (e.u.)
SSI dimer[a]	3.2×10^{-3}	23.8	20.9	23.2	7.7
SSI-S-BPN'[b]	0.9×10^{-4}	14.2[c]	23.0	13.6[c]	-31.5

a; dissociation SSI dimer into SSI monomer.

b; dissociation SSI-subtilisin BPN' complex into SSI and subtilisin BPN'

c: reculculated from the data of Uehara et al. (39)

Appendix-1

Behavior of SSI-subtilisin BPN' complex

SSI inhibits subtilisin BPN' strongly by forming an E_2I_2 complex in which two molecules of subtilisin BPN' (E) are bound to an SSI dimer (I_2). EI_2 and EII^*, in which only one subtilisin molecule was bound to I_2 and I^*_2, respectively, were formed under the conditions of $2[E] < [I_2]$ and $2[E] < [I^*_2]$, respectively. In this paragraph, dissociation-association of SSI at the dimer interface that occurs also in the SSI-subtilisin BPN' complex, and the rate constants and activation parameters for the dissociation of the complex are reported.

Materials and Methods

Proteins and PAGE - See this chapter.

Determination of dissociation rate constant - Following equations can be assumed for mixing of E_2I_2 complex and the inhibitor I_2:

$$\begin{array}{ccccccc} & I_2 & & & E_2I_2 & & \\ k_1 & \| & k_{-1} & k_1^* & \| & k_{-1}^* & k_1^{**} \\ & 2I & + & & 2EI & \rightleftharpoons & 2EII \\ & & & & & & k_{-1}^{**} \end{array} \qquad (5\text{-}7)$$

where E_2I_2 and EI_2 indicate enzyme-inhibitor complex of a dimer SSI and 2 moles of S-BPN' and of a dimer SSI and one mole of S-BPN' respectively; k_1, k_1^*, and k_1^{**} are the association rate constants and k_{-1}, k_{-1}^*, and k_{-1}^{**} are the dissociation rate constants at the respective steps indicated. The dissociation must be the rate determining step, so $[EI_2]$ or $[EII^*]$ were fitted to the first order equation, because the densities/mol of E_2I_2, EI_2, and I_2 on

PAGE are different.

$$[EI_2] \text{ or } [EII^*] = A(1 - \exp(-k_{-1} t)) \quad (5\text{-}8)$$

When E_2I_2 and I^*_2 were mixed, EII* was detected instead of EI^*_2 (see the Results) because the cleaved reactive site of I^*_2 was resynthesyzed ($EI^*_2 \rightarrow$ EII*) within 15 s by the action of S-BPN' as described in Chapter 4.

Determination of activation parameters - See this chapter.

Results

Formation of enzyme-inhibitor complexes, EI_2 and EII^* - Subtilisin BPN' (E) and an excess molar concentration of SSI (I_2) was mixed at pH 7.0, 25 ℃, and applied to PAGE. The band of E_2I_2 is shown in Fig. 5-5, lanes 1 and 2. Under the conditions of $2[E] < [I_2]$, the second band (X) from the top was observed, whose density was in proportion to the concentration of I_2 employed (lanes 3, 4, and 5). Proteins of X extracted from the gel was applied to PAGE again and gave the bands corresponding to E_2I_2, X, and I_2 (data not shown). Thus the band, X, was suggested to be EI_2 in which one enzyme molecule binds with an SSI dimer (I_2).

When subtilisin BPN' (E) and excess SSI^* (I^*_2) were mixed ($2[E] < [I^*_2]$), there were observed E_2I_2 and a band migrating a little further than EI_2, which was assumed to be the band EII^* (discussed below) (Fig. 5-5, lanes 8~10). When I^*_2 was mixed with subtilisin BPN', the cleaved reactive site of I^*_2 was found repaired within 15 s at room temperature, pH 7.0 and becomes I_2 (Chapter 4). Thus, the subunit of I^*_2 bound with E was repaired, and consequently, $E_2I^*_2$ in which I^*_2 is bound with 2 enzyme molecules and EI^*_2 in which I^*_2 is bound with an enzyme molecule were converted

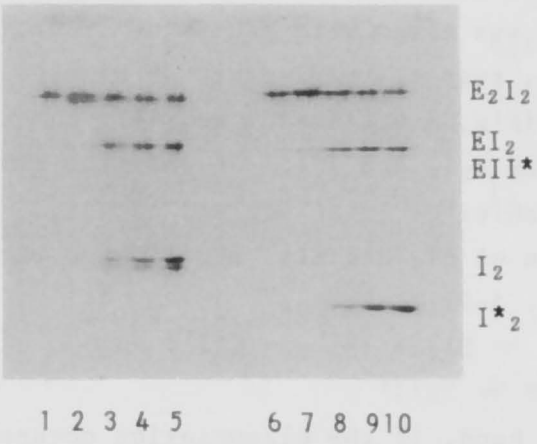

Fig. 5-5. Appearance of EI_2 and EII^* on PAGE. Subtilisin BPN' (E) was mixed with I_2 or I^*_2 at various molar ratio; Lanes 1 ~ 5 are for I_2, Lanes 6 ~ 10 for I^*_2. The molar ratio ($[I_2]$or $[I^*_2]/2[E]$ is 0.5 (lanes 1 & 6), 1.0 (lane 2 & 7), 2.0 (lane 3 & 8), 3.0 (lane 4 & 9), and 4.0 (lane 5 & 10).

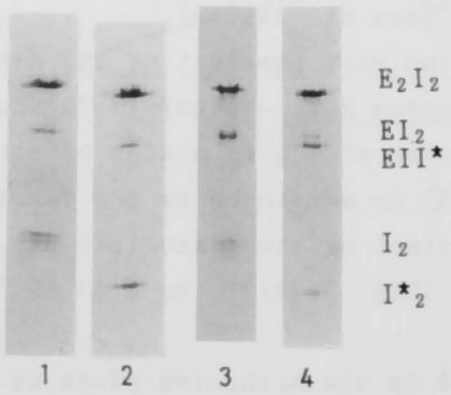

Fig. 5-6. Mixing of SSI-subtilisin BPN' complex (E_2I_2) with SSI or SSI*. $[E_2I_2]$=15 μM; lane 1, E_2I_2 + $2I_2$ after mixing for 10 min; lane 2, E_2I_2 + $2I^*_2$ after mixing for 10 min; lane 3, E_2I_2 + $2I_2$ after mixing for 6 h; lane 4, E_2I_2 + $2I^*_2$ after mixing for 6 h at pH 7.0, room temperature.

to E_2I_2 and EII*, respectively. The mobility on PAGE of EII* is faster than that of EI_2 (Fig. 5-5).

When E_2I_2 was mixed with excess of I_2 or I^*_2, EI_2 or EII* was observed, respectively within 10 minutes at room temperature (Fig. 5-6, lanes 1 and 2). Let us consider the case of mixing E_2I_2 and I^*_2. If only the dissociation at the enzyme-inhibitor interface had occurred, equimolar concentration of EI_2 and EII* should have been newly observed (Eq. 5-9).

$$EI_2E + I^*_2 = EI_2 + (EI^*_2 \rightarrow EII^*) \qquad (5\text{-}9)$$

$$EIIE + I^*I^* = 2EII^* \qquad (5\text{-}10)$$

On the other hand, if the dissociation occurred only at the SSI dimer interface, only EII* should be newly observed (Eq. 5-10). The results (Fig. 5-6, lane 2) shows that the latter (Eq. 5-10) is the case in this time scale. However, EI_2 was detected after 6 h of incubation (Fig. 5-6, lane 4); dissociation of the enzyme and the inhibitor must also have occurred, but much more slowly than that of the dimer dissociation (see discussion).

Dissociation rate constant of SSI dimer in enzyme inhibitor complex E_2I_2 - Figure 5-7a shows time dependence of the formation of EI_2 by mixing of equimolar (7 μM) E_2I_2 and I_2 at 26℃ as monitored by the density of spot on PAGE. The rate constant of the dissociation, k_{-1}, was determined with Eq. 5-8 (Fig. 5-7b) to be 3.0×10^{-3} s^{-1} at 26℃, pH 7.0.

Figure 5-8 is the Arrhenius plots of the dissociation rate constants obtained according to Eq. 5-8 for the systems of $E_2I_2 + I_2$ and $E_2I_2 + I^*_2$ together with the values for the system of $I_2 + I^*_2$ (shown in Fig. 5-4). The rate constant of dissociation at the dimer interface of SSI in the E_2I_2 complex was essentially the same, at each temperature (Table 5-3), as that of free I_2, and they have the same activation

(a)

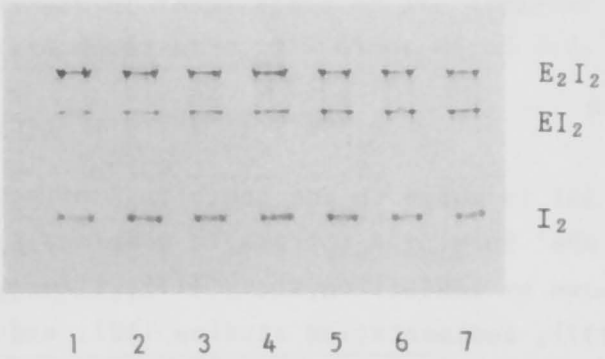

(b)

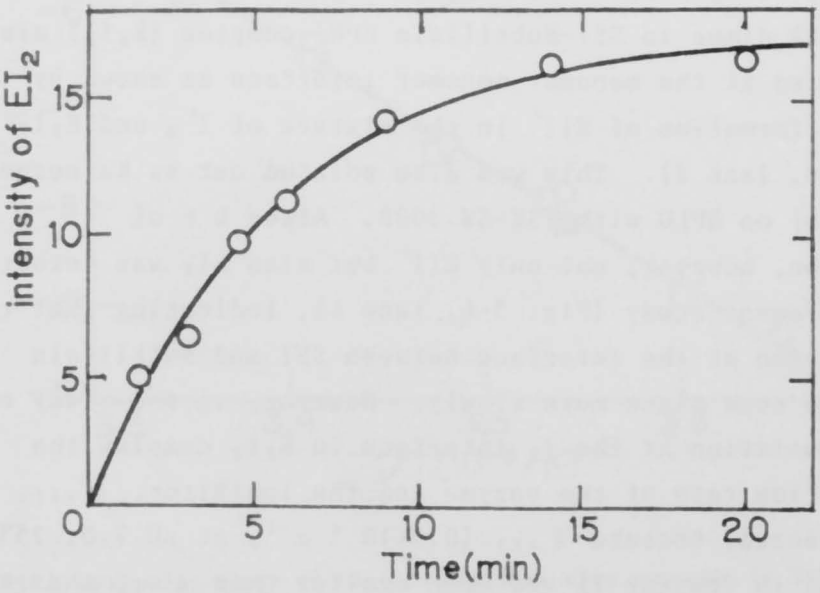

Fig. 5-7. Time course of formation of EI_2. Equal concentration of E_2I_2 complex and I_2 (28 μM) at 26 ℃. (a) PAGE. Reaction times (min) are; For lanes 1-7, the incuvation times were 1.5, 3, 4.5, 6, 9, 14, 20 min, respectively. 9.5 μg protein /lane were applied. (b) Time dependence of density of EI_2 band in PAGE. The solid line is the theoretical curve drown based on Eq. 5-8 with $k_{-1} = 3.0 \times 10^{-3}\ s^{-1}$.

energy (23.8 kcal/mol).

Discussion

A dimer SSI is bound to and inhibits 2 molecules of subtilisin BPN' forming a tetrameric complex, E_2I_2. This has been shown by inhibition study (17), fluorometric titration (57), sedimentation studies (18), and X-ray crystallographic studies (12-13). However, when an excess of the inhibitor exist over the enzyme, a molecular species EI_2, in which only one enzyme molecule is bound to a dimeric SSI is formed (85). Kainosho et al (86) reported that EI_2 gradually forms the species corresponding to I_2 and E_2I_2 to reach a static equilibrium: $2EI_2 = E_2I_2 + I_2$, and this disproportion reaction seems to proceed via dissociation at interface ($2EI_2 = 2EI + 2I = E_2I_2 + I_2$).

The SSI dimer in SSI-subtilisin BPN' complex (E_2I_2) also dissociated at the monomer-monomer interface as shown by the dominant formation of EI^* in the mixture of I^*_2 and E_2I_2 (Fig. 5-6, lane 2). This was also pointed out by Kainosho et al (86) on HPLC with TSK-SW 3000. After 6 h of incubation, however, not only EI^* but also EI_2 was detected in the present study (Fig. 5-6, lane 4), indicating that the dissociation at the interface between SSI and subtilisin BPN' also took place more slowly. However, in the study of the dissociation at the I_2 interface in E_2I_2 complex the dissociation rate of the enzyme and the inhibitor, k_{off}, was neglected, because k_{off} (0.9×10^{-4} s^{-1}, at pH 7.0, 25℃; described in Chapter 1) was much smaller than k_{-1}, the rate constant of SSI dimer dissociation.

The dissociation rate constant (k_{-1}) obtained in the experiments of mixing of E_2I_2 with I_2 or I^*_2 was equal with

TABLE 5-3: Effect of temperature on the apparent dissociation rate constant of SSI dimer at pH 7.0.

T (℃)	$E_2I_2+I_2$ (10^{-4} s^{-1})	$E_2I_2+I^*_2$ (10^{-4} s^{-1})
5	1.3	1.3
10	3.5	2.5
15	5.6	6.0
20	17	14
26	30	36

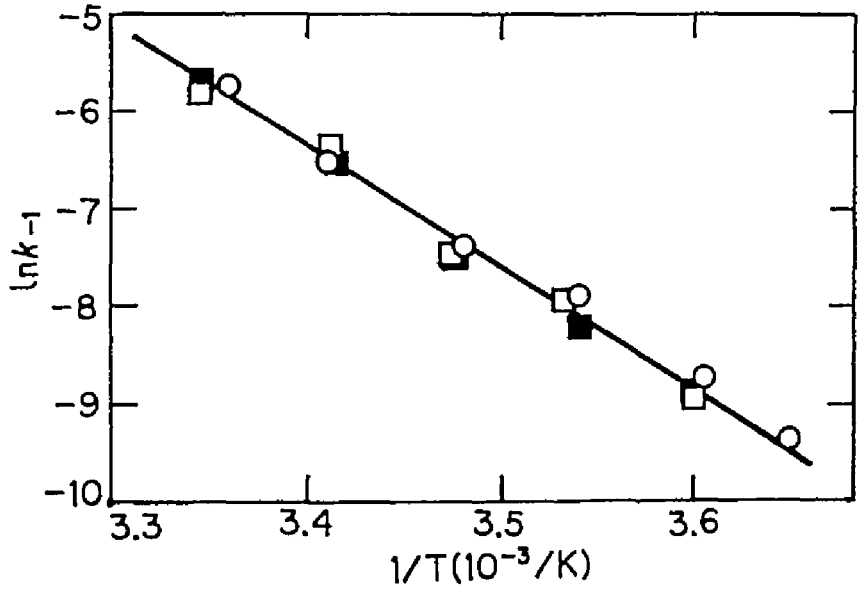

Fig. 5-8. Arrhenius plots of the dissociation rate constant of SSI dimer, k_{-1}, at pH 7.0.
○, $I_2 + I^*_2$; □, $E_2I_2 + I_2$; ■, $E_2I_2 + I^*_2$.

that obtained in the experiment of mixing of I_2 and I^*_2 (Fig. 5-8). These results suggest that the dissociation rate constants of I_2 and E_2I_2 at the dimer interface are equal (Table 5-3), namely that SSI dimer dissociates at the same rate both in the free form and in the form complexed with enzymes. This view is supported by the results of NMR (74) and X-ray crystallographic (13) studies that the β-sheets structure at dimeric interface of SSI has little change between free and enzyme bound SSI.

An interesting question in the SSI studies has been whether or not the monomeric SSI can inhibit the enzyme. SSI is a globular protein in the dimer structure (Fig. 5-1) which has been regarded necessary to keep the very stable structure and the strong inhibitory activity. The momentary dissociation of E_2I_2 complex into 2EI was revealed in the present study, and the monomeric SSI may inhibit an enzyme within a very short time.

Appendix-2
Thermal denaturation of SSI

Thermal denaturation of SSI has been studied by differential scanning calorimetry (DSC), and it was reported that the denaturation obeyed two state transition scheme (79);

$$N_2 \rightleftharpoons 2D \qquad (5\text{-}11)$$

in which N and D mean native and denatured protein, respectively. That means that SSI forms dimer in native state and monomer in denatured state.

In this paragraph, thermal denaturation of SSI* and the mixture of equimoler of SSI and SSI* was studied by DSC at pH 7.0. Calorimetric measurements (91) were made with DASM-4 scanning microcalorimeter at the temperature scanning rate of 1 K/min. The inhibitor concentration was 0.9 mg/ml in 25 mM phosphate buffer pH 7.0 (I = 0.1 M, NaCl).

Excess heat capacity curves for the thermal transition of SSI, SSI* and the mixture of SSI and SSI* at pH 7.0 are shown in Fig. 5-9. The peak temperatures of denaturation, T_p, of SSI and SSI* were 81.3 and 68.4℃, respectively. The curves of SSI and SSI* were fitted the theoretical curve in which the two state transition of dimer to monomer (Eq. 5-11). Excess heat capacity curves for the mixture of SSI and SSI* showed two peaks assigned to SSI* and SSI. When SSI and SSI* are mixed, II* should occur. So it was shown that SSI subunit denature independently.

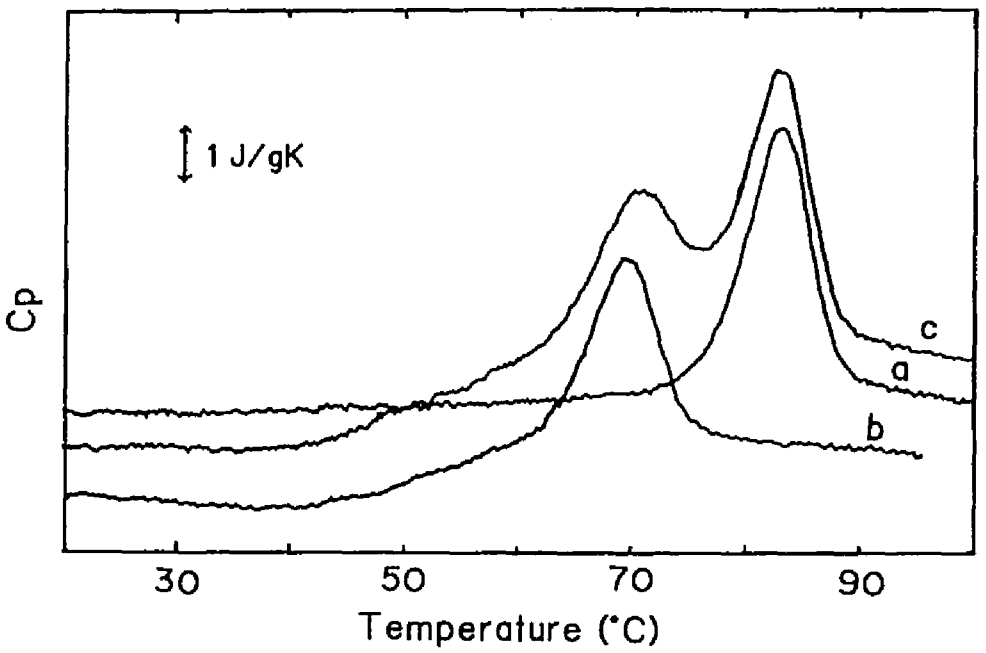

Fig. 5-9. Differential scanning calorimetry curves for SSIs at pH 7.0. Temperature scanning rate was 1 K/min. a, SSI; b. SSI*; c, SSI+SSI*.

Chapter 6

Role of Pro residues at around the reactive site of Streptomyces Subtilisin Inhibitor - Effects on the interaction with subtilisin BPN' and conformational stability

Streptomyces subtilisin inhibitor (SSI) is a proteinaceous proteinase inhibitor which inhibits strongly bacterial alkaline serine proteinases such as subtilisin BPN'. There are two Pro residues around the reactive site peptide bond, which are conserved in Kazal type serine proteinase inhibitor and natural mutant of SSI (Fig. 6-1) (87).

The interaction of SSI and subtilisin BPN' is considered to obey the standard mechanism of interaction of serine proteinase with inhibitor, which has been proposed as eq. 6-1:

$$E + I \underset{k_{off}}{\overset{k_{on}}{\rightleftharpoons}} EI \underset{k_{-c}}{\overset{k_{+c}}{\rightleftharpoons}} EI^* \underset{k_{on}^*}{\overset{k_{off}^*}{\rightleftharpoons}} E + I^* \qquad (6\text{-}1)$$

where E, I, I*, EI, and EI* represent an enzyme, an inhibitor, a modified inhibitor in which the reactive site peptide bond was cleaved, an enzyme-inhibitor complex, and an enzyme-modified inhibitor complex, respectively; and k_{on} and k_{on}^* are the association rate constants, k_{off} and k_{off}^* are dissociation rate constant, respectively. The rate constants of cleavage and resynthesis are represented in k_{+c} and k_{-c}, respectively. The stable complex of SSI-subtilisin BPN' is in the form of Michaelis complex (EI), in which the inhibitor and the target enzyme binds noncovalently (12-14).

Proline residues restrict the conformational freedom of the backbone of polypeptide chains (88), and are expected to

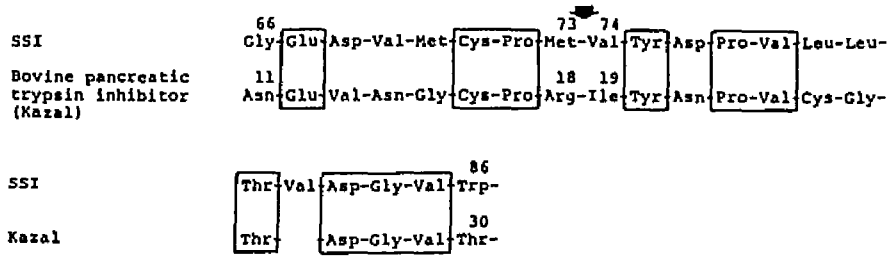

Fig. 6-1. Homology in the amino acid sequences of SSI and bovine pancreatic secretory trypsin inhibitor (Kazal) (87) .

stabilize protein structure by decreasing the conformational entropy of denaturation (89). In this study two Pro residues (Pro72 and Pro77) in SSI were replaced by Ala to investigate their role on structure and function of SSI. Equilibrium and kinetic parameters in the interaction of the Pro mutated SSI were compared with wild type SSI. Changes in the conformations and stability of intact and modified mutant SSIs were investigated by means of differential scanning calorimetry, CD and fluorescence study.

MATERIALS AND METHODS

Proteins - A subtilisin BPN' (EC 3.4.21.14) (lot No. 7370935) and SSI (SSI wild type (SSI(wt))) were prepared as described in Chapter 1. Mutant SSIs (SSIP72A, SSIP77A, and SSIP72A/P77A) were made by site-directed mutagenesis as described below and purified from the culture media by the method described previously in Chapter 1.

The protein concentration was determined spectrophotometrically as described in Chapter 1. SSI concentration in the text is represented as monomer concentration unless otherwise mentioned. Modified SSI (SSI*) was purified by the method of Tonomura (66) and

Chapter 3.

Site-directed mutagenesis of SSI gene - The mutations of Pro72 to Ala (SSIP72A) and Pro77 to Ala (SSIP77A) were performed by site-directed mutagenesis of a plasmid pSIAX (90). The mutagenic primers used for mutations are 5' TC-ATG-TGC-GCG-ATG-GTG 3' for Pro72 to Ala and 5' TG-TAC-GAC-GCG-GTG-CTG 3' for Pro77 to Ala where the asterisks indicate the mismatched bases. The plasmid pSIAX72A77A was obtained by codon substitution at Pro72 with Ala of pSIAX77A in which the Pro77 codon had been replaced by Ala codon. Mutations were verified by dideoxy sequencing (52) of the mutated plasmid. Reconstruction of mutated pSI52 from mutated pSIAX, and insertion of the SSI gene into streptomycete plasmid pIJ702, followed by transformation of S. lividans 66 were carried out as described previously (28).

Measurement of kinetic and static parameters - K_i, k_{on}, and k_{off} were determined as described in Chapter 1. K_{hyd} was determined as described in Chapter 3. The resynthesis rate constant, k_{-c}, was determined as described in Chapter 4.

CD measurement - The CD spectra were recorded with a Jasco J-720 spectropolarimeter. Spectra were scanned 3 times at the scan rate of 1 nm/min. The spectra were measured at inhibitor concentrations of 1.0 mg/ml in 25 mM phosphate buffer pH 7.0, using a cell of 0.1 mm (200-260 nm) or 10 mm (250-320 nm) light-path length at 25°C.

Calorimetric measurements - Calorimetric measurements (91) were made with DASM-4 scanning microcalorimeter at the temperature scanning rate of 1 K/min. The inhibitor concentration was 1.0 mg/ml in 25 mM phosphate buffer pH 7.0 (I = 0.1 M, NaCl).

Fluorescence study - Fluorescence intensity of the SSI-subtilisin BPN' complex was measured at 340 nm with

excitation at 280 nm with a Hitachi fluorescence spectrophotometer 850 at 25℃. Inhibitor solution (2μ M) in 25 mM phosphate buffer pH 7.0 was titrated by HCl and pH values was measured.

RESULTS

Interaction of SSIs with subtilisin BPN' - Equilibrium and kinetic parameters for the interaction of mutant SSIs and subtilisin BPN' are summarized in Table 6-1. There is no difference in the inhibitor constants, K_i, between SSI(wt) and Pro mutated SSIs. Further similar kinetic parameters of association (k_{on}) and dissociation (k_{off}) of intact (reactive site peptide bond is not cleaved) SSIs were obtained. These results indicate that these Pro residues (Pro72 and Pro77) of SSI make little contribution to the interaction between intact inhibitor and subtilisin BPN'. As for modified (reactive site peptide bond cleaved) inhibitors (SSI*), however, association rate constants (k_{on}*) were decreased compared with intact SSIs and the value of k_{on}* of SSIP72A/P77A* was decreased compared to SSI*. The equilibrium constants of hydrolysis, K_{hyd}, for SSIP77A and SSIP72A/P77A, were 1.5 and 1.9, respectively and they are more than unity (Fig. 6-2). Further these three mutant SSIs were digested by 30 mol% of subtilisin BPN' within 30 days and modified inhibitors were digested faster than intact form. The resynthesis rate constants, k_{-c}, of all Pro mutated SSIs were around 1 s^{-1}, twice as much as that of SSI(wt). This means that mutant SSIs are resynthesized faster than that of SSI(wt). The half-life of resynthesis was calculated to be 0.7 s and 1.4 s for mutant SSIs and SSI(wt), respectively. The resynthesis rate was

TABLE 6-1. Equilibrium and kinetic parameters for the binding of subtilisin BPN' and inhibitors, at pH 7.0, 25℃.

	K_i (10^{-11}M)	k_{on} (10^6/(M·s))	k_{off} (10^{-4}/s)	k_{-2} (/s)	K_{hyd}
SSI(wt)	1.8(±0.3)[a]	6.5(±0.1)[a]	0.9(±0.2)[a]	0.45	0.3
SSIP72A	0.6	5.9(±0.2)	1.4(±0.2)	1.2	0.3
SSIP77A	1.4	6.3	2.9	1.1	1.5
SSIP72A/P77A	1.5	4.6(±0.3)	2.7(±0.4)	1.0	1.9
SSI(wt)*	ND	3.6(±0.07)[b]	ND		
SSIP72A*	ND	2.3(±0.08)[b]	ND		
SSIP77A*	ND	1.8(±0.07)[b]	ND		
SSIP72AP77A*	ND	1.3(±0.05)[b]	ND		

[a]reported in Chapter 1; [b]calculated by Eq. 1-11 ; ND, not determined

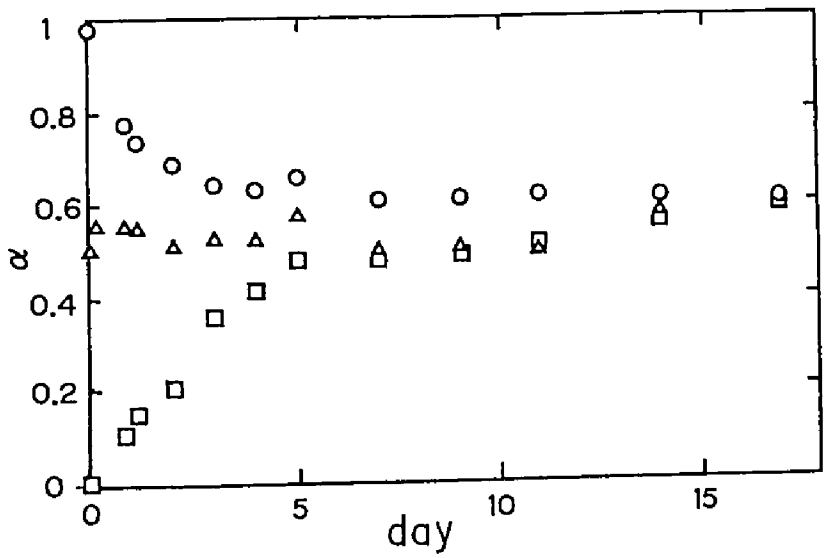

Fig. 6-2. Time course the fraction α (=[I*]/([I]+[I*])) of SSIP77A* at pH 7.0, 25℃. $[I]_0$ = 40 μM, $[E]_0$ = 12 μM. Starting conditions: ○, α = 1; △, α = 0.5; □, α = 0.

not obtained k_{off}* and K_i* (=[E][I*]/[EI*]) by the methods in this text (see Discussion).

Calorimetric studies on the mutant SSIs - Excess heat capacity curves for the thermal transition of all SSI derivatives at pH 7.0 are shown in Fig. 6-3. The peak temperatures of denaturation, T_p, the calorimetric enthalpies, ΔH_{cal}, and the van't Hoff enthalpies, ΔH_{vH}, are listed in Table 6-2. T_p values of Pro mutated SSIs were decreased in the order of SSIP72A/P77A, SSIP77A, and SSIP72A compared to the T_p value of SSI(wt) that exceeds 80℃ as reported previously (79). These results suggest that substitutions of Pro residues affect the heat denaturation process of SSI. The T_p values of modified SSIs were decreased similarly to the order of T_p of intact inhibitors. The reversibility of the thermal denaturation of SSI* was confirmed by reheating the protein solution in the calorimeter cell immediately after cooling from the first run. All curves were fitted the theoretical curve in which the two state transition of dimer to monomer was assumed: $N_2 \rightleftharpoons 2D$ (6-2) in which N and D mean native and denatured protein, respectively.

CD spectra - The CD spectra of inhibitors in the region of 200-260 nm at pH 7.0, 25℃ are shown in Fig. 6-4. There is little difference among CD spectra of intact three Pro mutant SSIs. However, the negative CD values of SSI* was a little decreased and that of modified mutant SSIs were remarkably decreased, suggesting that the secondary structure content of SSI was reduced by replacing Pro residue by Ala. The CD spectra in the aromatic region (260-320 nm) of all the inhibitors were similar.

Acid denaturation - Acid denaturation of SSIs at 25℃ were monitored by fluorescence intensity (Fig. 6-5). It was reported that the fluorescence of Trp86, the sole Trp

TABLE 6-2. Summary of DSC data for SSI unfolding at pH 7.0.

	T_p (°C)	ΔH_{cal} (cal/mol)	ΔH_{vH} (cal/mol)
SSI(wt)	81.27	82.2	82.2
SSIP72A	79.05	79.7	79.7
SSIP77A	72.53	68.8	71.8
SSIP72A/P77A	69.49	62.4	67.9
SSI(wt)*	68.35	68.1	71.1
SSIP72A*	68.39	59.6	64.8
SSIP77A*	65.10	69.9	57.8
SSIP72AP77A*	63.80	57.1	57.1

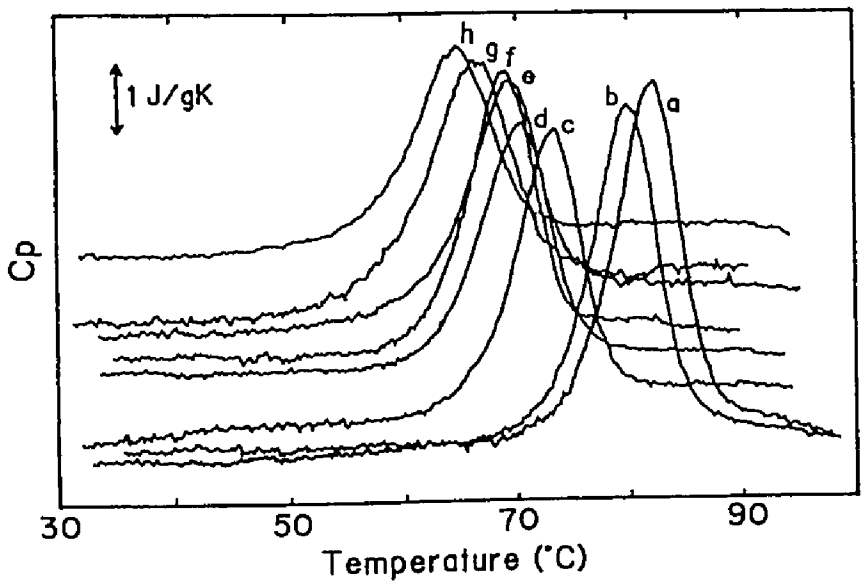

Fig. 6-3. Differential scanning calorimetry curves for SSIs at pH 7.0. Temperature scanning rate was 1 K/min. a, SSI; b. SSIP72A; c, SSIP77A; d, SSIP72A/P77A; e, SSI*; f. SSIP72A*; g, SSIP77A*; h, SSIP72A/P77A*.

residue in SSI, is strongly quenched in the native state, and a large increase in the Trp fluorescence was brought about upon denaturation by lowing pH (57). The fluorescence intensity of Pro mutated SSIs at below pH 3 were higher than that of SSI, and SSIP72A/P77A began to denature at pH 4, 1 more unit than SSI(wt). SSI* also began to denature at higher pH than did intact SSI and showed higher fluorescence intensity. Modified mutant SSIs showed similar pH profiles of acid denaturation to SSI*; however, the fluorescence intensity of SSIP72A/P77A* was higher than that of other inhibitors at pH 7.0, indicating more denatured structure at neutral pH.

DISCUSSION

Generally, the strength of proteinase inhibitor is evaluated by the inhibitor constant in the simplest binding mechanism represented as below:

$$E + I \underset{k_{off}}{\overset{k_{on}}{\rightleftharpoons}} EI \quad (6\text{-}3), \qquad K_i = \frac{[E][I]}{[EI]} = \frac{k_{off}}{k_{on}} \quad (6\text{-}4).$$

There were no difference in these kinetic and equilibrium parameters between SSI(wt) and Pro mutant SSIs (Table 6-1), that means these Pro residues (Pro72 and Pro77) of SSI have little contribution to the interaction between intact inhibitor and subtilisin BPN'. The author investigated the interaction including modified Pro mutant inhibitors, and some differences were obtained (Table 6-1). At first, the equilibrium constants of hydrolysis, K_{hyd}, were increased to larger than unity for SSIP77A and SSIP72A/P77A, indicating that modified form is thermodynamically more stable than intact form in these cases, which is contrary to the case of SSI(wt). The small K_{hyd} values at neutral pH

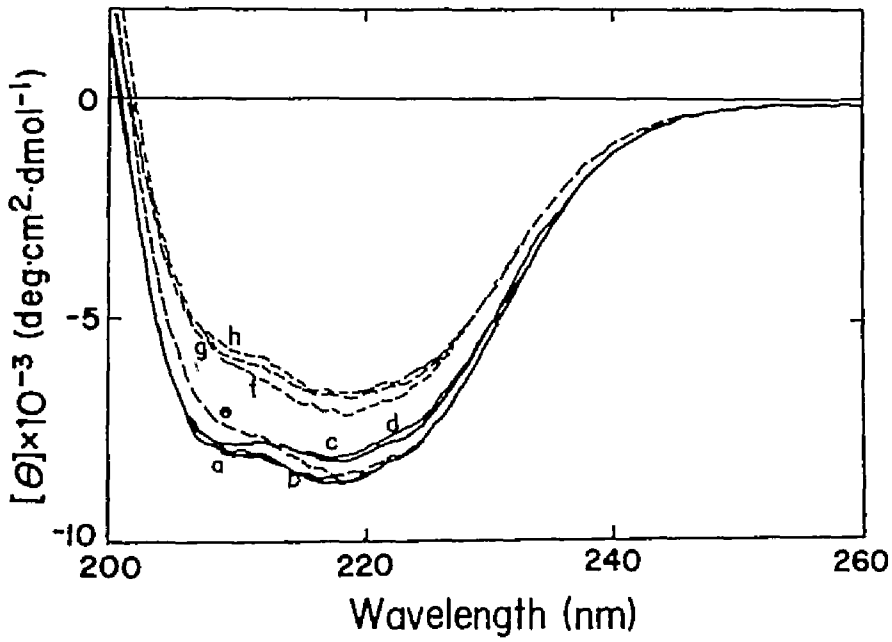

Fig. 6-4. CD spectra of SSIs at pH 7.0, 25℃. a, SSI; b. SSIP72A; c, SSIP77A; d, SSIP72A/P77A; e, SSI*; f. SSIP72A*; g, SSIP77A*; h, SSIP72A/P77A*.

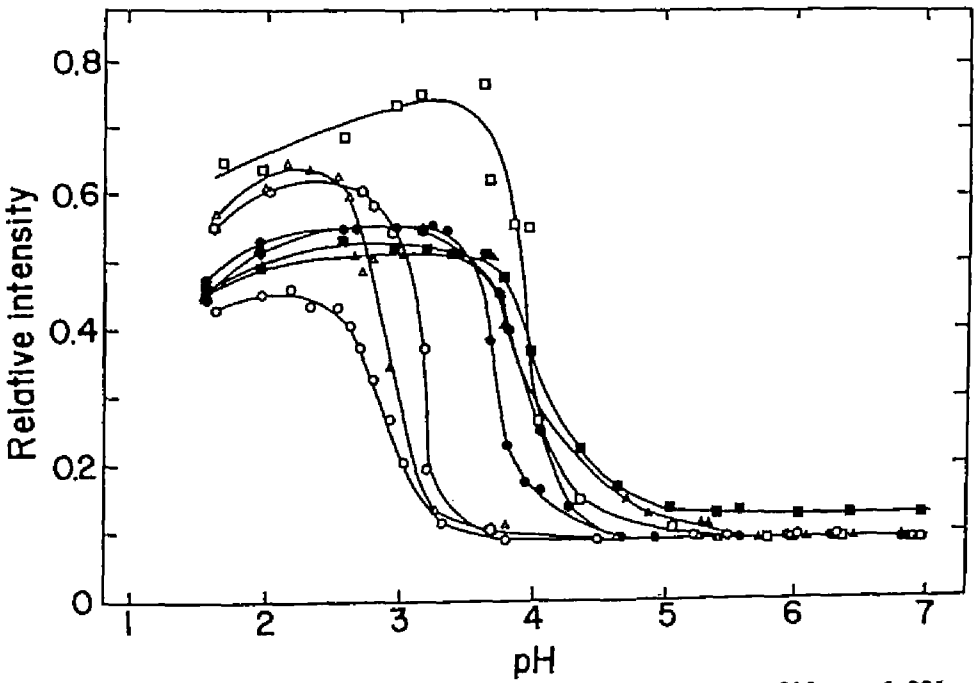

Fig. 6-5. pH dependence of the fluorescence intensity at 340 nm of SSIs at 25℃. $[I]_0$ = 2.0 μM. Excitation at 280 nm. The desired pH was obtained by adding HCl to the solvent at neutral pH of phosphate buffer. ○, SSI; ○ . SSIP72A; △, SSIP77A; □, SSIP72A/P77A; ●, SSI*; ● . SSIP72A*; ▲, SSIP77A*; ■, SSIP72A/P77A*.

were reported only for the Kazal type serine proteinase inhibitors (62). Homology in the amino acid sequences of SSI and Kazal type inhibitors was reported, in which these Pro residues at around the reactive site are conserved (87). They are assumed to contribute to the small K_{hyd} value. Double mutated SSI had the largest K_{hyd} value, but it seems that Pro77 has more important role than Pro72. This tendency was also observed on the conformational stability study described in Results. Although there is a disulfide bond next to the Pro72 (Cys71-Cys101) to link the reactive site peptide bond to the core region, Pro77 is located at the end of β4-sheet, so that these results seem to be reasonable. Recently, many natural mutants of SSI are discovered from Streptomyces (92), and these Pro residue especially at the position of 77 of SSI are completely conserved (Taguchi et al., personal communication).

The resynthesis rate of the reactive site peptide bond (EI*→EI), k_{-c}, of Pro mutated SSIs were larger than that of SSI(wt), and it is speculated that the energy barrier of the equilibrium between EI and EI* of mutants would be smaller than that of SSI(wt); accordingly the scissile bond would be more easily cleaved and resynthesized in the case of mutants. The k_{-c} values are considerably fast for four inhibitors. This means that EI complex is more stable than EI* complex, and it is calculated that EI* changes to EI within 15 sec. When SSI*s and subtilisin BPN' were used in the experiment to obtain k_{on}* and k_{off}* or K_i*, it would take more than 20 min for measurement, which is enough for EI* to change to EI, so that one could not obtain k_{off}* and K_i* (= [E][I*]/[EI*]) directly. The small k_{on}* value obtained (see Methods) for SSIP72A/P77A* represents the weakness as an inhibitor.

Differences in the interaction with subtilisin BPN' were

observed especially with the modified form of Pro mutant SSIs as mentioned above, so that the stability of these intact and modified mutants were investigated. The differences of T_p values of heat denaturation compared to that of SSI(wt) were 2.22, 8.74, and 11.78℃ decrease for SSIP72A, SSIP77A and SSIP72A/P77A, respectively. Thus Pro72 and Pro77 seem to contribute to the stability of heat denaturation independently. The T_p value of SSI* decreased 12.92℃ from T_p of SSI(wt), indicating that the thermal stability of SSI was decreased by one nick in the globular protein. The T_p values of modified Pro mutants were also decreased, and these Pro residues seem to contribute to the stability of protein core. The ΔH_{cal} values of each modified inhibitor was also reduced compared with intact form. All the calorimetric curves were fitted to the theoretical curve led from Eq. 6-2, which indicated that native and denatured form are dimer and monomer, respectively. Two polypeptide fragments of SSI* are still linked by disulfide bond (Cys71-Cys101), that supports the results of analysis and reheating experiment of SSI*.

Judging form CD spectra in the far-UV region (200-260 nm), the secondary structure of the three intact Pro mutants were not affected at pH 7.0, 25℃. For the modified proteins, however, the negative CD values were decreased significantly. These results suggest that the secondary structure of the Pro mutated SSIs were destroyed in the modified form and that these Pro residues located around the reactive site peptide bond play important role in maintaining the structure of modified inhibitor.

The fluorescence intensity of SSIP72A/P77A* was higher than that of other inhibitors at pH 7.0, indicating it was a little denatured even at neutral pH, 25℃ and that was supported by the CD spectrum although the fluorescence

intensity of SSIP72A* and SSIP77A* were not affected at pH 7.0. The higher fluorescence intensity of Pro mutated SSIs at acid condition (less than pH 3) indicated that they were more denatured in acid condition, and that fluorescence of Trp86 which was strongly quenched in the native state has appeared. There are another interesting results which were obtained for modified inhibitors. All the modified species, wild-type and Pro mutants as well, showed rather similar pH dependence of fluorescence intensity, whereas in the intact species replacement of those Pro residues have resulted in significant difference of fluorescence behaviors.

The present results indicate that the conserved Pro residues of SSI play roles in the conformational stability especially in the cases of the modified (reactive site peptide bond cleaved) form. The role of Pro residue on conformational stability were investigated in some proteins. Substitution of conserved Pro of tryptophan synthase α subunit by Ala or Gly (93), and of nucleoside diphosphate kinase (94) by Ser decreased stability. In contrast, introduction of Pro to Bacillus stearothermophilus neutral protease (95) and T4 lysozyme increased stability.

One of the reasons why SSI is a very strong inhibitor is considered that SSI* is still stable protein and it can inhibit the enzyme. However, these Pro mutants were digested, especially faster in the case of modified form, by catalytic amounts of proteinases. From these results, it is considered that these conserved Pro residues cause the stability of not only intact SSI but also modified SSI in order not to accept the attack by proteinases.

SUMMARY

Chapter 1

Kinetic analysis was performed on the interaction between subtilisin BPN' and recombinant species of a proteinaceous proteinase inhibitor, Streptomyces subtilisin inhibitor (SSI) of which the P_1 site amino acid residue, Met73, was replaced by site-directed mutagenesis. The inhibitor constant, K_i, was determined from the residual enzyme activity by using a peptide substrate. The rate constant of binding, k_{on}, and the rate constant of dissociation, k_{off}, were determined from a progress curve of the substrate hydrolysis in the presence of the inhibitor by using newly derived equations. A recombinant SSI in which Met73 was replaced by Ile showed an affinity ($1/K_i$) toward subtilisin BPN' of only about 7% of that of the wild-type SSI, and the kinetic analysis revealed that the increase of k_{off} was responsible for this difference. The affinity of other SSI mutants in which Met73 was replaced by Glu or Asp decreased significantly as pH became increasingly alkaline. The decrease in the affinity of these recombinants was due to the decrease of k_{on} rather than the increase of k_{off}. Stopped-flow studies revealed that the binding reaction was reconcilable with a two-step mechanism, and the kinetic parameters for each step were obtained for the binding of the enzyme and recombinant SSIs.

Chapter 2

An ultraviolet absorption difference spectrum characteristic of the ionization change of a tyrosyl residue was observed on the binding of subtilisin BPN' with Streptomyces subtilisin inhibitor (SSI) at alkaline pH. This difference spectrum was considered to be induced by a

pK_a shift (from 9.7 to ≧ 11.5) of a tyrosyl residue of subtilisin BPN' in the interaction with carboxyls of SSI (Inouye et al., (1979) J. Biochem. 85, 1115-1126). In the present study, the tyrosyl residue in subtilisin BPN' and the carboxyls in SSI were identified by analyzing the difference spectrum using mutants of subtilisin BPN' and SSI: naturally occurring mutants and those prepared by site-directed and cassette mutagenesis. The difference spectrum disappeared on the binding of a mutant subtilisin BPN' of which Tyr104 was replaced by Phe (S-BPN'Y104F) and SSI at pH 9.8. The magnitude of the absorption difference was much smaller when subtilisin BPN' was bound with a mutant SSI of which both Glu67 and Asp68 were replaced by Gly than with the wild-type SSI. These lines of evidence indicated that the difference spectrum was caused by Tyr104 of subtilisin BPN' interacting with Glu67 and Asp68 of SSI.

The binding of subtilisin BPN' and SSI is accompanied by an increase of tryptophan fluorescence, which is pH-dependent in the range of pH 7-11 (Uehara et al., (1978) J. Biochem. 84, 1195-1202). In the present study, this pH-dependence of the fluorescence diminished when SSI bound with S-BPN'Y104F. This suggested that the fluorescence increase was due to Trp106 of subtilisin BPN' and was influenced by the ionization of Tyr104.

Chapter 3

The pH dependence of the equilibrium constant K_{hyd} for the hydrolysis of the reactive site peptide-bond of proteinaceous proteinase inhibitor, Streptomyces subtilisin inhibitor (SSI) was investigated over the pH range 3-9.5. Solutions of SSI, modified SSI (SSI*) with the Met73-Val74 peptide bond cleaved, and mixture of both species were incubated with catalytic amount of subtilisin BPN. The

state of equilibrium was determined by polyacrylamide gel electrophoresis at pH 9.4. The K_{hyd} values obtained essentially obey the equation of Dobry et al. ((1952) J. Biol. Chem. 195, 149-155). The pH-independent equilibrium constant was obtained to be 0.37, indicating that the intact form is thermodynamically more stable than the modified form. The pK_a values of the Met73 carboxyl group and of the Val74 amino group, which were newly appeared in the modified species, were 3.6 and 9.0, respectively.

Chapter 4

Apparent rate constant of resynthesis of the cleaved reactive site (Met73-Val74) of modified Streptomyces subtilisin inhibitor, by subtilisin BPN' was determined to be 0.45 s^{-1} at pH 7.0, 25℃. Formation of the intact inhibitor was followed as a function of time after mixing of the modified inhibitor and subtilisin BPN'. A simple apparatus with three sets of pulse-motor driven pumps was constructed for this purpose. The reaction was found to be first order and yielded predominantly intact inhibitor. It is considered that the reactive site of Streptomyces subtilisin inhibitor is intact in the most stable complex with subtilisin BPN' and that this agrees with the results by X-ray crystallographic study and NMR study.

The dissociation constant of subtilisin BPN'-SSI* complex to subtilisin BPN' and SSI*, K_i*, was obtained to be 2.5×10^{-6} M from the analysis of reactant concentration dependence of apparent rate constant of resynthesis. The overall equation of the interaction of SSI and subtilisin BPN' was discussed.

Chapter 5

Streptomyces subtilisin inhibitor (SSI), a proteinaceous inhibitor of subtilisin, is a stable homodimer of molecular weight with 23000. The rate constant of dissociation of the dimer into monomers was determined by measuring the rate of formation of a heterodimer (II*) formed by mixing SSI (I_2) and modified SSI (I^*_2) in which the reactive site against subtilisin BPN' was cleaved. The rate constant was 3.2×10^{-3} s^{-1} at pH 7.0, 25 ℃. The activation energy for the dissociation was 23.8 kcal/mol. SSI inhibits subtilisin BPN' strongly by forming an E_2I_2 complex in which two molecules of subtilisin BPN' (E) are bound to an SSI dimer (I_2). However, EI_2 and EI^*, in which only one subtilisin molecule was bound to I_2 and I^*_2, respectively, were formed under the conditions of $2[E] < [I_2]$ and $2[E] < [I^*_2]$, respectively. When E_2I_2 and I^*_2 were mixed, only EI^* but no EI_2 was detected first. This indicates that dissociation-association of SSI at the dimer interface occurs also in the SSI-subtilisin BPN' complex, and the rate constants and activation parameters for the dissociation of the complex were found similar to those obtained for free SSI (I_2).

Excess heat capacity curves for the equimoler mixture of SSI and SSI* showed two peaks and this suggests that SSI subunit denatures independently.

Chapter 6

There are two proline residues in Streptomyces subtilisin inhibitor (SSI) (Pro72 and Pro77), which frank both sides of the reactive site peptide bond (Met73-Val74) and are conserved in Kazal type serine proteinase inhibitor. These Pro residues were replaced by Ala by site directed mutagenesis to study their role on the interaction with

subtilisin BPN' and conformational stability of the protein. There was no difference in inhibitory activity of three mutant SSIs with Ala in place of Pro (SSIP72A, SSIP77A and SSIP72A/P77) against subtilisin BPN', but larger K_{hyd} was obtained for SSIP77A and SSIP72A/P77A. The far UV CD spectra of these mutants were identical to the spectrum of the wild type SSI (SSI(wt)); however, the negative CD values of modified inhibitors in which reactive site peptide bond was cleaved were decreased. The rate of resynthesis of cleaved reactive site peptide bond was of each mutant SSIs twice of that of SSI(wt).

Peak temperature of thermal denaturation obtained by calorimetric measurements of these mutants were decreased and modified mutant SSIs further decreased. The decreases of stability for acid were observed on these mutant proteins monitored by the fluorescence intensity of tryptophan residue. These Pro residues seem to contribute to the stability of SSI and to play not to be digested by proteinase as inhibitor.

References

1. Gebhard, W. & Hochstrasser, K. (1986) in Proteinase Inhibitors (Barrett & Salvesen, Eds.) pp 389-401, Elsevier, Amsterdam.
2. Carrell, R. W. (1988) Nature 331, 478-479
3. Laskowski, M., Jr. & Sealock, R. W. (1971) in The Enzymes 3rd. Ed. vol Ⅲ Hydrolysis: Petide bonds (Boyer, P. D. Ed.) pp 375-473, Academic Press, New York
4. Read, R. J. & James, M. N. G. (1986) in Proteinase Inhibitors (Barrett & Salvesen, Eds.) pp 301-336, Elsevier, Amsterdam
5. Kunitz, M. & Northrop J.H. (1936) J. Gen. Physiol. 19, 991-1007
6. Laskowski, M., Jr. & Kato, I. (1980) Ann. Rev. Biochem. 49, 593-626
7. Murao, S. & Sato, S. (1972) Agric. Biol. Chem. 36, 160-163
8. Hiromi, K., Akasaka, K., Mitsui, Y., Tonomura, B., & Murao, S. (1985) Protein Protease Inhibitor - The Case of Streptomyces Subtilisin Inhibitor (SSI), Elsevier, Amsterdam
9. Ikenaka, T., Odani, S., Sakai, M., Nabeshima, Y., Sato, S. & Murao, S. (1974) J. Biochem. 76, 1191-1209
10. Mitsui, Y., Satow, Y., Sakamaki, T., & Iitaka, Y. (1977) J. Biochem. 82, 295-298
11. Mitsui, Y., Satow, Y., Watanabe, Y., & Iitaka, Y. (1979) J. Mol. Biol. 131, 697-724
12. Hirono, S., Akagawa, H., Mitsui, Y., & Iitaka, Y. (1984) J. Mol. Biol. 178, 389-413
13. Takeuchi, Y., Satow, Y., Nakamura K., & Mitsui, Y. (1991) J. Mol. Biol. 221, 309-325
14. Kainosho, M. & Tsuji, T. (1985) in Protein Protease

Inhibitor - The Case of Streptomyces Subtilisin Inhibitor (SSI), (Hiromi, K., Akasaka, K., Mitsui, Y., Tonomura, B., & Murao, S. Eds.) pp 322-332, Elsevier, Amsterdam

15. Obata, S., Taguchi, S., Kumagai, I., & Miura, K. (1989) J. Biochem. 105, 367-371
16. Obata, S., Furukubo, S., Kumagai, I., Takahashi, H., & Miura, K. (1989) J. Biochem. 105, 372-376
17. Inouye, K., Tonomura, B., Hiromi, K., Sato, S., & Murao, S. (1977) J. Biochem. 82, 961-967
18. Inouye, K., Tonomura, B., Hiromi, K., Kotaka, T., Inagaki, H., Sato, S., & Murao, S. (1978) J. Biochem. 84, 843-853
19. Sato, S. & Murao, S. (1973) Agric. Biol. Chem. 37, 1067-1074
20. Sato, S. & Murao, S. (1974) Agric. Biol. Chem. 38, 587-594
21. Omichi, K., Nagura, N., & Ikenaka, T. (1980) J. Biochem. 87, 483-489
22. Marquart, M., Walter, J., Deisenhofer, J., Bode, W. & Huber, R. (1983) Acta Crystallogr. B39, 480-490
23. Read, R. J., Fujinaga, M., Sielecki, A. R., & James, M. N. G. (1983) Biochemistry 22, 4420-4433
24. McPhalen, C. A. & James, M. N. G. (1988) Biochemistry 27, 6582-6598
25. Schechter, I. & Berger, A. (1967) Biochem. Biophys. Res. Commun. 27, 157-162
26. Empie, M. W. & Laskowski, M., Jr. (1982) Biochemistry, 21, 2274-2284
27. Longstaff, C., Campbell, A. F., & Fersht. A. R. (1990) Biochemistry, 29, 7339-7347
28. Kojima, S., Nishiyama, Y., Kumagai, I., & Miura, K. (1991) J. Biochem. 109, 377-382

29. Bender, M. L., Begué-Cantón, M. L., Blakeley, R. L., Brubacher, L. J., Feder, J., Gunter, C. R., Kézdy, F. J., Killheffer, J. V., Jr., Marshall, T. H., Miller, C. G., Roeske, R. W., & Stoops, J. K. (1966) J. Amer. Chem. Soc. 88, 5890-5913
30. Markland, F. S. & Smith, E. L. (1967) J. Biol. Chem. 242, 5198-5211
31. Tashiro, M., Kihira, Y., Katayama, Y., & Maki, Z. (1989) Agric. Biol. Chem. 53, 443-451
32. Bieth, J. (1974) in Bayer Symposium V, "Proteinase Inhibitors" (Fritz, H., Tschesche, H., Greene, L. J., and Truscheit, E. Eds.) pp 463-469, Springer-Verlag, Berlin
33. Schweitz, H., Vincent, J. P., & Lazdunski, M. (1973) Biochemistry 12, 2841-2846
34. Guggenheim, E. A. (1926) Phil. Mag. 2, 538
35. Green, N. M. (1957) Biochem. J. 66, 407-415
36. Eigen, M., and De Maeyer, L. (1974) in Techniques of Chemistry (Weissberger, A., Ed.) 3rd ed., Vol. 6, Pt. Ⅱ, pp 63-146, Wiley, New York
37. Williams, J. W. & Morrison, J. F. (1979) in Methods in Enzymology 63 (Purich, D. L. Ed.) pp 437-467, Academic Press, London
38. Zhou. J-M., Liu, C., & Tsou, C-L. (1989) Biochemistry 28, 1070-1076
39. Uehara, Y., Tonomura, B., & Hiromi, K. (1980) Arch. Biochem. Biophys. 202, 250-258
40. Matsumori, S., Tonomura, B., & Hiromi, K. (1981) Nippon Nogeikagakukai Taikaikouenyoushishu 56, 457 (in Japanese)
41. Wells, J. A., Cunningham, B. C., Graycar, T. P., & Estell, D. A. (1987) Proc. Natl. Acad. Sci. USA 84, 5167-5171

42. Matsubara, H., Kasper, C. B., Brown, D. M., & Smith, E. L. (1965) J. Biol. Chem. 240, 1125-1130
43. Inouye, K., Tonomura, B., & Hiromi, K. (1979) J. Biochem. 85, 1115-1126
44. Uehara, Y., Tonomura, B., & Hiromi, K. (1978) J. Biochem. 84, 1195-1202
45. Tonomura, B., Uehara, Y., Inouye, K., & Hiromi, K. (1979) Abstracts of 2nd Annual Meeting of Japanese Society of Molecular Biology (Fukuoka) P. 15, (in Japanese)
46. Tamura, A., Kanaori, K., Kojima, S., Kumagai, I., Miura, K., & Akasaka, K. (1991) Biochemistry 30, 5275-5286
48. Kakinuma, A., Sugino, H., Moriya, N., & Isono, M. (1978) J. Biol. Chem. 253, 1529-1537
49. Suzuki, K., Uyeda, M. & Shibata, M. (1978) Agric. Biol. Chem. 42, 1539-1543
50. Schultz, S. C. & Richards, J. H. (1986) Proc. Natl. Acad. Sci. U. S. A. 83, 1588-1592
51. Kojima, S., Obata, S., Kumagai, I., & Miura, K. (1993) Protein Engng. 6, 297-303
52. Hattori, M. & Sakaki, Y. (1986) Anal. Biochem. 152, 232-238
53. Wells, J.A., Ferrari, E., Henner, D.J., Estell, D.A. & Chen, E.Y. (1983) Nucleic Acid Res. 11, 7911-7925
54. Vasantha, N., Thompson, L.D., Rhodes, C., Banner, C., Nagle, J. & Filpula, D. (1984) J. Bacteriol. 159, 811-819
55. Ishiwa, H. & Shibahara, H. (1985) Jpn. J. Genet. 60, 235-243
56. Kakinuma, A., Sugino, H., Matsushima, M., Kamiya, N., Uyeda, M., & Mitsui, Y. in Protein Protease Inhibitor - The Case of Streptomyces Subtilisin Inhibitor (SSI), (Hiromi, K., Akasaka, K., Mitsui, Y., Tonomura, B., &

Murao, S. Eds.) (1985) pp 363-391, Elsevier, Amsterdam
57. Uehara, Y., Tonomura, B., & Hiromi, K. (1976) Biochim. Biophys. Acta 453, 513-520
58. Inouye, K. Doctoral Dissertation (Kyoto University) (1977)
59. Robertus, J. D., Kraut, J., Alden, R. A., & Birktoft, J. J. (1972) Biochemistry 11, 4293-4303
60. Niekamp, C.W., Hixson, H.F., Jr., and Laskowski, M., Jr. (1969) Biochemistry 8, 16-22
61. Mattis, J.A., amd Laskowski, M., Jr. (1973) Biochemistry 12, 2239-2245
62. Sealock, R.W. and Laskowski, M., Jr. (1973) Biochemistry 12, 3139-3146
63. Estell, D.A., Wilson, K.A., and Laskowski, M., Jr. (1980) Biochemistry 19, 131-137
64. Siekmann, J., Wenzel, H.R., Matuszak, E., Goldammer, E., and Tschesche, H. (1988) J. Protein Chemistry 7, 633-640
65. Ardelt, W., and Laskowski, M., Jr. (1991) J. Mol. Biol. 220, 1041-1053
66. Tonomura, B. in "Protein Protease Inhibitor-The Case of Streptomyces Subtilisin Inhibitor(SSI)," Elsevier, Hiromi, K., Akasaka, K., Mitsui, Y., Tonomura, B., & Murao, S., Eds. Amsterdam (1985) pp. 351-352
67. Davis, B. J. (1964) Ann. N. Y. Acad. Sci. 121, 404
68. Dobry, A., Fruton, J.S., and Sturtevant, J.M. (1952) J. Biol. Chem. 195, 124-131
69. Laskowski, M., Jr. (1970) Struc. Funct. Relat. Proteolytic Enzymes, Desnuelle, P., Neurath, H., and Ottesen, M., eds.) pp. 89, Munksgaard, Copenhagen
70. Kainosho, M., Tsuji, T., Akagawa, H. & Mitsui, Y. (1982) Tampakushitsu Kakusan Koso 27, 1556-1569. (in Japanese)
71. Musil, D., Bode, W., Huber, R., Laskowski, M., Jr., Lin, T-Y., and Ardelt, W. (1991) J. Mol. Biol. 220, 739-

755

72. Ardelt, W., and Laskowski, M., Jr. (1983) Acta Biochem. Polon. 30, 115-126
73. Tonomura, B., Iwanari, H., Ishikawa, H., Toyono, T., Hiromi, K., & Kano, K. (1984) Tanpaku kozo toronkai 35, 77 (in Japanese)
74. Kainosho, M. & Miyake, Y. (1988) Nippon Nögeikagaku Kaishi 12, 1822-1827 (in Japanese)
75. Yosimasa, K., Momma, K. & Tonomura, B. (1989) Seikagaku 61, 983 (in Japanese)
76. Hixson, H.F., Jr. & Laskowski, M., Jr. (1970) J. Biol. Chem. 245, 2027-2035
77. Quast, U., Engel, J., Steffen, E., Tschesche, H., & Kupfer S. (1978) Biochemistry 17, 1675-1682
78. Inouye, K., Tonomura, B., & Hiromi, K. (1979) Arch. Biochem. Biophys. 192, 260-269
79. Takahashi, K., & Sturtevant, J.M. (1981) Biochemstry 20, 6185-6190
80. Tamura, A., Kimura, K., Takahara, H., & Akasaka., K. (1991) Biochemistry 30, 11307-11313
81. Akasaka, K., Fujii, S., Hayashi, F., Rokushika, S., & Hatano, H. (1982) Biochem. Int. 5, 637-642
82. Hiromi, K. "Kinetics of Fast Enzyme Reactions" HALSTED PRESS, New York (1979) P.256
83. Satow, Y., Watanabe, Y & Mitsui, Y. (1980) J. Biochem. 88, 1739-1755
84. Korenm R. & Hammes, G.G. (1976) Biochemistry 15, 1165-1171
85. Tamura, A., Kanaori, K., Kojima, S., Kumagai, I., Miura, K., & Akasaka, K. (1991) Biochemistry 30, 5275-5286
86. Kainosho, M., & Imamura, Y. (1983) Seikagaku 55, 630 (in Japanese)
87. Ikenaka, T. (1985) in Protein Protease Inhibitor - The

Case of Streptomyces Subtilisin Inhibitor (SSI), (Hiromi, K., Akasaka, K., Mitsui, Y., Tonomura, B., & Murao, S. Eds.) pp. 159-163, Elsevier, Amsterdam

88. Yun, R.H., Anderson, A., & Hermans, J. (1991) PROTEINS 10, 219-228
89. Matthews, B.W., Nicholson, H., & Becktel, W.J. (1987) Proc. Natl. Acad. Sci. USA 84, 6663-6667
90. Kojima, S., Obata, S., Kumagai, I., & Miura, K. (1990) Bio/Technology 8, 449-452
91. Privalov, P. L. (1979) Adv. Protein Chem. 33, 167-241
92. Taguchi, S., Kikuchi, H., Kojima, S., Kumagai, I., Nakase, T., Miura, K., & Momose, H. (1993) Biosci. Biotech. Biochem. 57, 522-525
93. Yutani, K., Hayashi, S., Sugisaki, Y., & Ogasahara, K. (1991) PROTEINS 9, 90-98
94. Lascu, I., Deville-Bonne, D., Glaser, P., & Veron, M. (1993) J. Biol. Chem. 268, 20268-20275
95. Hardy, F., Vriend, G., Veltman, O.R., van der Vinne, B., Venema, G., & Eijsink, V.G.H. (1993) FEBS 317, 89-92

Acknowledgments

I would like to express my sincere gratitude to Prof. Ben'ichiro Tonomura of Kyoto University for his invaluable guidance, useful discussion, constant encouragement throughout the course of these studies.

I am deeply grateful to Assoc. Prof. Kuniyo Inouye of Kyoto University for his constant and valuable advice and discussions during the course of these studies and his critical reading of the manuscript.

I am greatly indebted to Prof. Emeritus Keitaro Hiromi of Kyoto University (presently at Fukuyama University) for his generous suggestion and encouragement.

I would like to express my appreciation to Dr. Hiroshi Nakatani of Kyoto University for his useful advises and suggestions.

I am greatly indebted to Prof. Emeritus Sawao Murao of University of Osaka Prefecture (presently at University of Kumamoto Institute) for his kind gift of Streptomyces subtilisin inhibitor, to Prof. Masatake Kainosho of Tokyo Metropolitan University for his generous gift of Plasminostreptin, API-2C' and mutant SSI's, and also indebted to Prof. Kazuyuki Akasaka of Kyoto University (presently at Kobe University) for his kind gift of mutant SSI's and useful discussions.

I appreciate generous guidance to prepare mutant SSI's and mutant subtilisin BPN' by site-directed mutagenesis from Prof. Kin-ichiro Miura and Assoc. Prof. Shuichi Kojima of Gakushuin University.

I thank to Assoc. Prof. Kenji Yamamoto of Kyoto University for his kind guidance of Streptomyces culture and

Prof. Etsuro Sugimoto and Dr. Teruo Kawada of Kyoto University for permitting me to use a densitometer and for the help in the measurements.

I wish to express my gratitude to Prof. Misao Tashiro of Kyoto Prefectural University for providing me with a computer program for K_i determination and to Assoc. Prof. Shuji Adachi of Kyoto University for the help in derivation of the equations and for useful discussion on the kinetic analysis.

I am greatly indebted to Prof. Masaaki Hirose of Kyoto University for his help in measurements and analysis of CD spectra.

Acknowledgments are also made to Prof. Saburo Hara and Dr. Kaeko Hayashi-Kamei of Kyoto Institute of Technology for the analysis of amino acid composition.

I wish to appreciate the kind help of Prof. Katsutada Takahashi and Dr. Harumi Fukada in measurement and analysis of differential scanning calorimetry.

I thank Prof. Yukio Mitsui of Nagaoka University of Technology for advice in drawing the stereo view of SSI-subtilisin BPN' interface.

My deep thanks are due to Ms. Kayo Yoshimasa-Sumida, Ms. Mitsuko Okamura, Ms. Hiromi Kawaguchi, Mr. Tstsuya Hatanaka, Ms. Yasuko Fukushima, and Mr. Shoji Yamasaki for their kind collaborations and discussions throughout these studies.

I am grateful to Dr. Teisuke Takita, Dr. Hiroshi Yamashita, Ms. Yukue Maruoka, and all the members of the Laboratory of Enzyme Chemistry, Department of Food Science and Technology, Fuculty of Agriculture, Kyoto university for their useful discussion and kind encouragement during the course of study.

Finally but not least, I express my great appreciation to my parents Tokio and Kiyoko Momma, and my hasband Seiji Masuda. These studies would not have been completed without them.

Kyoto 1994
Keiko Momma-Masuda

List of publications

1.

Keiko MASUDA-MOMMA, Tatsuya HATANAKA, Kuniyo INOUYE, Kenji KANAORI, Atsuo TAMURA, Kazuyuki AKASAKA, Shuichi KOJIMA, Izumi KUMAGAI, Kin-ichiro MIURA, and Ben'ichiro TONOMURA: Interaction of Subtilisin BPN' and Recombinant Streptomyces Subtilisin Inhibitor with Substitured P_1 Site Resiues
J. Biochem. (1993) 114, 553-559

2.

Keiko MASUDA-MOMMA, Toyohiro SHIMAKAWA, Kuniyo INOUYE, Keitaro HIROMI, Shuichi KOJIMA, Izumi KUMAGAI, Kin-ichiro MIURA, and Ben'ichiro TONOMURA : Identification of Amino Acid Residues Responsible for the Changes of Absorption and Fluorescence Spectra on the binding of Subtilisin BPN' and Streptomyces Subtilisin Inhibitor
J. Biochem. (1993) 114, 906-911

3.

Ben'ichiro TONOMURA, Keiko MASUDA-MOMMA, Mitsuko OKAMURA, Kayo YOSHIMASA-SUMIDA, and Keitaro HIROMI : Resynthesis of scissile bond of Streptomyces Subtilisin Inhibitor (SSI) by subtilisin BPN' in preparation

4.

Keiko MASUDA-MOMMA, Kayo SUMIDA-YOSHIMASA, Kuniyo INOUYE, and Ben'ichiro TONOMURA : Kinetic and thermodynamic studies on the dissociation of a dimeric protein, Streptomyces Subtilisin Inhibitor (SSI) in preparation

5.

Keiko MASUDA-MOMMA, Kayo SUMIDA-YOSHIMASA, Mitsuko OKAMURA, Kuniyo INOUYE, Ben'ichiro TONOMURA : Equilibrium constants K_{hyd} for the hydrolysis of the reactive-site peptide bond of Streptomyces Subtilisin Inhibitor in preparation

6.

Keiko MASUDA-MOMMA, Kuniyo INOUYE, Shuichi KOJIMA, Izumi KUMAGAI, Kin-ichiro MIURA, and Ben'ichiro TONOMURA : Role of Pro residues at around the reactive site of Streptomyces Subtilisin Inhibitor in preparation